Physiology-based biokinetic modelling and reverse dosimetry using biomonitoring data of pesticide exposures for humans and animals

Paul T. Scheepers, Nina Wieland, Noa Dominicus, Martien Graumans, Jonatan Dias, Hedwig van Hove, Rick Greupink, Annelies Noorlander, Benthe van der Lugt, Hans Mol

Deliverable number: D3.4

Due date: Month 48

Dissemination level: Public (after 6 months of submission date)
Lead beneficiary: SKU

Deliverable type: Report

Version: 1

Disclaimer: This report is part of a project that has received funding by the European Union's Horizon 2020 research and innovation program under grant agreement number 862568.

PROJECT INFORMATION	
Project Title	Sustainable Plant Protection Transition; A global health approach
Project Acronym	SPRINT
Call Identifier	H2020-SFS-2019-2; Sustainable Food Security
Grant Agreement no.	862568
Starting Date	01-09-2020
End Date	31-08-2025
Project duration	60 months
Website address	www.sprint-h2020.eu
Project coordinator	Wageningen University
Overall Project coordinator	Prof. Dr. V. Geissen +31317485144 (violette.geissen@wur.nl)
Scientific Project Manager	V. Felix da Graça Silva, PhD (vera.felixdagracasilva@wur.nl)
REPORT INFORMATION	
Report Title	Physiology-based biokinetic modelling and reverse dosimetry using biomonitoring data of pesticide exposures for humans and animals
Principle Author(s)	Paul T.J. Scheepers PhD
Principle Author e-mail	paul.scheepers@ru.nl
Deliverable Number	D3.6
Work Package	3
WP Leader	SKU
Other partners involved	UU, WSFR
Nature	Report
Dissemination	Public (after 6 months of submission)
Review	Nicoleta Suciu PhD
Report Due Date	31-08-2024
Report publish date	01-03-2025

List of abbreviations

ADI	Acceptable daily intake
ADME	uptake, distribution, metabolism and excretion
AOEL	Acceptable operator exposure level
AUC	Area under curve
CSS	Case study site
EM	Extensive metaboliser
EU	European Union
F	Foetal
GI	Gastrointestinal
HBM	Human biomonitoring
HCB	Hexachlorobenzene
HCH	Hexachlorocyclohexane
M	Maternal
LOD	Limit of detection
LOQ	Limit of quantification
MRL	Maximum residue level
NHANES	National Health and Nutrition Examination Survey
LOAEL	Lowest observed adverse effect level
NOAEL	No observed adverse effect level
PBK	Physiologically based biokinetic
PM	Poor metaboliser
PPE	Personal Protective Equipment
PPP	Plant Protection Product
QSAR	Quantitative structure activity relationship
SPRINT	Sustainable Plant Protection Transition
UER	Urinary excretion rate

Contents

List of abbreviations iii
Summary of main findings 1
1. Introduction 2
2. Methods for human PBK modelling 3
2.1. Substance selection for humans 3
2.2. Human volunteer study 4
2.2.1. Study design 4
2.2.2. Recruitment of study participants 6
2.2.3. Analysis of pesticides 6
2.2.4. Calculations and data analysis 7
2.3. PBK Modelling for humans 8
2.3.1. Generic toxicokinetic modelling 8
2.3.2. Dedicated toxicokinetic models 13
2.3.2. Pregnancy model 20
3. Methods for animal PBK modelling 25
3.1. Substance selection for animals 25
3.2. PBK modelling for animals 25
3.2.1. Generic modelling for animals 26
3.2.2. Model components 27
3.2.3. Reverse dosimetry 27
3.3. Liver S9 metabolism studies 28
4. Results Human PBK modelling 31
4.1. Generic PBK modelling 31
4.2. Substance specific PBK modelling 31
4.2.1. Acetamiprid 31
4.2.1.1. Oral 31
4.2.2.2. Skin 33
4.2.2. Glyphosate 35
4.2.3. Tebuconazole 36
4.3. Results of ex vivo placenta perfusion study 38
4.4. Reverse dosimetry of Human HBM data 41
4.4.2. Reverse dosimetry using dedicated models 41

5. PBK modelling for animals 46
5.1. Generic PBK modelling for each animal species 46
5.2 Farm animal species 46
5.2.1. Liver S9 metabolism studies 46
5.2.2. Model outcome with inclusion of the intrinsic clearance 46
5.2.3. Predicted transfer from pesticides to milk and eggs 48
5.2.4. Reverse dosimetry and assessment of pesticide concentrations in feed 49
5.2.5. Assessment maximum calculated intake of selected pesticides 49
5.2.6. Comparison of the predicted pesticide intake with the maximum calculated intake 51
6. Discussion 53
6.1. Human 53
6.2. Animal 55
7. Data gaps and future research 58
7.1. Human 58
7.2. Animal 58
8. Conclusions 60
8.1. Humans 60
8.2. Animals 60
9. References 61

Annexes i
Annex 1. Model code for the generic model ii
Annex 2. Human tissue parameters v
Annex 3: Physiological parameters for humans and all animal species of interest. x
Annex 4. Substance-specific modelling parameters. xii
Annex 5. MRM details on the LC-MS/MS analysis. xiv

Summary of main findings

Background - Physiology-based biokinetic (PBK) modelling describes the absorption, distribution, metabolism and excretion (ADME) of chemicals in humans and animals. This modelling approach was used to interpret human biomonitoring (HBM) data in the framework of existing reference values.

Aim - Use PBK modelling to calculate back from biomonitoring data to human and farm animal exposure to pesticides.

Methods - Human PBK modelling was supported by human volunteer studies according to a protocol approved by the ethics committee. Controlled exposures below the acceptable daily intake (ADI) were studied for acetamiprid and glyphosate. These pesticides were studied for ingestion and skin absorption on separate occasions in same study subject. For a third substance, tebuconazole, existing human kinetic data was used to develop a PBK model. With these human data, three substance-specific PBK models were constructed to generate exposure estimates by back-calculation from available HBM data. Additionally, placenta transfer was estimated using a human placenta model generating data that were used in a PBK model corresponding to 3rd trimester pregnancy. For other pesticides a less precise generic modelling was applied. In parallel, PBK models were developed for specific farm animal species (chicken, cow, goat, pig, sheep and cat). These models were parameterised with existing animal species-specific data from literature complemented with experimental data for metabolic conversion factors. Uptake was back-calculated from HBM data obtained in the SPRINT field campaign.

Results and discussion - For all substances in all sub-groups (farmers, neighbours and consumers) the back-calculated median values were below the current acceptable daily intake (ADI) and accepted operator exposure level (AOEL) by 2-4 orders of magnitude. Results are expressed as the median % of the (ADI), ranging from 5th to 95th percentile (P5-P95). For acetamiprid these values were 0.16% (0.02-1.8%) of the recently reduced ADI. For glyphosate these values were 0.06% (0.02-0.3%) of the ADI and 0.3% (0.1-1.6%) of the AOEL. For tebuconazole these values were 0.03% (0.001-0.6%) of the ADI. Using the generic model, the 95th percentile of chlorpyrifos of all blood samples analysed from the SPRINT study participants corresponds to 8.9% of the ADI. Forward dosimetry studies combining PBK models with *ex vivo* placental transfer data demonstrate how this approach can be used to estimate internal fetal exposure following external maternal exposure. In farm animals for hexachlorobenzene, indoxacarb, MPCA, pendimethalin and tri-allate, most of the predicted dose levels exceeded the MRL-based maximum concentration in feed (at MRL-values). For MCPA, some datapoints calculated for cat and cow were below the MRL-based maximum concentrations in feed (at MRL-values). For bromoxynil in cat, cow, goat and sheep predicted oral doses were exceeding estimated total concentrations of bromoxynil in feed at MRL values in all animal species. For 2,4-D and pyrethrin II, none of the predicted doses exceeded the MRL-based maximum concentration in feed. PBK modelling and its use to interpret human and animal biomonitoring data is a demonstration of principle. Some of the calculations should be interpreted with caution regarding assumptions made to cover data gaps.

Conclusion – PBK models were developed for interpretation of HBM data in the field campaign. For humans no indications of exceeding the ADI and AOEL were found. For farm animals our modelling results predict exceedance at MRL-based maximum concentrations in feed. With this the role of PBK modelling in the interpretation of HBM data was demonstrated showing opportunities for further development and addressing gaps in knowledge.

1. Introduction

During the SPRINT field campaign samples of biological matrices were collected to describe the exposure status of human subjects and for selected farm animals (cow, pig, sheep, goat and chicken). Analysis of these samples for active ingredients of plant protection products (PPPs) provides information about their internal exposure. Diet is assumed to be the driving factor but, depending on the specific substance, other non-dietary routes and sources of exposure may contribute.

In WP3 we used two methods to study the link between the results of biomonitoring data and environmental exposures: Statistical models (in D3.3) and physiology-based biokinetic (PBK) models (in D3.4). These models simulate the physiology of uptake, distribution, metabolism and excretion after substances become systemically available. Such models can be used to describe the kinetics of pharmaceuticals (pharmacokinetics) and toxic substances (toxicokinetics) to generate predictions of the concentration time pattern in the blood circulation and in internal organs and tissues. Such models can also be used to calculate back to uptake according to certain exposure scenarios of interest. Based on the type of biological matrix this can be done from samples of blood, urine and feces. In the proposal we also included saliva as a less invasive alternative. As we have been able to obtain ethics approval for collection of blood, we did not use this alternative sampling matrix.

The term 'pesticides' is used to refer to active ingredients of PPPs also including any other uses next to plant protection including biocide use or use as veterinary medicine. Where relevant we will specifically refer to any known other uses than plant protection.

This report describes the use of PBK modelling on to calculate back from biomonitoring data to exposure from uptake by humans and by farm animal species. The human volunteer study the human PBK modelling and the analysis of HBM data was done by SRU and the placenta transfer study was done at SRUMC. The animal PBK modelling was done by WUR as well as the chemical analyses on the human volunteer and placenta studies.

This deliverable used HBM data from the field campaign described in D2.3 and D2.4 for the most frequently occurring pesticides. The current report provides insights for WP4 e.g. on the bioavailability and kinetics of pesticides and their metabolites in the fetus. This deliverable also provides information on the level of aggregated internal exposure relevant to health impact assessment in WP5.

The main objective is to collect human data of the kinetics of pesticides after a single oral or dermal dose to create a physiology-base pharmacokinetic (PBK) model.

The secondary objectives are to use the parametrised PBK models to:
a. perform calculations of the dose of the parent and its metabolites in internal organs for follow-up testing of specific organ toxicity;
b. perform back-calculations (reverse-dosimetry) related exposure scenarios observed in real life to evaluate how HBM findings are related to currently established safe values.

2. Methods for human PBK modelling

PBK models are essentially a set of mathematical formulas which represent the rate of change in the amount of substance in each compartment. A model consists of multiple compartments (or: organs) which have eliminating or non-eliminating functions. An assumption that is often made in modelling is that the organs are 'well-stirred', meaning that upon entering of a said compound is immediately distributed among the whole organ. In these models, a dose input to the gastrointestinal tract lung or skin can be made to simulate exposure through any of these routes. PBK models require both chemical substance specific and physiological input parameters. PBK models are often used to estimate target dose or predict excretion in an application called 'forward dosimetry' (**Figure 1**). Models can also be used to do back-calculations from human biomonitoring (HBM) data back to uptake in a process referred to as 'reverse dosimetry'. Below the methods for the human PBK modelling will be introduced in more detail.

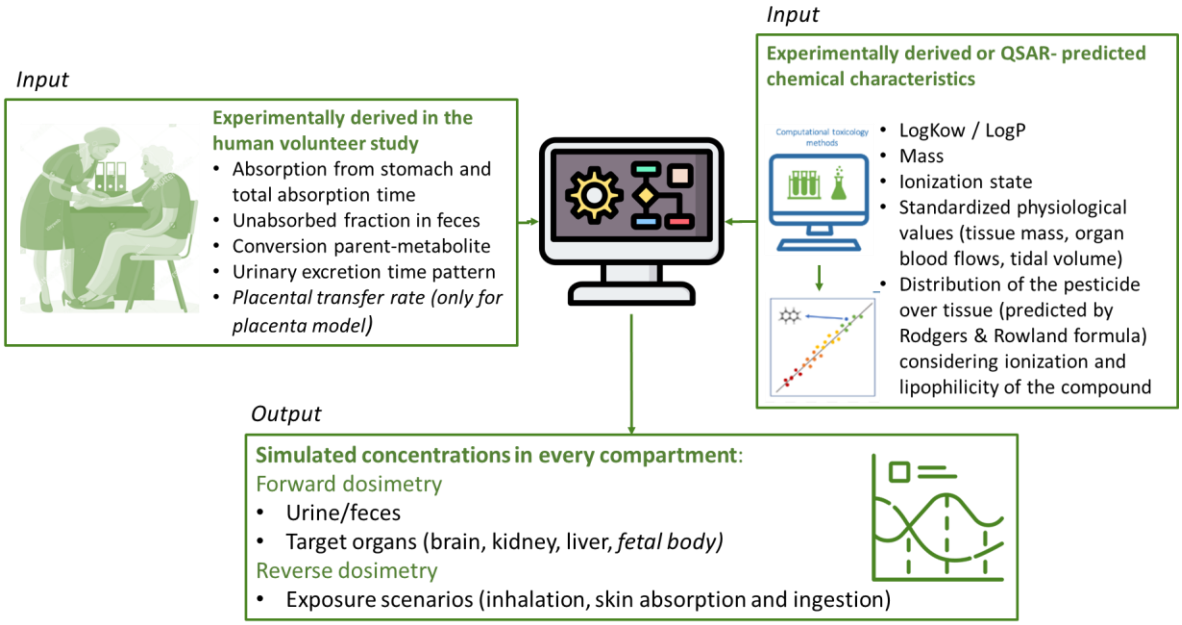

Figure 1. *Schematic specified PBK model input parameters and expected output tailored to the application for human biomonitoring (forward and reverse dosimetry).*

2.1. Substance selection for humans

The selection of pesticides for human PBK modelling is in line with the tiered approach already presented in WP4 deliverables. Three substances were selected as outcome of tier-3 corresponding to the substances that were tested in the in vivo animal studies in WP4: acetamiprid, glyphosate and tebuconazole (**Table 1**).

Table 1. Substance selection of active ingredients used in dedicated modelling.

Substances	Metabolites included[a]
Acetamiprid[b]	Acetamiprid-N-desmethyl
Glyphosate	Not applicable
Tebuconazole[c]	5 Hydroxy-tebuconazole

[a] Metabolites selected due to data availability and analytical capabilities; [b] Limited dual used for a single commercial product in France; [c] Extensive dual use as wood preservative (406 commercial products) in many countries in the EU (ECHA database, accessed 15-12-2024).

For the substances in the tier-1 longlist and tier-2 shortlist we have adopted a generic modelling strategy for kinetic modelling. Further selections were (only) made due to limited data availability. Based on the available data from high-throughput databases such as CompTox, which mainly contained pesticides that have been banned a long time ago, the compound chlorpyrifos was selected. The CompTox database contained data on this chemical and was also measured as part of the SPRINT biomonitoring campaign.

2.2. Human volunteer study

The study protocol has been submitted for ethics approval that was granted and the study was registered in the Trial register of the Netherlands (Netherlands trial register)

2.2.1. Study design

The design is a laboratory-based controlled kinetic study (**Figure 2**). Study subjects will be their own reference as we will start to collect samples of body fluids before the pesticide of interest will be administered. All study participants will receive the same dose and samples of body fluids will be collected over time. A similar study design has been used in our research group by Oerlemans et al. (2019) to study kinetics of tebuconazole in healthy volunteers (3). Study participants will be asked to participate in two single exposure scenarios (oral and skin absorption) separated by a wash-out period of at least one week to avoid carry-over.

Exposure at baseline will be verified before the administration of the pesticide of interest. Study subjects will be advised to avoid foods and beverages known to contain high residue levels of the pesticide of interest, and document this prior to their visit. During the visit the research department food and beverages will be provided. The dose will not exceed the ADI for that pesticide. One session will be dedicated to oral administration and the other session involves dermal exposure of the substance of interest dissolved in a volatile organic solvent (ethanol) that will evaporate, leaving a known topical dose on the skin surface. For reasons of comparison, each volunteer will be exposed to the same substance orally and dermally.

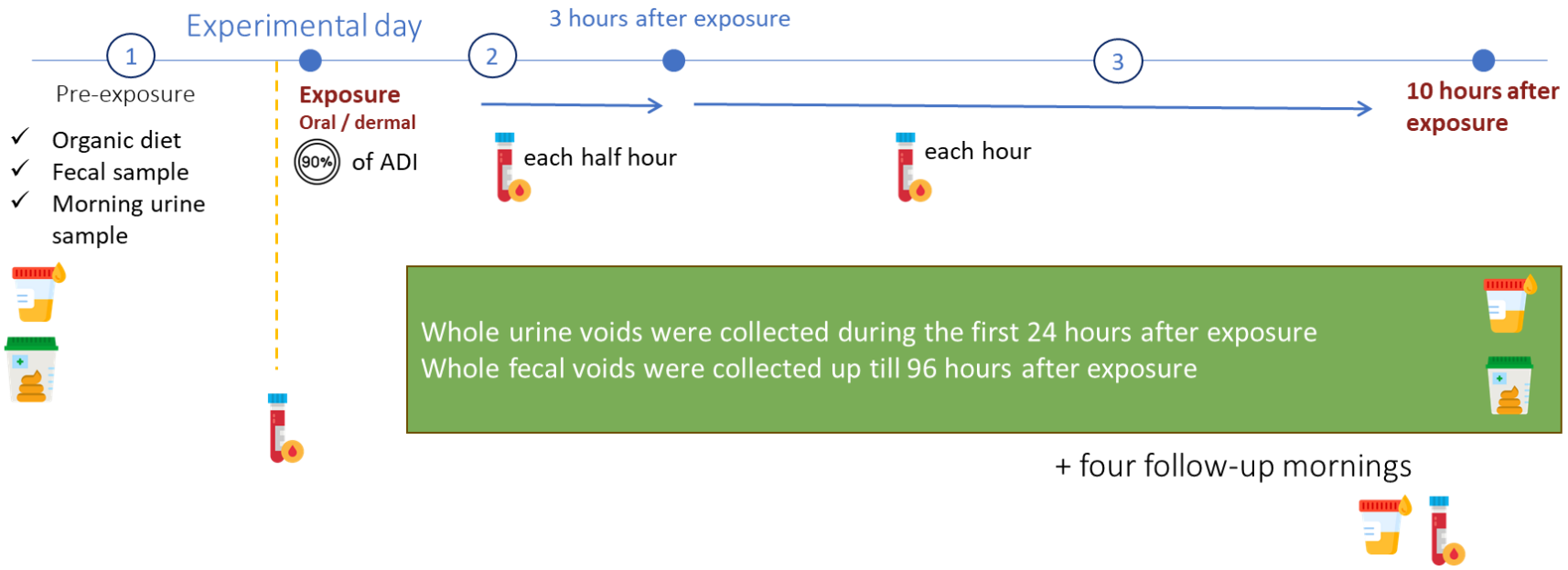

Figure 2. *Timeline of the study starting with a pre-exposure sample (1), the exposure (2) and the post-exposure collection of follow-up samples (3).*

2.2.2. Recruitment of study participants

For this study we recruited healthy subjects in range of 18 to 64 years. The plan is to find participants in a wide age range and a balance in male and female participants.

Inclusion criteria - Good general health i.e. no use of prescribed or OTC medication (except oral contraceptives) that could change the kinetics of pesticides during the study period; - Age between 18 and 55 years; - BMI between 20 and 25; - Alcohol consumption (on average) less than two units of alcohol consumption per day; Exclusion criteria - People using OTC or prescribed medication that induces or decreases CYP-enzyme activity, or could otherwise influence metabolism. - Pregnancy or (partner) intention to become pregnant during the study period; - Lactating mothers; - Skin disorders, e.g. sensitivity to natural or synthetic pyrethroids, atopic eczema, psoriasis, or other chronic skin diseases that causes hyperkeratosis; - Skin abnormalities on the non-dominant forearm, e.g. scars and injuries; - Smoking; - Any direct contact with pesticides (e.g. work-related).

2.2.3. Analysis of pesticides

For analysis of pesticides and/or their metabolites (previously) validated methods were used. These have been described in previous deliverables, and/or will be described in full detail in scientific publications.

2.2.3.1. Blood

Glyphosate in blood (plasma): the method involved addition of an isotope labelled glyphosate, protein precipitation using acetonitrile, addition of EDTA to avoid complexation of glyphosate with metals, cleanup using solid phase extraction (Strong Anion Exchange, SAX), derivatization with FMOC, and then determination of the derivative by LC-MS/MS (ESI, negative mode). This method was also used to support the analyses for the placenta perfusion studies.

For the analysis of acetamiprid and its metabolite acetamiprid-n-desmethyl (dr. Erhrenstoffer analytical standards, purity >95%, was purchased from LGC Ltd. (Teddington, UK). Stock solutions with a concentration of 1 mg/mL were prepared and subsequently diluted into 1 µg/mL work solution. The work solution was directly spiked in 1mL Krebs buffer or pooled human plasma with French origin (SEQENS, Lyon, France). Calibration standards with a range from 0.125 – 25 ng/mL (n = 7) freshly prepared were for each analysis and subsequently extracted using the previously validated QuEChERS SPRINT methodology. In short, 1 mL plasma was spiked with 5µL of internal standard solution (Chloridazon-D5 (pos), Bentazone-D6 (neg)) ~ 2ng/µL), subsequently 3 mL of acetonitrile 0.1% v/v formic acid was added, and the sample was vortexed. An aliquot of 1.5g of $MgSO_4$/sodium acetate was then added to dehydrate the plasma. After 10 min centrifuging at 3148 rcf, 1 mL of the supernatant was collected, spiked with 10 µL DMSO and evaporated under a stream of nitrogen at 40°C. The dried sample was reconstituted in 100 µL 50:50 (v/v) 5 mM ammonium formate:methanol solution, 5 min centrifuged and subsequently transferred to an vial containing 5µL LC-internal standard (Diuron-D6 (pos), 2,4-D 13-C6 (neg)) ~ 0.2 ng/µL. Multiple reaction monitoring analysis was applied during LC-MS/MS analysis to detect acetamiprid and acetamiprid-n-desmethyl (ESI, positive mode).

2.2.3.2. Urine

Glyphosate in urine: the method involved addition of an isotope labelled glyphosate, cleanup using solid phase extraction (SPE, Strong Anion Exchange, SAX), derivatization

with FMOC, and then determination of the derivative by LC-MS/MS (ESI, negative mode). AMPA in urine was analysed as glyphosate, but without the SPE cleanup.

Multi-method urine: approx. 45 pesticides, mostly urinary metabolites, were determined by liquid-liquid extraction/salt-out partitioning into acetonitrile. After an evaporative concentration/solvent switch into water/methanol, the extract was analyse using LC-MS/MS (ESI positive and ESI negative mode). Quantification was based using isotope labelled standards as far as available, and otherwise using matrix-matched calibration. For desmethyl-N-acetamiprid specific analyses, LC-MS/MS ESI was used in positive mode.

2.2.3.3. Feces

Glyphosate and AMPA: were extracted from feces after addition of isotope labelled internal standards using acidified water/methanol. The extract was analysed by LC-MS/MS using a HILIC column and ESI in negative mode.

Multi-method feces (LC-MS/MS): feces was extracted after addition of (isotope labelled) internal standards using water/acetonitrile followed by a salt-induced phase separation (QuEChERS). For LC-MS/MS analysis, an aliquot of the extract was diluted with water and analysed by LC-MS/MS (ESI, positive and negative mode)

Multi-method feces (GC-MS/MS): an aliquot of the acetonitrile extract obtained for the LC-MS/MS multimethod was diluted 1:1 with acetonitrile and cleanup by dispersive solid phase extraction (dSPE, C18/PSA/MgSO4). The extract was analysed by GC-MS/MS (EI). Combined, the multi-methods for feces covered 185 pesticides. For desmethyl-N-acetamiprid specific analyses, LC-MS/MS ESI was used in positive mode.

2.2.4. Calculations and data analysis

Rstudio (version 2023.12.1) and Microsoft Excel (Version 1404) were used to calculate toxicokinetic parameters. For each individual, toxicokinetic parameters of the parent and metabolite were calculated for the oral and dermal exposure scenario. In blood plasma, maximum plasma concentrations (Cmax), time to maximum plasma concentrations (Tmax), plasma half-life (t ½), and the area under the curve (AUC) were determined using the NonCompart package in R Studio. This package defines kinetic parameters within a one-compartment model with first-order kinetics such as blood. This model assumes a dynamic equilibrium between tissue and plasma concentration levels (on CRAN, CRAN: Package NonCompart (r-project.org). In addition, cumulative urinary excretion and excretion rate plots were made for the first 24 hours after exposure. The first 24 hours were chosen for analysis because the whole urine void was collected during this period. The points of urinary excretion on the timely were derived by calculation of the midpoint between two micturition's. The peak excretion time and urinary half-life (t ½) were identified from concentration-time plots. In addition, the half-life in urine was calculated using a lognormal curve fit to the pooled data of all participants in R. Equation 1 was used to fit a curve to the data. In this equation, N is the concentration of the compound in ng/mL, t is the difference in time, and t ½ is the compound's half-life in hours.

$$N(t)=N(0)\cdot \left[1/2\right]^{((t/(t\ ½)))}$$

The cumulative urinary excreted percentage after 24 hours was calculated as a percentage of the administered dose. Based on the total void collection in the first 24 hours after exposure, combined with four morning urine spot samples, the estimated

cumulative urinary excretion over 96 hours after oral exposure was calculated. The median void volume and the number of voids over one day were used to calculate the predicted excretion for each individual. The estimated dose per void for day 2 up to day 5 in urine was calculated via Equation 2. These estimated doses were used to predict the excreted percentage after 96 hours. This was applied to the metabolite after oral exposure.

dose in void = median void volume (mL)·morning urine concentration (ng/mL)

Urinary conversion factors were determined by dividing the administered dose of the parent compound (in mg) by the total cumulative amount of metabolite in urine (in mg) after 24 hours. All urine data on acetamiprid-N-desmethyl were also adjusted for dilution using creatinine corrections. The excreted percentage of parent and metabolite via feces after 96 hours was determined for each individual. Each variable's geometric mean of all participants was determined, including standard deviation. The conversion factor was calculated based on urinary excretion rates (UERs). in mg/h or mol/h

2.3. PBK Modelling for humans

2.3.1. Generic toxicokinetic modelling

The purpose of the generic model was to create a generally applicable model which could be applied to a large set of pesticides for the purpose of reverse dosimetry. The generic model is based on an existing physiologically-based biokinetic model (PBK) model developed for the httk R package by Pearce et al. 2017 The abbreviation HTTK stands for High-Throughput Toxicokinetics and supports a generic solution supporting predictions of kinetics based on *in vitro* human data, using animal-free methods (EPA website https://www.epa.gov/comptox-tools/high-throughput-toxicokinetics-httk-r-package).

2.3.1.1. Model structure

Model code was run from R. Volumes were presented in liters and concentrations in µM and µmol. An area under curve (AUC) was calculated in µM*days. Organs included in the model were gut lumen and gut tissue, liver, kidney, skin and lung. The other organs were grouped in a 'Rest of Body' compartment. After intake, the compound is firstly taken up by the gut tissue and transported to the liver, mimicking the first-pass effect. Here it is distributed to the venous blood and arterial blood via the lungs. From the arterial blood compartment, the compound returns with the blood flow to the gut tissue, the liver, kidney, skin and rest of body. From the kidney compartment the compound is cleared. The complete R script is provided in **Annex 1**.

2.3.1.2. Input parameters

Physiological and physicochemical data are the parameters in the model that need to be fulfilled in order to run the calculations. In this model, to keep it widely applicable, only a limited set of parameters was used. Partition coefficients were calculated using Schmitt's method (Schmitt 2008).

Tissue volumes and blood flows were obtained from Brown (1997) similar to the base model from *httk*.

A fast absorption rate of 1 h^{-1} was used for absorption from the gut lumen into the gut tissue. The fraction absorbed (*fa)* is set to 1 (100%) when data was unavailable but can be adjusted if known.

The conversion of the parent compound into one or more metabolites in the liver is estimated based on *in vitro* hepatic clearance assays with human or rat hepatocytes. Full-liver hepatic clearance ($CL_{metabolism}$) is calculated by scaling *in vitro* hepatic clearance (CL_{int}, *µl/min/10⁶ cells)* with hepatocyte density (*1.1 x 10⁸ hepatocytes per gram liver*) and liver density (*1.05 g/mL*). Renal elimination occurs through passive glomerular filtration through the kidneys. It is assumed that metabolite formation occurs solely through hepatic metabolism and clearance from the body occurs through the kidney only.

2.3.1.3. Model formulas

R is used to calculate the concentrations in each compartment over time or calculate back from plasma concentration to dose using the solver. Differential equations calculate the change in concentration within perfused tissue over time.

The oral dose is deposited in the gut lumen compartment and absorption from the gut lumen to the gut is modelled using the following equation:

$$\frac{d}{dt}A_{gutlumen} = -k_{gutabs}A_{gutlumen} + g(t)$$

$$\frac{d}{dt}C_{gut} = \left(k_{gutabs}A_{gutlumen} + Q_{gut}\left(C_{art} - \frac{R_{blood2plasma}}{K_{gut2pu}f_{ub}}C_{gut}\right)\right) \Big/ V_{gut}$$

Where:

- -k_gutsabs = the absorption rate constant
- A_gutlumen = the amount in the gut lumen (equal to the dose
- Qgut = blood flow towards and from the gut
- Cart = concentration in the arterial blood
- Rblood2plasma = the ratio in distribution of compound between whole blood and plasma
- Vgut = gut volume
- Kgut2pu = partitioning between blood plasma and gut tissue
- Fub = fraction unbound
- Cgut = concentration in the gut tissue

Distribution in the liver, first-pass effect and metabolism in the liver:

$$\frac{d}{dt}C_{liver} = \left(Q_{liver}C_{art} + \frac{Q_{gut}R_{blood2plasma}}{K_{gut2pu}f_{ub}}C_{gut} - \frac{(Q_{liver}+Q_{gut})R_{blood2plasma}}{K_{liver2pu}f_{ub}}C_{liver} - \frac{Cl_{metabolism}}{K_{liver2pu}}C_{liver}\right) \Big/ V_{liver}$$

$$\frac{d}{dt}C_{ven} = \left(\left(\frac{Q_{liver}+Q_{gut}}{K_{liver2pu}}C_{liver} + \frac{Q_{kidney}}{K_{kidney2pu}}C_{kidney} + \frac{Q_{rest}}{K_{rest2pu}}C_{rest}\right)\frac{R_{blood2plasma}}{f_{ub}} - Q_{cardiac}C_{ven}\right) \Big/ V_{ven}$$

Where:

- $CL_{metabolism}$ (L/day)
- K_liver2pu

In this model, the liver functions as a metabolising organ and the kidney as an elimination organ. Their differential equations are slightly different from the other organs, which function for distribution. For non-elimination or metabolizing organs, the following formula structure is used:

$$\frac{d}{dt}C_{organ} = \frac{Q_{organ}\left(C_{art} - \frac{R_{blood2plasma}}{K_{lung2pu} * f_{ub}} * C_{organ}\right)}{V_{organ}}$$

Where:

- d/dt C_organ = the change in the concentration of pesticide in the organ
- Q_organ = the blood flow to the organ
- C_art = the concentration of pesticide in the arterial blood (inflow to organ)
- R_blood2plasma / K_lung2pu * fub = a factor to scale the partitioning between blood plasma:organ tissue
- C_rest = the concentration in the organ compartment
- V_organ = the volume of the organ in liters

The venous blood receives input from the liver, kidney and rest of body, and expels blood to the lung tissue. Blood enters the arterial blood after passing through the lung and expels back to the organs. Thus, the concentration of the arterial blood is calculated as 'everything that doesn't remain in the lung compartment'.

$$\frac{d}{dt}C_{lung} = Q_{cardiac}\left(C_{ven} - \frac{R_{blood2plasma}}{K_{lung2pu}f_{ub}}C_{lung}\right) \Big/ V_{lung}$$

$$\frac{d}{dt}C_{art} = Q_{cardiac}\left(\frac{R_{blood2plasma}}{K_{lung2pu}f_{ub}}C_{lung} - C_{art}\right) \Big/ V_{art}$$

$$\frac{d}{dt}C_{rest} = Q_{rest}\left(C_{art} - \frac{R_{blood2plasma}}{K_{rest2pu}f_{ub}}C_{rest}\right) \Big/ V_{rest}$$

$$\frac{d}{dt}C_{ven} = \left(\left(\frac{Q_{liver}+Q_{gut}}{K_{liver2pu}}C_{liver} + \frac{Q_{kidney}}{K_{kidney2pu}}C_{kidney} + \frac{Q_{rest}}{K_{rest2pu}}C_{rest}\right)\frac{R_{blood2plasma}}{f_{ub}} - Q_{cardiac}C_{ven}\right) \Big/ V_{ven}$$

The kidney receives blood from the arterial blood compartment. The amount that is passively renally cleared through the GFR is removed from this compartment into a urinary compartment.

$$\frac{d}{dt}C_{kidney} = \left(Q_{kidney}C_{art} - \frac{Q_{Kidney}R_{blood2plasma}}{K_{kidney2pu}f_{ub}}C_{kidney} - \frac{Q_{gfr}}{K_{kidney2pu}}C_{kidney}\right) \Big/ V_{kidney}$$

Table 3. Chemical and physiological input data for chlorpyrifos as input for the generic PBK model. The required tissue parameters are presented in **Annex 2**.

1. Chemical physical and in vitro data			
Parameter	**Value**	**Unit**	**Source**
CAS	2921-88-2	n/a	n/a
LogP	4.96	log10 unitless ratio	OPERAv2.9
Molecular weight	350.6	g/mol	EPA
Human.Clint	2.6	µL/min/10^6 hepatocytes	Tonnelier 2012
Human.Fabs	*MISSING*	n/a	n/a
Human.Fgut	*MISSING*	n/a	n/a
Human.Fhep	*MISSING*	n/a	n/a
Human.Foral	*MISSING*	n/a	n/a
Human.Funbound.plasma	0.007932	Fraction	Wetmore 2015
Human.Rblood2plasma	0.7333	Ratio	TNO
2. Physiological data			
Plasma volume	42.86	ml/kg	See text above or Pearce 2017
Cardiac Output	231.4	ml/min/kg^(3/4)	
Average body weight	70	Kg	
Total plasma protein	0.07400	g/ml	
Hematocrit	0.440	Fraction	
Urine	0.040	ml/min/kg^(3/4)	
Glomular filtration ratio (GFR)	5.16	ml/min/kg^(3/4)	
Plasma protein volume fraction	0.069	Fraction	
Pulmonary ventilation rate	27.75	l/h/kg^(3/4)	
Alveolar Dead Space Fraction	0.33	n/a	
3. Tissue parameters			
See Annex 2			

The available databases in the online application were used and screened for compounds that were available from the high-throughput experiments from *httk* and included in the SPRINT biomonitoring campaign. Of all compounds, chlorpyrifos was the most data rich (**Figure 3**). Basic physicochemical parameters LogP and molecular weight were included to7 compute physiological parameters and predict partitioning. However, human data on blood tissue partitioning are missing.

Step 1: Derive *in vitro* chemical data

Standard chemical parameters were derived using httk in R with function:

$$chlorpyrifos.1 = chem.physical_and_invitro.data \,\%>\% filter(DTXSID == 'DTXSID4020458')$$

The substance properties octanol water partition coefficient (LogP) was computed, and the molecular weight (Molweight) was measured. Intrinsic clearance was determined in *vitro*. The fraction unbound to protein (Funbound) and the ratio between blood cells and plasma (Rblood2plasma) were experimentally derived.

Step 2: Physiological and tissue data

Physiological and tissue parameters were derived from existing databases included in the httk functions *physiology.data* and *tissue.data*. These data were used to parameterize the base model. The physiological parameters are presented in **Table 4**.

Step 3: Calculate parameters for running the model

Compute partitioning coefficients using Schmitt's method:

Partitioning coefficients are calculated using Schmitt's method, which takes into account the cellular composition of each tissue, the water content, the pH and the fraction unbound in plasma (F*up)*.

After running these steps, the solver was parameterised and run to back-calculate to the dose from a blood plasma concentration. This is assumed to be at steady-state. Other kinetic parameters, such as AUC and half-life can also be calculated.

Table 4. Physiological parameters

Partitioning Parameter name	Partitioning value
Krbc2pu	190
Kliver2pu	7218
Kkidney2pu	5707
Klung2pu	481.9
Krest2pu	2466
Kgut2pu	3811
Partitioning Parameter name	**Fractional volume value**
Vliverc	0.02448
Vkidneyc	0.00419
Vlungsc	0.007235
Vrestc	0.7765
Vgutc	0.0158
Partitioning Parameter name	**Fractional blood flow value**
Qtotal.liverf	0.2589
Qkidneyf	0.2214
Qlungf	0.025
Qrestf	0.4757
Qgutf	0.2054

2.3.2. Dedicated toxicokinetic models

An introduction to PBK modelling is written in the generic modelling part.

2.3.2.1. Introduction to dedicated PBK modelling

Dedicated PBK models were developed with the goal of creating substance-specific models to support reverse dosimetry calculations using human biomonitoring data. These models contain parameters determined in human volunteer studies. The BPK model can be modified to support pregnancy (**Figure 3**).

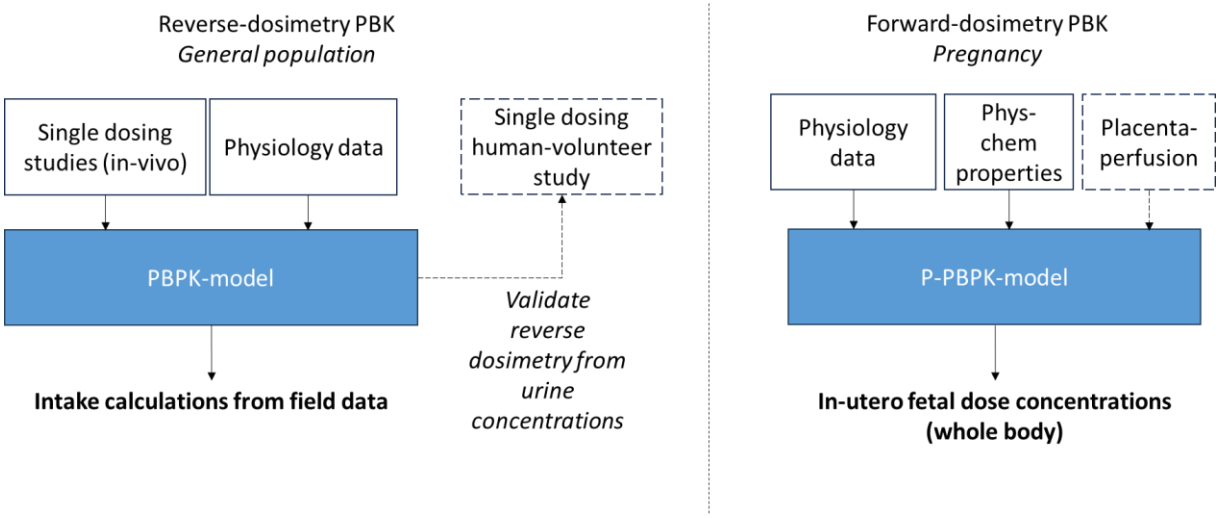

Figure 3. *Development of dedicated PBK modelling for reverse dosimetry (left panel) and forward dosimetry (right panel).*

2.3.2.2. Prioritised substances

Three active ingredients used in products for plan production have been prioritised for study involving human volunteers. This selection was coordinated with in vivo toxicity studies performed in WP4.

2.3.2.3. *Acetamiprid*

Acetamiprid is an insecticide that is mainly used for plant protection. There is only one biocide application registered in France for a single product. In mammals acetamiprid is metabolized by demethylation of the nitrogen, hence the metabolite is called acetamiprid-N-desmethyl (**Figure 4)**.

Figure 4. *Chemical structures of acetamiprid and its main metabolite in mammals (acetamiprid-N-desmethyl). Me = methyl group (-CH_3).*

2.3.2.4. 2.3.2.2.2. Glyphosate

Glyphosate is a herbicide used for plant protection. The main metabolite aminomethylphosphonic acid (AMPA) is also formed as a degradation product in the environment and as a residue in the diet (**Figure 5).**

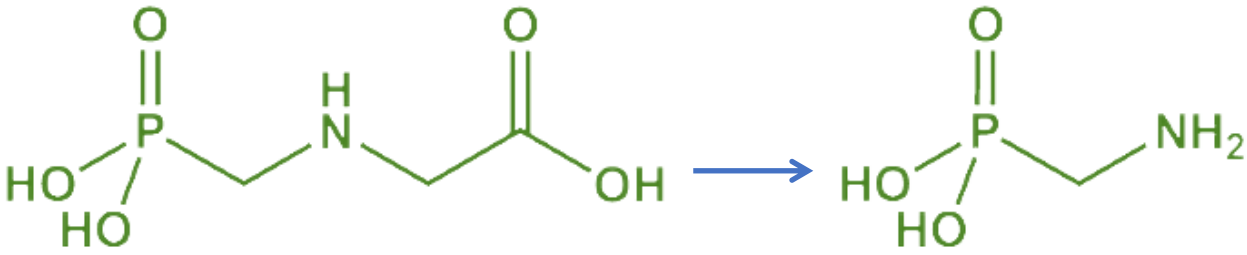

Figure 5. *Chemical structures of glyphosate and its metabolite aminomethylphosphonic acid (AMPA) in animals and in the environment.*

2.3.2.5. Tebuconazole

Tebuconazole is a fungicide that is mainly used for plant protection and also authorised as a biocide in wood preservation. In mammals tebuconazole is metabolized by hydroxylation, to 5-hydroxy-tebuconazole (**Figure 6)**. In the environment there is a wider spectrum of metabolism described by Youness et al. 2018.

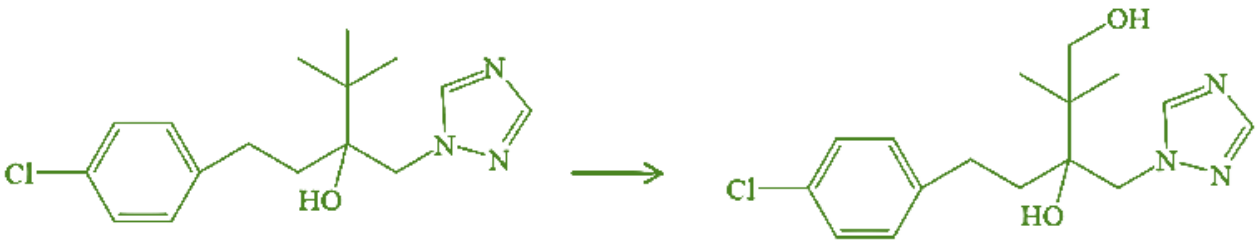

Figure 6. *Chemical structures of tebuconazole and one of its metabolites 5-hydroxy-tebubononazole in mammals.*

2.3.2.6. Overview developed models and scenario's

In total, several dedicated models and sub-models were developed for this deliverable:

Model A: Acetamiprid and acetamiprid-N-desmethyl

- Model A1 – Healthy male humans
- Model A2 – Fremle pregnancy model, third trimester

Model B: Tebuconazole and 5-hydroxy-tebuconazole

- Model B1 – Healthy male humans
- Model B2 – Female pregnancy model, third trimester

Model C: Glyphosate

- Model C1 – Healthy male humans
- Model C2 – Female pregnancy model, third trimester

The following scenarios were selected to apply these models to:

Scenario 1 – Oral exposure

Scenario 2 – Dermal exposure

Scenario 3 – Inhalation exposure

Scenario 4 – Combined exposure from oral, dermal and inhalation routes

2.3.2.7. Model structure

The model structure supports the different exposure scenarios, ingestion, inhalation and dermal absorption (figure 4a-c). The pregnancy scenario was added for forward dosimetry and is presented in Figure 4d. All models were developed using Berkeley Madonna software (UC, Berkeley, CA, USA version 10.2.8).

An existing PBK model describing human kinetics for tebuconazole and its metabolite 5-hydroxy-tebuconazole by Oerlemans et al (2019) was used to start developing the dedicated models for acetamiprid and glyphosate. Organ volumes were presented in liters, time in minutes, mass in mg and organ weights in kilograms. Organs included as compartments in the model were lung, adipose, gut, liver, kidney, skin, venous blood, arterial blood, rapidly perfused tissues (containing the brain, spleen, heart, pancreas, thyroid and adrenal glands) and slowly perfused tissues (bone and muscle). Each compartment is assumed to be well-stirred. Organ masses were scaled to a % of the bodyweight. A cardiac output of 5.2 L/min was used which represents residual tissues and organs (rest). Organ blood flows were determined as fractions of the cardiac output, where the lung compartment received 100% of the cardiac output.

In the oral exposure scenario exposure is simulated by assuming a fixed amount of the parent compound into the (gut) lumen compartment (**Figure 7a**). A pre-defined oral absorption fraction (%) and oral absorption constant (/min) were added for absorption from the lumen into the gut (tissue) compartment. From the gut lumen, a first-pass effect is simulated by passing the outward blood flow from the gut directly into the liver compartment where metabolism is simulated. The parent compound is removed, and the metabolite is added to the sub-model for the metabolite in the liver. Unmetabolized parent and metabolites then flow outwards to the venous blood, through the lungs and into the arterial blood circulation, where they are redistributed over the whole body. Here also passes the kidneys is passed, where renal elimination of the metabolite and thus removal of the metabolite from the body is simulated for a period of five days.

For the inhalation exposure (**Figure 7b**), a 100% absorption from air is assumed. Currently the dose is fixed to 1 µg/kg/d with a fixed bodyweight of 70kg to calculate dose (70 µg). When measured concentrations in µg/m^3 are available a dose can be calculated by multiplying the concentration in air in µg/m^3 with tidal volume (in m^3/h) and subsequently multiplied by the duration of the exposure (h). Blood:air partitioning can be calculated using QSAR (2).

In the dermal exposure scenario (**Figure 7c**), the deposition of the parent compound occurs in the stratum corneum compartment, similar to the lumen from the oral exposure scenario. A dermal absorption fraction (%) and dermal absorption constant (/h) are derived from available rat studies in literature.

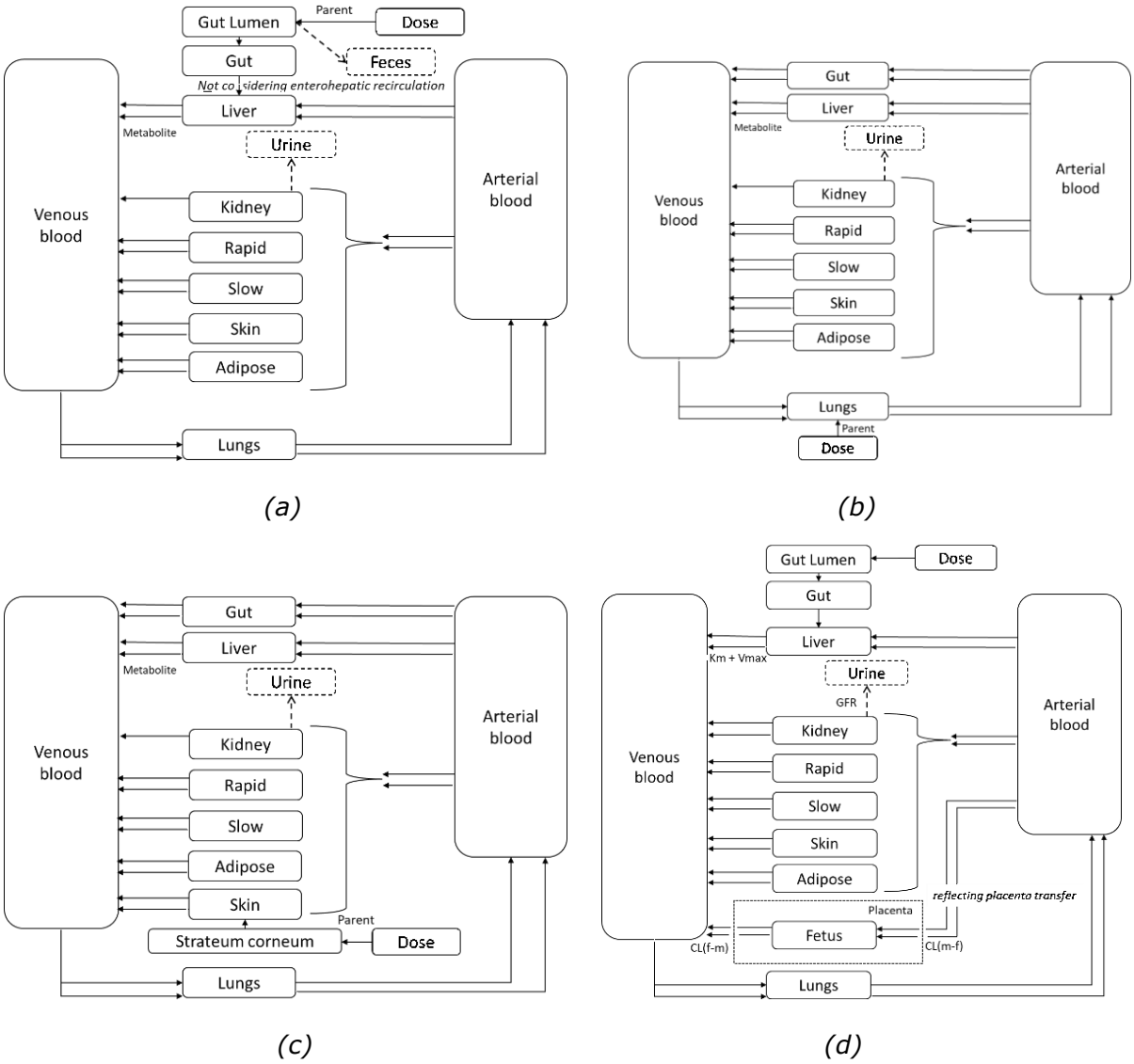

Figure 7. *PBK model structure to support the reverse-dosimetry calculations in the different exposure scenarios: ingestion (a), inhalation (b), dermal absorption (c) and the ingestion model with the placenta perfusion (d).*

In all models, hepatic clearance by metabolism was based assuming Michaelis-Menten kinetics using Vmax and Km for a single metabolite and renal clearance of the parent and metabolite.

Models A2, B2 and C2 – Third trimester pregnancy model

The maternal part of the pregnancy model is the same as the general population model. Some adjustments were made to correct for female body composition (**Figure 7d**). The cardiac output and bodyweight were scaled according to Abduljalil *et al.* (3). Gestational

age was set to 34 weeks (third trimester). Fetal volumes in L were calculated according to Abduljalil *et al.* as fixed fractions of the maternal bodyweight. Exchange between the amniotic fluid and the fetal blood is modelled using a fetal swallowing constant (L/min) and a fetal oral, nasal, tracheal and pulmonary secretion constant (L/min).

The fetal exposure is modelled using fetal blood, rest of body and amniotic fluid compartment. The fetal blood receives inflow from the arterial blood of the mother. An exchange between the amniotic fluid and the fetal blood is calculated using fetal oral, nasal, tracheal and pulmonary secretion constants and a fetal swallowing constant (L/min). Compound clearance from the maternal arterial blood compartment was modelled using ex-vivo placental clearance values. Clearance values obtained from the ex-vivo experiments were scaled to represent the summed capacity of cotyledons in the placenta that facilitate delivery of oxygen and nutrients to fetal blood (see **Figure 8**).

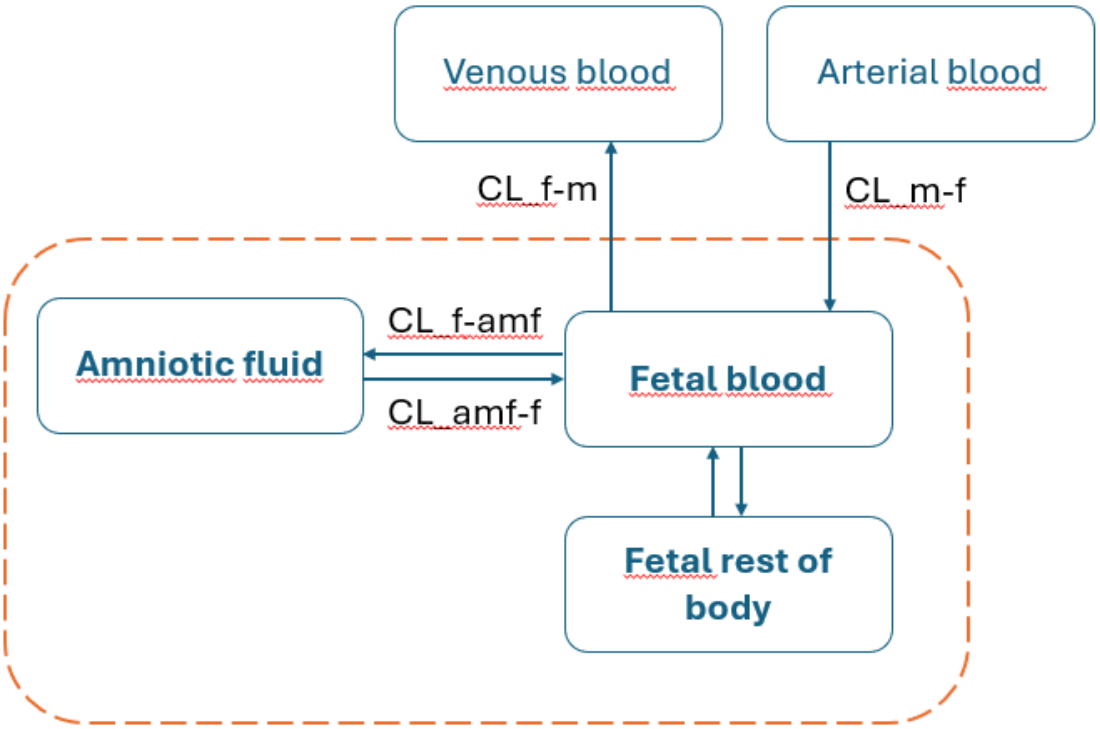

Figure 8. *Conceptual model to describe the kinetics of the placenta transfer of the parent and the metabolite from the maternal blood to the fetus and back to the mother.*

2.3.2.8. Model inputs

For acetamiprid partition coefficients are calculated using Rodger and Rowland's method, taking into account pH and logP of a compound (**Table 6a**). For the metabolite desmethyl-N-acetamprid additional parameters were used (**Table 6b**).

Table 6a. Input parameters for acetamiprid PBK model

Abbreviation	Parameter	Unit	Value	Source
Oka	Oral absorption rate constant	/min	0.334	RAR, scaled from rats
Fabs	Fraction absorbed from the gut lumen	w%	0.955	RAR
Fu	Fraction unbound in plasma	w%	0.482	HTTK [QSAR]
B:P	Blood:plasma partitioning coefficient	-	1	Assumption
Kfecal	Fecal transfer rate	/min	0.001	Calculated from human volunteer study data
Vmax	Maximum velocity	mg/min	31.9	Kolanzky
Km	Michaelis-Menten constant	mg/L	24.49	Kolanzky
Dose	Administered dose	mg	ADI*0.90*BW	Computed
Fdose	Dose corrected for bioavailability	mg	Dose*fabs	Computed

Table 6b. Input parameters for the acetamiprid-N-desmethyl module.

Abbreviation	Parameter	Unit	Value	Source
Fu	Fraction unbound in plasma	w%	0.482	Assumed same as parent
B:P	Blood:plasma partitioning coefficient	-	1	Assumption
ER	Excretion rate	mg/min	0.005	Fit to cumulative urine excretion

For glyphosate partition coefficients are calculated using Rodger and Rowland's method, taking into account pH and logP (**Table 7**). Glyphosate is not as extensively metabolized as acetamiprid or tebuconazole and Km and Vmax values were not available from literature. Thus, no sub-model for the metabolite was included for this compound and only clearance of the parent was modelled renally.

Table 7. Input parameters for the glyphosate PBK model.

Abbreviation	Parameter	Unit	Value	Source
Oka	Oral absorption rate constant	/min	0.2963	Calculated from Tmax in rats
Fabs	Fraction absorbed from the gut lumen	w%	0.25	RAR
Fu	Fraction unbound in plasma	w%	0.99	Smith-Roe 2023 (computed using ADMET predictor)
B:P	Blood:plasma partitioning coefficient	-	1	Assumption
kfecal	Fecal transfer rate	/min	0.00048	Fit to human volunteer data
Dose	Administered dose	mg	8.75	25% of the ADI
Fdose	Dose corrected for bioavailability	mg	8.75*0.25	
ER	Excretion rate	L/min	0.00074258	Fit to human volunteer data

For tebuconazole partition coefficients are calculated using Rodger and Rowland's method, taking into account pH and logP of a compound (**Table 8**).

Table 8. Input parameters for the tebuconazole model.

Parameter	Parameter	Unit	Value	Source
Oka	Oral absorption rate constant	/min	0.06	Oerlemans 2019
Fabs	Fraction absorbed from the gut lumen	w%	1	Oerlemans 2019
Fu	Fraction unbound in plasma	w%	0.34	Jónsdóttir 2016
B:P	Blood:plasma partitioning coefficient	-	1	
kfecal	Fecal transfer rate	/min	0	100% absorption is assumed → no fecal excretion
Dose	Administered dose	Mg	1.5	
Fdose	Dose corrected for bioavailability	w%	1.5	
ER	Excretion rate	l/min	0.125	Oerlemans
Km	Michaelis-menten constant	mg/l	4.16	Jónsdóttir 2016
Vmax	Maximum velocity	mg/min	19.68	Jónsdóttir 2016

2.3.2. Pregnancy model

All physicochemical parameters for the compound partitioning during pregnancy and in blood are derived using the pregnancy-QSARs in SimCyp for acetamprid (**Table 9**) and tebuconazole (**Table 10**). Clearance of compounds across the placenta were determined in ex vivo experiments with human term placenta tissue.

Table 9. Input parameters for the acetamiprid pregnancy model.

Parameter	Unit	Value	Source
Clearance fetal blood – maternal blood	L/min/cotyledon	0.00326	Experimentally derived
Clearance maternal blood - fetal blood	L/min/cotyledon	0.00172	Experimentally derived
Fraction unbound in maternal perfusion buffer		0.14167	Assumed same as fraction unbound in blood
Fraction unbound in fetal perfusion buffer		0.14167	Assumed same as fraction unbound in blood
Number of cotyledons per placenta	N	30	Freriksen et al.
Fetal cardiac output	L/min	553 * VtotalF * (60/1000) / 60	De Smedt. Et al 1987
Fetal oral, nasal, tracheal, and pulmonary secretion constant	(L/min)	(0.275/A_SF) * (1/24)/60	Underwood et al. 2005
Fetal swallowing constant	(L/min)	(0.774*A_SF) * (1/24)/60	Underwood et al. 2005
Partitioning coefficients			Simcyp
Fraction unbound in fetal blood		0.41167	Simcyp
Fraction unbound in maternal blood		0.41167	Simcyp

Table 10. Input parameters for the tebuconazole pregnancy model.

Parameter	Unit	Value	Source
Clearance fetal blood – maternal blood	L/min/cotyledon	0.00278	Experimentally derived
Clearance maternal blood - fetal blood	L/min/cotyledon	0.00356	Experimentally derived
Fraction unbound in maternal perfusion buffer		0.061	Assumed same as fraction unbound in blood
Fraction unbound in fetal perfusion buffer		0.061	Assumed same as fraction unbound in blood
Number of cotyledons per placenta	N	30	Freriksen et al.
Fetal cardiac output	L/min	553 * VtotalF * (60/1000) / 60	De Smedt. Et al 1987
Fetal oral, nasal, tracheal, and pulmonary secretion constant	(L/min)	(0.275/A_SF) * (1/24)/60	Underwood et al. 2005
Fetal swallowing constant	(L/min)	(0.774*A_SF) * (1/24)/60	Underwood et al. 2005
Fraction unbound in fetal blood		0.061	Simcyp

2.3.3.1. Ex-vivo placenta perfusion

Ex vivo placenta perfusion studies were performed in term human placenta tissue, as described earlier by our laboratory (Freriksen et al., 2020). In this study, we determined bi-directional placental intrinsic clearance values by studying both maternal-to-fetal (MTF) as well as fetal-to-maternal (FTM) transport of acetamiprid and tebuconazole. A closed-open perfusion set-up experimental design was used to maintain sink conditions and thus obtain estimates of intrinsic clearance in either direction.

The Local Ethics Committee of the Radboudumc (Nijmegen, the Netherlands) approved the use of placental tissue for the conduction of *ex vivo* dual-side cotyledon perfusion studies. After signing informed consent, placentas were collected immediately after delivery. Perfusion experiments were conducted as follows. Within 20 minutes after birth an intact cotyledon was selected based on integrity of the maternal side. The fetal circulation of an individual cotyledon was re-established by cannulation of a matching artery and vein, applying a flow of 6 mL/min. Subsequently, four cannulas were inserted through the decidual plate into the intervillous space, thereby resembling the maternal spiral arteries *in vivo*. A maternal flow rate of 12 mL/min was applied. By collecting the perfusion buffer flowing from the intervillous space back into the perfusion chamber, the maternal circulation was also reestablished. The perfusion medium consisted of Krebs-Henseleit buffer, supplemented with 11.1 mM glucose and 2500 IU/L heparin (LEO Pharma, The Netherlands). Albumin (Albuman®, Sanquin, The Netherlands) was added to the maternal and the fetal circulation (29 g/L and 34 g/L, respectively) (4). The medium was oxygenated with 95% O_2 and 5% CO_2, while being kept at 37 °C at a pH between 7.2 and 7.5. Initially, both circulations were left open for approximately 30 minutes to wash out residual blood. Thereafter, either the maternal or the fetal circulation was closed (200 mL), with the other circulation left open to maintain sink conditions. In this way, maternal-to-fetal (MTF) as well as fetal-to-maternal (FTM) transport of the compounds could be studied. Both reservoirs were sampled at regular intervals. Samples were analysed for test compounds via LC-MS/MS.

Elimination rate constants (ke) for compound disappearance were calculated by linear regression analysis of the ln-transformed compound concentration in the closed reservoir, taking into account the terminal phase of the curve. Bidirectional clearance values were determined using the following formula:

$$CL_{app\ cot} = ke * V$$

where CLapp cot represents the apparent intrinsic cotyledon clearance, ke is a placental elimination rate constant calculated from the slope of the Ln-transformed concentration-time profile, and V represents the volume of the buffer in the closed circulation (200 mL). A schematic representation of the placenta perfusion setup is shown in **Figure 9**. Calculated placental transfer clearance values are listed in tables x (acetamiprid) and x (tebuconazole).

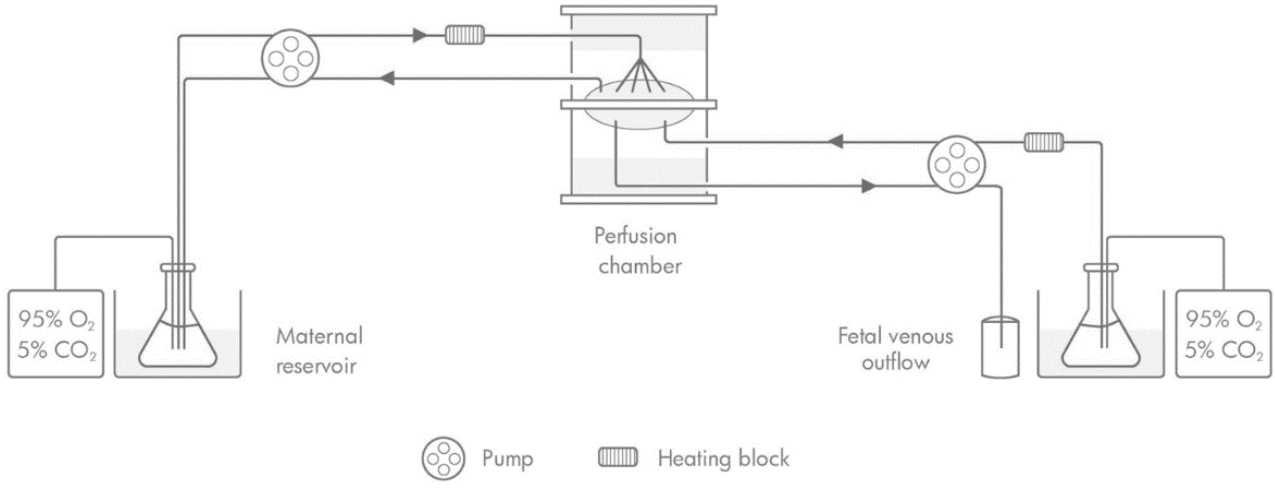

Figure 9. *Illustration of the ex vivo dual-side cotyledon perfusion model*

Four cannulas were inserted in the cotyledon positioned in the perfusion chamber. To study maternal-to-fetal transport of acetamiprid and tebuconazole, a closed maternal reservoir was established with an open fetal venous outflow to maintain sink conditions, as depicted. To study transport from the fetal to the maternal circulation, a closed fetal reservoir with an open maternal outflow was used.

2.3.3.2. Reverse dosimetry

A method to perform reverse dosimetry using the dedicated general population models was developed. Study participants were asked to collect a morning urine sample defined as the first morning void of the day (Silva et al., 2019). For the dose calculation we assumed that the urine micturition during the day occurred over a period of eight hours and that the parent and metabolite concentration in the morning void reflected exposure of the previous day (Goh et al., 2018). Thus, Δt (the time between previous and current void) was set to be 8 hours (= 480 minutes).

The PBK model was run 100 times taking a random distribution of doses between 10% above or under the ADI using bootstrapping. For each run, the cumulative excreted metabolite was determined at 8 hours exposure. A nocturnal urinary production rate of 0.99 ml/min was assumed to result in an estimated morning void volume of 475.2 mL. The cumulative excreted amount at t = 8h was divided by 475.2 mL to achieve the concentration excreted. For the parent this concentration is proportional to the administered dose, resulting in a linear relationship for the reverse dosimetry calculations:

$$Dose = urinary\ concentration * x + b$$

This equation was applied to the SPRINT biomonitoring data. Only samples >LOQ were used in the reverse dosimetry calculations, since concentrations reported <LOQ cannot be reliably quantified. It was assumed that the SPRINT participants were orally exposed 8 hours before the urine sample was taken. It was also assumed that the dose and urinary concentration overnight are linearly correlated.

3. Methods for animal PBK modelling

3.1. Substance selection for animals

Two sets of pesticides were selected for PBK modelling (**Table 11**). For the first set of pesticides the *in vitro* intrinsic clearance (CL_{int}) was determined using liver subcellular fractions (liver S9) for six species (cat, chicken, cow, pig, rat, and human). Some of the included pesticides were selected based on their (potential) nephrotoxicity (i.e. glyphosate and pyrimethanil) (Mazuryk et al. 2024; Seneff and Orlando., 2018; FAO/WHO, 2007) and *in vitro* toxicity testing for these substances was executed in WP4, simultaneously. These sets include pesticides used for plant protection as biocide and some substances that have been banned.

Table 11. Sets of pesticides included in PBK-modelling of animals and human**.**

	Cat	Chicken	Cow	Goat	Human*	Pig	Rat	Sheep
First set of pesticides								
Chlorpropham	x	x	x		x	x	x	
Chlorpyrifos	x	x	x		x	x	x	
Glyphosate	x	x	x		x	x	x	
Imidacloprid	x	x	x		x	x	x	
Piperonyl butoxide	x	x	x		x	x	x	
Prosulfocarb	x	x	x		x	x	x	
Pyrimethanil	x	x	x		x	x	x	
Tebuconazole	x	x	x		x	x	x	
Second set of pesticides								
Bromoxynil	x		x	x				x
Hexachlorobenzene		x						
Indoxacarb						x		
MCPA	x		x					x
Pendimethalin						x		
Pyretrhin II								x
Tri-allate	x							
2,4-D	x							

*A second set for human was absent in this table as human reverse dosimetry is included separately

Other pesticides in the first set were selected based on the frequent detection of their residues in food and feed. The second set of pesticides was included based on their occurrence in blood in at least three animals (based on data collected in SPRINT project) and were subsequently used for reverse dosimetry.

3.2. PBK modelling for animals

PBK modelling describes the absorption, distribution, metabolism and excretion (ADME) of chemicals. The aim was to use PBK modelling to calculate back from biomonitoring data to farm animal exposure to pesticides. Below an approach is described of applying a model generic to the pesticides but tailored to some of the relevant farm animal species. In this exercise human and rat were added for comparison.

3.2.1. Generic modelling for animals

PBK models were developed for human, chicken, cow, pig, goat, sheep, cat and rat. Berkeley Madonna software (UC, Berkeley, CA, USA version 10.2.8) was used for goat and sheep, applying the Rosenbrock-stiff model. For the other species, the PBK model was developed in R 4.3.3 using rtools43 and the packages rxode2, tidyverse and ggplot2. Despite the difference in software, the approach for generic PBK modelling was similar.

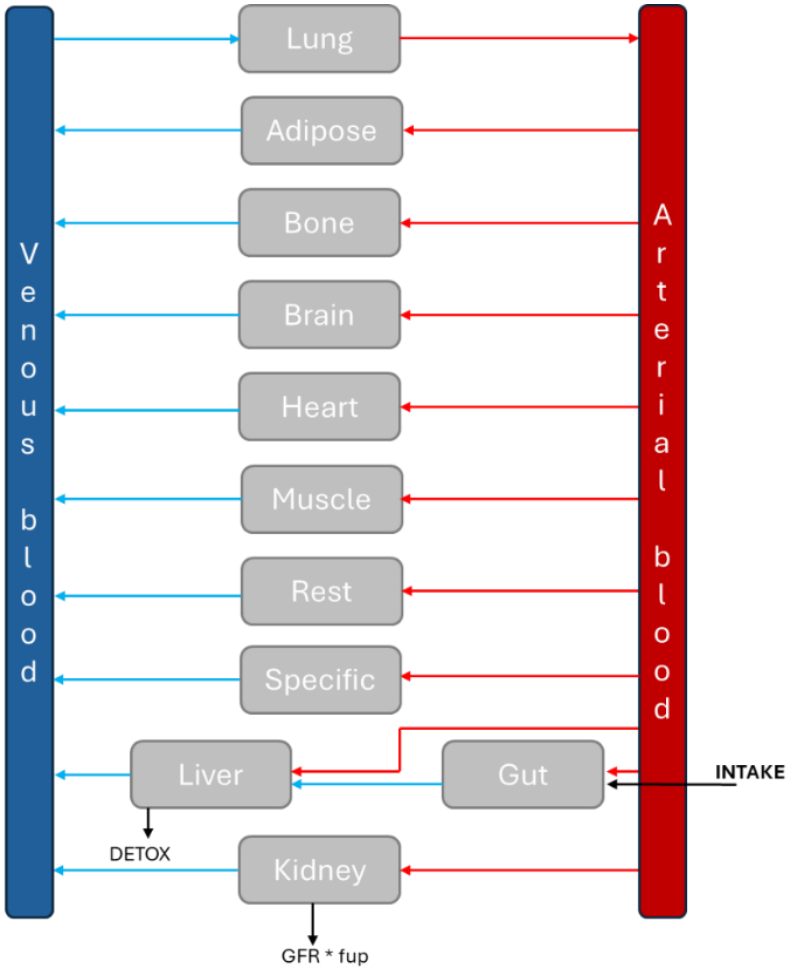

Figure 10. *Conceptual model used for the different species. The specific compartment refers to the mammary glands in dairy cows or the reproductive organs in chicken. Liver clearance (DETOX) and glomerular filtration (the glomerular filtration rate (GFR) multiplied with the free plasma concentration (concentration in plasma multiplied by fraction unbound in plasma (fup)) are incorporated in the model for each species.*

For chicken, cow, pig, human, cat and rat, the models consisted of separate compartments for lung, adipose tissue, bone, brain, heart, liver, gut, kidney and muscle, which was based on previous PBK models for these animals (Noorlander et al, 2024; Lautz et al., 2024). For cow and chicken, specific compartments were added that represent the mammary gland in cow and reproductive organs in chicken to simulate transfer to milk and eggs, respectively (**Figure 10**). Regarding goat and sheep, the

compartments adipose tissue, kidney, liver, gastrointestinal tract and muscle were included, as these were considered the most relevant organs for these species. For all species, the remaining organs and tissues were collated under a residual compartment (rest).

The parameters for tissue weight and tissue blood flow fractions were derived from literature (**Annex 3**). Partition coefficients and the fraction unbound in plasma were calculated using the web-based QIVIVE Tool according to Berezhkovskiy's method (Berezhkovskiy, 2004). Unless stated otherwise, a blood to plasma ratio of 1 was assumed. All substance-specific parameters per species are given in **Annex 4**.

In the PBK models described in this report, only an oral exposure route was included as it was assumed that exposure to pesticides occurred via feed. Other potential exposure routes, such as via inhalation and via skin, were not included, since these were expected to only contribute to a negligible amount (Lautz et al., 2022).

3.2.2. Model components

In contrast to the other species, no complete datasets with concentration/plasma values were obtained for goat and sheep in the current study. Therefore, these PBK models were evaluated using experimental data from so-called model components. A literature search was performed to select suitable model components, taking into account that both blood and urine concentrations over time were reported in the respective species (i.e., goat and/or sheep). For both species, veterinary drugs were selected as suitable components. For the goat model, demeclocycline was chosen using data reported in Jha et al. (1989, 2013). For the sheep model, probenecid was selected as model compound, based on data reported by Guerrini et al. 1985. From the graphs with experimental data (i.e., plasma and urine concentrations) of the model components, data points were extracted using WebPlotDigitizer (Automris) version 5 and transferred to Berkeley Madonna to recreate the graphs. After addition of all physiological and physicochemical parameters, the models were run.

3.2.3. Reverse dosimetry

Reverse dosimetry was performed in Berkeley Madonna (for goat and sheep) and R (for the other species) to predict the oral intake of the selected pesticides (Table 1). For both strategies, the maximum concentration (C_{max}) in plasma was used, as this reflects a worst-case scenario. After running the model in Berkeley Madonna 100 times, the results were transferred to Microsoft Excel. The predicted oral doses were plotted against the C_{max} in plasma using Microsoft Excel, under the assumption of linearity between dose and C_{max}, a slope and intercept were extracted. With regard to reverse dosimetry calculations in R, two arbitrary chosen doses (1 and 5 mg/kg BW) were used and the predicted C_{max} values were obtained and transferred to Microsoft Excel. Similar to Berkeley Madonna, linearity between dose and C_{max} was assumed, and a slope and intercept were extracted to calculate pesticide concentration in blood. The calculated concentrations were converted to a possible exposure dose in mg/kg BW.

Importantly, due to the lack of kinetic data (i.e., clearance data) for the selected pesticides, an estimation of the intrinsic hepatic clearance (CL_{int}) was made. To represent variation in a population of animals, two hepatic clearances were included, namely a "poor metabolizer" and an "extensive metabolizer". The simulation of a poor metabolizer (PM) was done by taking a "low" clearance (CL) value of 0.2 L/hr. The simulation of an

extensive metabolizer (EM) was performed by applying a clearance value resulting in a 40% lower C_{max} than a poor metabolizer Kirchheinder et al., 2004

3.3. Liver S9 metabolism studies

For the biotransformation of the pesticides of interest the hepatic metabolism was studied to derive the parameters that describe the enzymatic metabolism of the liver. Liver S9 fraction contains a mixture of cytosolic and microsomal enzymes expressing a wide range of enzyme activities for a variety of substrates. These in vitro assays are used to describe biokinetic parameters such as in this the intrinsic clearance. These kinetic parameters are needed to describe the clearance of the parent substance from the blood circulation by conversion to metabolites.

For some species (human, rat, chicken, cow, pig, cat) some kinetic parameters for liver metabolism were not available from the literature. Below it is described how this missing data was generated.

3.3.1. Chemicals and reagents

Chlorpropham, tebuconazole, imidacloprid, prosulfocarb, chlorpyrifos, adenosine 3'-phosphate 5'-phosphosulfate lithium salt hydrate (PAPS), uridine 5'-diphosphoglucuronic acid trisodium salt, (UDPGA), dimethyl sulfoxide (DMSO) Hybri-Max, potassium phosphate dibasic and ammonium formate were purchased from Sigma Aldrich (Zwijndrecht, The Netherlands). Piperonyl butoxide was purchased from Dr. Ehrenstorfer (Augsburg, Germany), and pyrimethanil from HPC standards (Borsdorf, Germany). Dihydronicotinamide-adenine dinucleotide phosphate (NADPH) was purchased from Roche (Mannheim, Germany). Potassium dihydrogen phosphate, magnesium chloride, and alamethicin were purchased from Merck Chemicals (Amsterdam, The Netherlands). Methanol Ultra LC-MS and formic acid LC-MS were purchased from Actu-All Chemicals (Oss, The Netherlands). Human and rat liver S9 fractions were purchased from Corning Life Sciences (Amsterdam, The Netherlands).

3.3.2. Preparation of liver S9 fraction

The preparation of liver S9 fraction has previously been described (Punt et al., 2021 and Lautz et al., 2022). Briefly, livers of the farm animals (chicken, cow, and pig) were collected at a slaughterhouse and livers of previously deceased feral cats were collected in the lab. For cow and pig, only a part of the liver was taken for the subsequent experiment. All collected livers were washed with ice-cold DPBS or Krebs buffer (pH 7.4) containing 10 mM HEPES, 25 mM sodium bicarbonate and 25 mM glucose, minced, snap-frozen in liquid nitrogen, and stored at −80°C. Preparation of the liver S9 homogenate started with homogenizing the livers in ice-cold Tris/KCl buffer (1.15% KCl in 50 mM Tris/HCl pH 7.4) in a pre-cooled stainless-steel blender at a ratio of 1 g liver tissue to 2 mL of buffer. The crude homogenate was centrifuged in a pre-cooled rotor for 25 min at 8,960 rcf at 4°C. Supernatant was collected and 500 µL aliquots were snap-frozen in liquid nitrogen and stored at −80°C. The protein concentration was determined using the Biorad DC Protein Assay (Biorad, Lunteren, The Netherlands) according to the manufacturer's protocol. Bovine Serum Albumin (BSA) (Sigma Aldrich, Zwijndrecht, The Netherlands) was used as the calibration standard.

3.3.3. In vitro metabolism assay

The *in vitro* metabolism studies were performed in 1.5 mL protein Eppendorf tubes at 37°C. The incubation mixture of 100 µL contained a final concentration of 1 µM of a pesticide compound (0.1% DMSO), 0.025 mg/mL alamethicin, 3 mM NADPH, 5 mM UDPGA, 0.2 mM PAPS, and an optimized concentration of liver S9 fraction (varying per

compound and species from 0.02 to 4 mg/mL) in KPI buffer (100 mM potassium phosphate buffer with 5 mM MgCl2 pH 7.4). After a pre-incubation of 5 minutes at 37°C reactions were started by addition of the cofactors. The reactions were stopped by adding 100 µL ice-cold methanol after 0, 5, 10, 15, 30, and 60 minutes of incubation. The samples were vortexed thoroughly and put on ice. For sample t = 0, first ice-cold methanol was added after the pre-incubation step prior to the addition of the cofactor mix. Two control conditions were included, namely: 1) an incubation in the absence of liver S9 and 2) an incubation in the absence of cofactors. The samples were stored at −20°C.

3.3.4. LC-MS/MS analysis

Samples were thawed, mixed thoroughly, and centrifuged for 10 min at 14,000 rpm at room temperature. The supernatants were transferred to LC/MS vials and analysed on a Waters Acquity UPLC Class system coupled to a triple quadrupole mass spectrometer (Xevo TQ-S) equipped with an autosampler set at 10°C. Compounds were chromatographically separated on a Waters Acquity C18 UPLC column (Acquity UPLC HSS C18 1.8 µm column, 2.1 × 100 mm, Waters, Etten-Leur, The Netherlands) set at a temperature of 60°C by gradient elution altering the mobile phase (gradient: 0.00–3.00 min 100% A, 3.00–6.00 min 50:50% A:B, 6.00–8.30 min 100% B, 8.30–11.00 min 100% A). The mobile phase consisted of water (A) and 90% methanol + 10% water (B) both containing 0.1% (v/v) formic acid and 1 mM ammonium formate. The mass spectrophotometer was equipped with an electrospray ionization interface (ESI). The ESI was operated in positive mode (ESI+) with a capillary voltage of 3 kV, a desolvation gas temperature of 400°C, and a source temperature of 150°C. The injection was set for 10 minutes at a flow rate of 0.4 mL/min. MassLynx software (version 4.1) was used to record and analyse the peaks and data were acquired in MRM mode (**Annex 5**).

3.3.5. Calculating the intrinsic clearance (CLint)

The intrinsic clearance (CL_{int}) values were determined by plotting the substrate concentrations' natural logarithm (ln) against the incubation time. The slope of the linear part of these ln-transformed substrate depletion curves represents the elimination rate constants (k, min-1). The half-life of each compound was calculated by $t_{1/2}$ (min) = ln(2)/k (min^{-1}) and the incubation volume by V (µL/mg) = 1000 / [liver S9] (mg/mL). After calculation of the half-life and volume of incubation, the intrinsic clearance can be calculated as follows (Equation (1):

$$Cl_{int}\ (\mu l/min/mg\ S9\ protein = \left(\frac{Ln(2)}{t_{\frac{1}{2}}}\right) \times Volume\ (\mu L/mg\ S9\ protein)$$

The *in vitro* kinetic parameters for the metabolism of the present study are scaled to *in vivo* situations using an S9 protein yield (S9PL) of 140 mg/g liver (Musther et al. 2017). No species differences are assumed to occur in the partition coefficient, fraction unbound and S9PL.

3.3.6. Comparison of predicted oral intake and estimated pesticide concentration in feed

The reverse dosimetry-based predicted oral intake of the selected pesticides was used to assess if there were indications for exceedance of maximum residue levels (MRL) based on human biomonitoring data from the SPRINT field study. First, feed intake per species was calculated based on three assumptions:

1) Pesticide exposure was only calculated for concentrate feeds, thereby neglecting the potential presence of pesticides in roughage (i.e., pasture, hay and silage,

which include a considerable part of the diet of cow, goat and sheep) and other types of feed.

2) Commercially available concentrate feed (www.welkoop.nl) for chicken, cow, goat, pig and sheep was used as example representing the composition, and thus intake of specific ingredients. As the exact composition of the ingredients was not provided, an estimation was made based on Table 4 of the EFSA Scientific Report on animal dietary exposure (EFSA, 2019) giving examples of feed ingredients as percentages of animal diets.
3) The maximum recommended intake of concentrate feed was applied, and the MRLs of pesticides per food ingredient (EU Pesticides Database) were used to calculate the total concentration of individual pesticides. Thus, we assumed that the substance was present in feed at MRL, which can be considered as worst-case scenario.

Next, the total concentration of the individual pesticides was calculated by taking the sum of the concentrations calculated per ingredient. These total pesticide concentrations were compared to the predicted exposures (as determined by reverse dosimetry in Section 3.1.3) for both poor and extensive metabolizers (i.e., PM and EM).

4. Results Human PBK modelling

The construction of PBK models and their applications to pesticides will be discussed for humans and farm animals separately. The results of generic and dedicated PBK models will be presented. For the dedicated models the results of human volunteer studies as unique new data will be described. We also describe the role of human placenta study to support prediction of placenta transfer in the pregnant female to the unborn child.

4.1. Generic PBK modelling

The highest measured plasma concentration for chlorpyrifos from the SPRINT biomonitoring campaign was 0.05 ng/mL. The httk application accepts inputs as µM. The concentration in plasma is equal to 0.1426 µM. After running the steps described earlier, an intake of 0.0008896 mg/kg bw/day calculated dose at as plasma concentration of 0.05 ng/mL corresponding to the 95th percentile of the highest exposed individuals in the SPRINT dataset. This is 8.9 % of the ADI of 0.01 mg/kg btw.

4.2. Substance specific PBK modelling

For parameterisation of the the PBK models dedicated to the priority substances acetamiprid, glyphosate and tebuconazole, the results of the human volunteer studies are presented below.

4.2.1. Acetamiprid

4.2.1.1. Oral

Both acetamiprid and acetamiprid-N-desmethyl were found in plasma after oral exposure (**Figure 11**). A rapid absorption of acetamiprid was observed following ingestion. The measured concentrations of acetamiprid varied between 0 and 17.9 ng/mL, with an average Cmax of 15.2 ± 1.3 ng/mL. Acetamiprid-N-desmethyl ranged from 0 to 23.8 ng/mL concentrations, with an average Cmax of 21.3 ± 1.1 ng/mL (oral) and 1.08 ± 1.3 ng/mL (dermal). On average, the concentrations of the metabolite were higher in blood plasma compared to the parent compound. The mean Tmax was 0.820 ± 1.7 hours for acetamiprid and 7.80 ± 1.2 hours for acetamiprid-N-desmethyl. Urine was found to be the main route of excretion for acetamiprid-N-desmethyl (**Figure 12**).

On average, participants collected 8 urine samples during the first 24 hours after exposure. After oral exposure, the average peak excretion time was 2.91 ± 2.9 h for the parent and 12.0 ± 2.1 h for the metabolite. The estimated urinary half-life was (GM± GSD): 3.80 ± 2.6 h for the parent and 29.9 ± 1.3 h for the metabolite. After 24 hours, on average 0.420 ± 3.6 % of the parent was excreted in the urine, and 14.4 ± 1.7 % of the administered dose was excreted as the metabolite. The cumulative urinary excretion of acetamiprid-N-desmethyl for all participants during the first 24 hours after exposure is shown in Figure 8. Furthermore, the estimated cumulative urinary excretion of the parent after 96 hours was 74.5 ± 1.3 %. Conversion factors were calculated based on the UER and amounted to a molar ratio of metabolite to parent of 7 (check/compare with Wrobel et al 2023a).

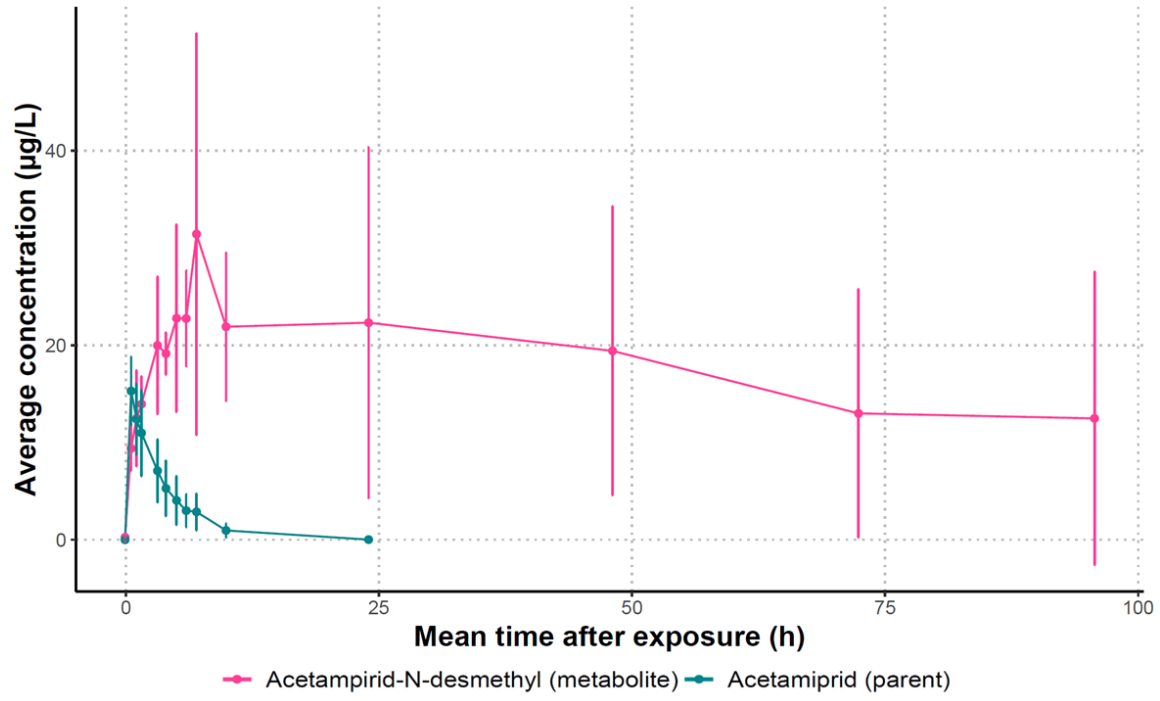

Figure 11. *Concentration time pattern of acetamiprid and its primary metabolite acetamiprid-desmethyl in plasma.*

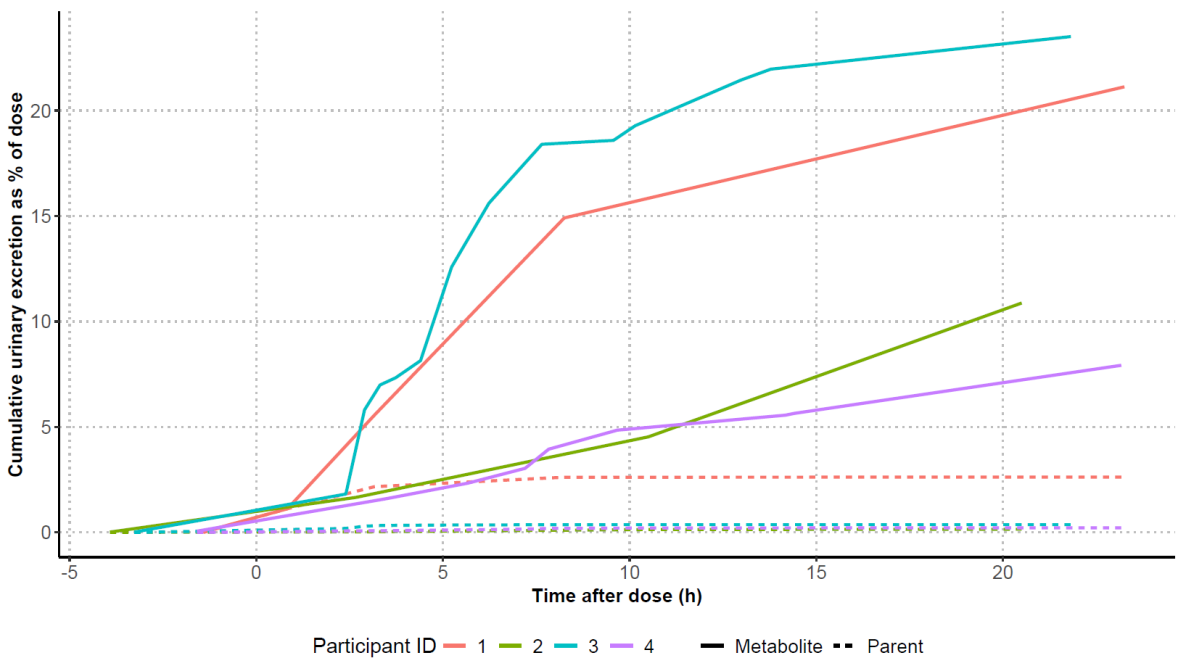

Figure 12. *Concentration time pattern of acetamiprid (dotted) and the metabolite acetamiprid-N-desmethyl (solid) presented as cumulative urinary excretion expressed as % of administered dose. Participants 1-3 are male, participant 4 is female.*

Overall, low fecal excretion was observed. The maximum concentrations measured over all voids were 9.17 and 12.72 µg/kg for the parent and metabolite, respectively. After

approx 96 h, 0.0350 ± 6.0 % of the administered dose of acetamiprid was excreted. For acetamiprid-N-desmethyl, this was 1.02 ± 1.2 % (**Figure 13**).

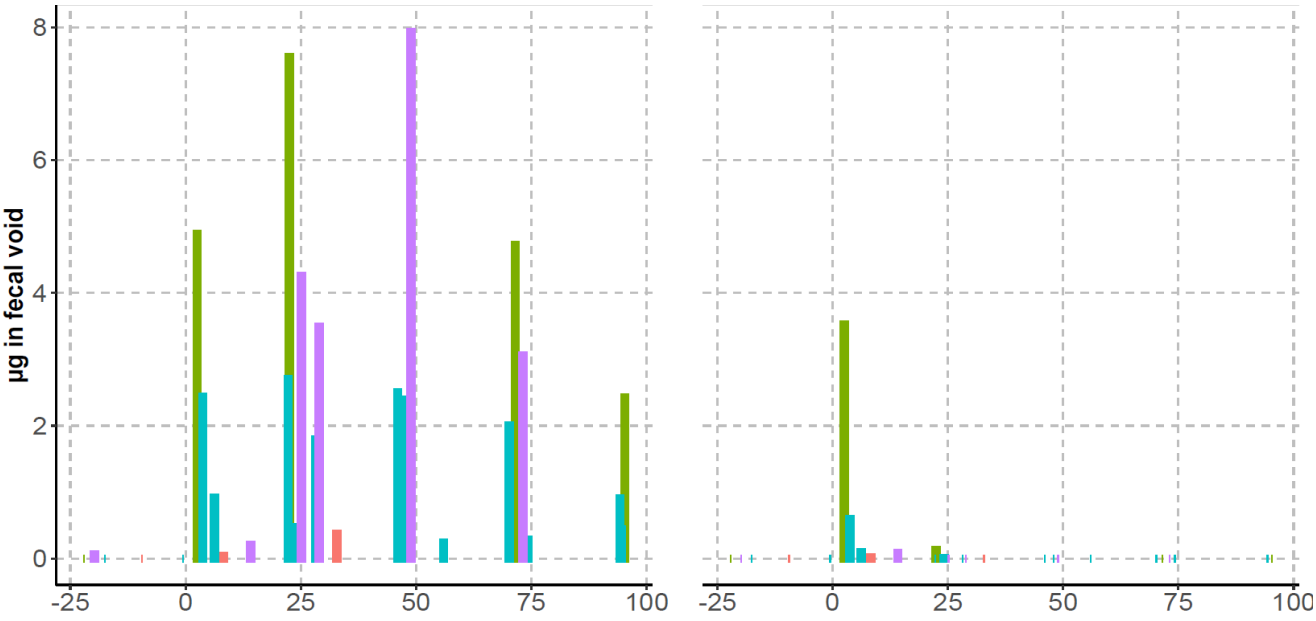

Figure 13. *Fecal excretion of acetamiprid-N-desmethyl (left panel) and acetamiprid (right panel) in µg/void following ingestion. Colors correspond to individual study participants (see Fig. 10).*

4.2.2.2. Skin

According to protocol the skin exposure as done 7 days after the oral administrations assuming a completed washout in one week. Due to unexpected very slow urinary excretion of acetamiprid-N-desmethyl the pre-exposure concentration was not yet at back baseline and may have influenced the interpretation of the dermal absorption findings for the metabolite (**Figures 14 and 15**).

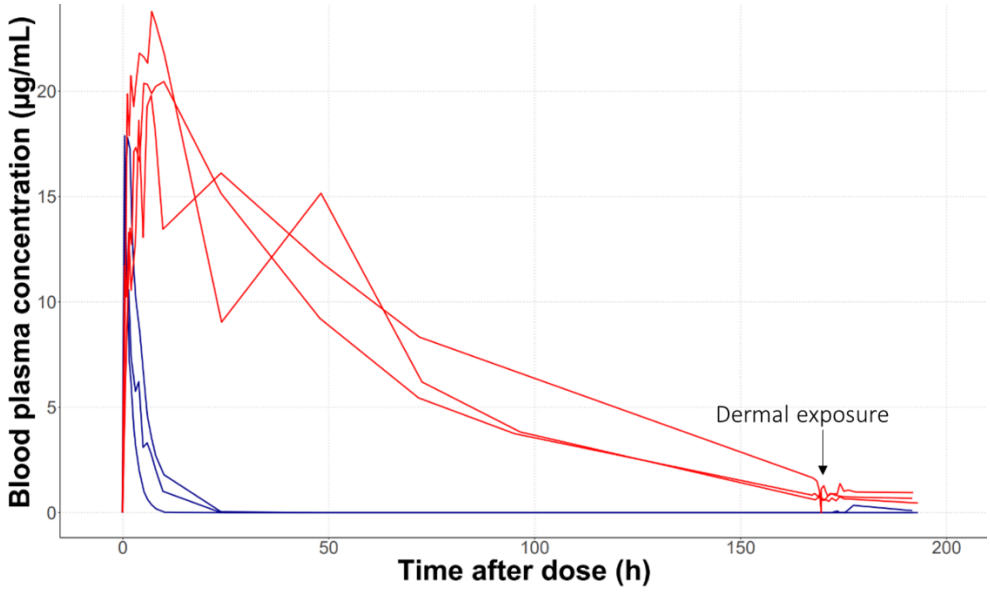

Figure 14. *Concentration time pattern for acetamiprid (blue lines) and acetamiprid-N-desmethyl (red lines). Following start of oral administration (t=0) and start of dermal exposure (t=168 h).*

After dermal exposure, no acetamiprid was detected in any of the urine samples as parent compound. Acetamiprid-N-desmethyl was found, but the concentrations much compared to the oral exposure scenario (Figure 10).

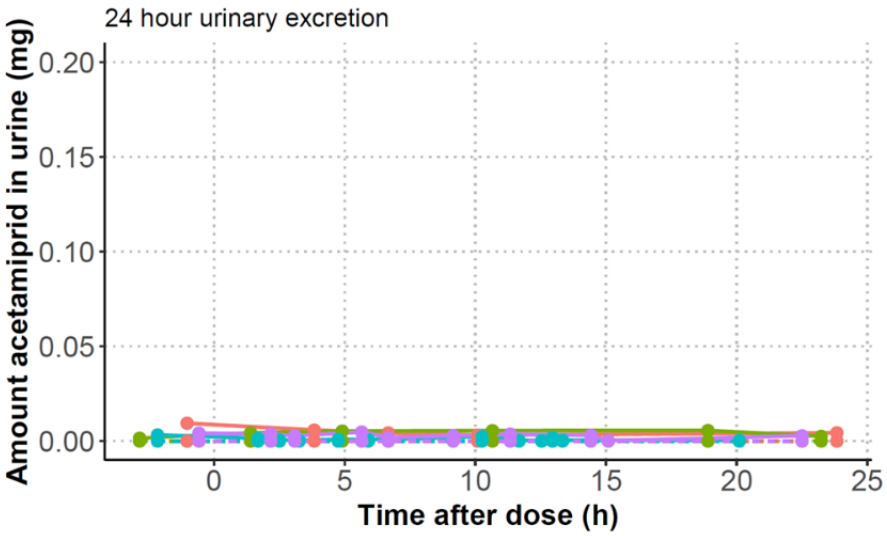

Figure 15. *Concentration time pattern for urinary excretion of acetamiprid in individual study participants (see Fig. 8 for legend).*

After dermal exposure, the concentration of parent and metabolite in feces remained very low compared with oral exposure (**Figure 16**). Also here we cannot rule out a contribution from the oral exposure of one week earlier.

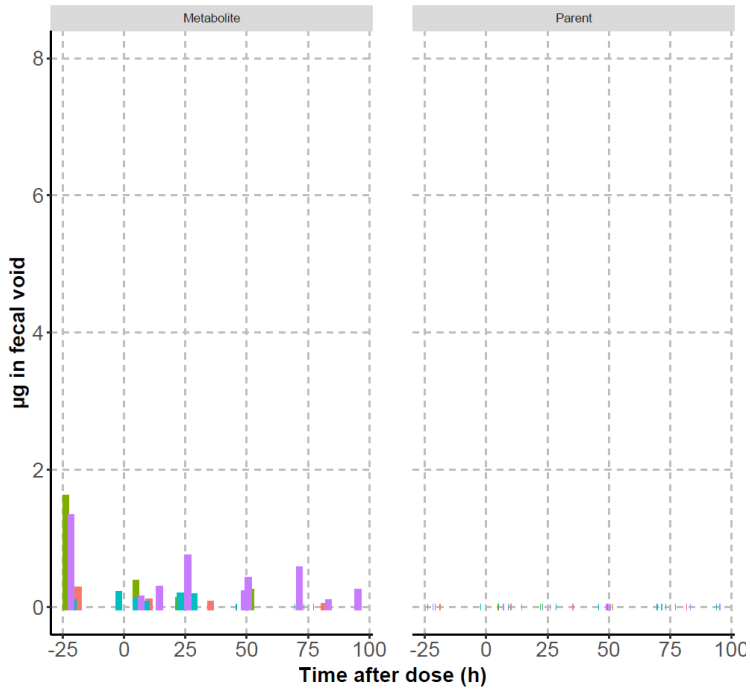

Figure 16. *Concentration time pattern for fecal excretion of acetamiprid in individual study participants (see Fig. 11 for legend).*

4.2.2. Glyphosate

4.2.2.1. Oral

Below in **Figure 17** the cumulative urinary excretion glyphosate is shown following oral exposure. The data for the concentration time pattern of glyphoste in blood is not yet available.

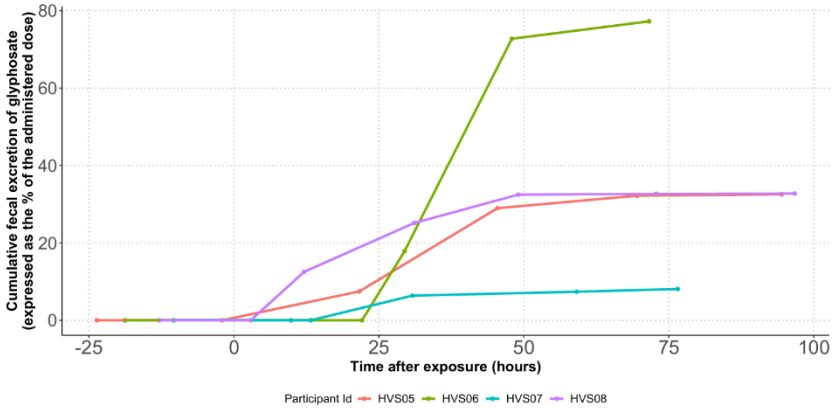

Figure 17. *Concentration time pattern of glyphosate presented as cumulative urinary excretion expressed as % of administered dose.*

4.2.2.2. Skin

After skin exposure we did not observe detectable levels of glyphosate in urine and therefore no graphs are shown here.

4.2.3. Tebuconazole

Tebuconazole is a mixture of isomers that has been tested as such in toxicity assays. Six healthy volunteers (three males and three females) received on separate occasions a single oral dose of 1.5 mg of TEB and a single dermal dose of 2.5 mg during 1 h. In addition to a pre-exposure urine sample, complete urine voids were collected over 48 h post-administration. The main metabolite 5-hydroxytebuconazole was quantified in each urine sample.

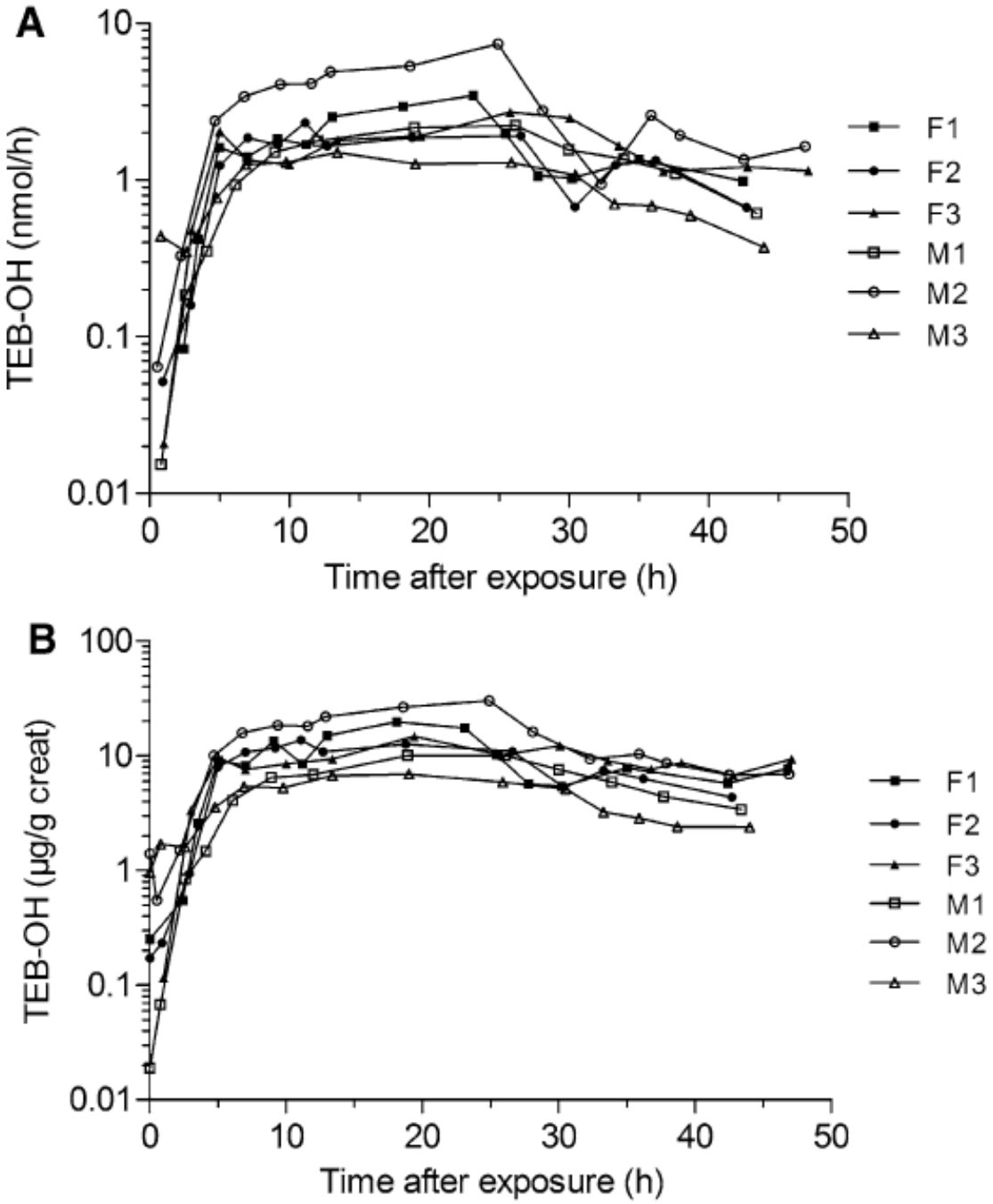

Figure 18. *Time course of the urinary excretion of TEB-OH after dermal administration in six human volunteers on a semi-logarithmic scale:* ***A*** *represents the excretion rate in nmol/h,* ***B*** *shows the creatinine corrected TEB-OH concentrations in µg/g creatinine (Oerlemans et al., 2019).*

Peak excretion rates after oral and dermal administration were reached after 1.4 and 21 h (**Figure 18**), mean elimination half-lives were 7.8 and 16 h, and recoveries within 48 h were 38% and 1%, respectively (**Figure 19**). The time courses of excretion were compared to simulations with an existing PBK model by Jónsdóttiret and co-workers (2016) that was extended with a parallel model for 5-hydroxytebuconazole. Overall, this metabolite was rapidly excreted into urine after oral exposure, and elimination was much slower after dermal exposure. Urinary time courses between individuals were similar. The PBK model predictions were in good agreement with the observed time courses of excretion. Due to time constraints, the data from another human volunteer study was used to validate the urinary excretion curves in Berkeley-Madonna. Data was extracted from the appendix of Oerlemans (2019) and cumulative excretion was calculated. The data from the model was fit to this excretion pattern.

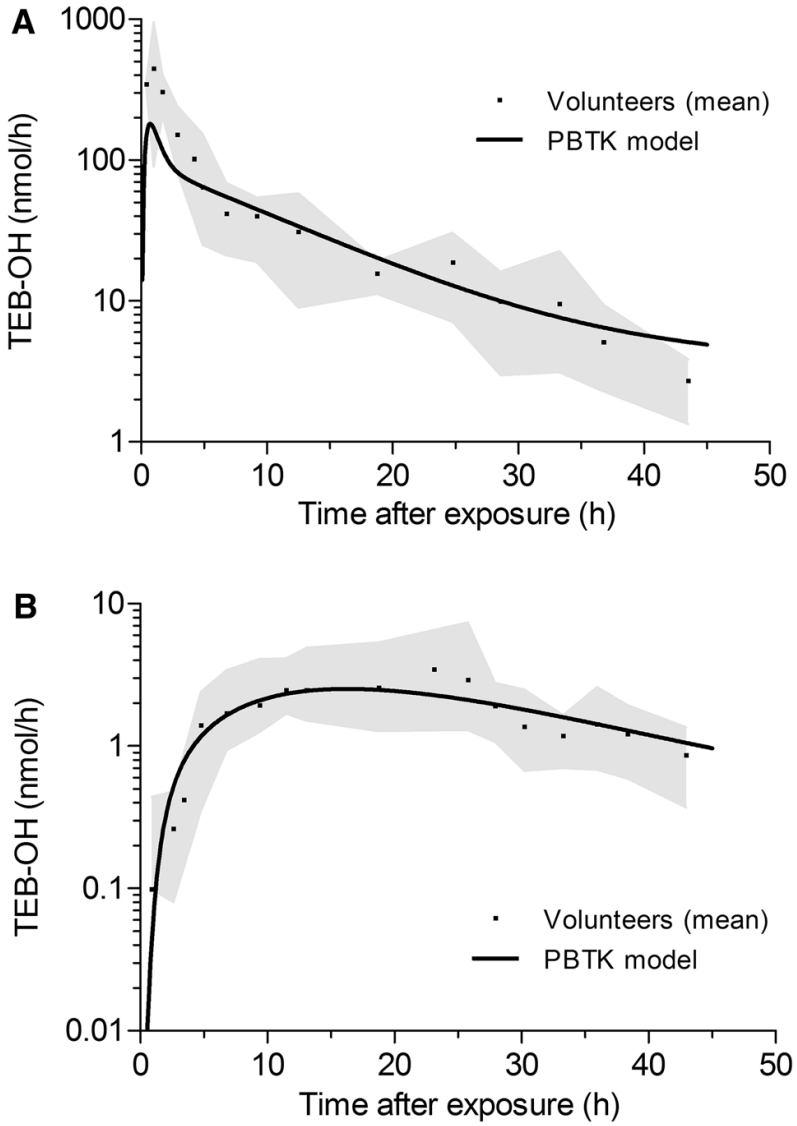

Figure 19. *Comparison of the mean time course of the urinary excretion rate of TEB-OH after oral (**A**) and dermal (**B**) administration in six human volunteers (dots) versus the simulated excretion rate using the adjusted PBK model (line). The grey area represents the range of the observed values in the volunteers; outliers were excluded in these figures (Oerlemans et al., 2019).*

4.3. Results of ex vivo placenta perfusion study

Ex vivo placenta perfusions studies indicate that both acetamiprid and tebuconazole are expected to traverse the placenta in both the maternal-to-fetal, as well as the fetal-to-maternal direction (see **Figure 20-23**).

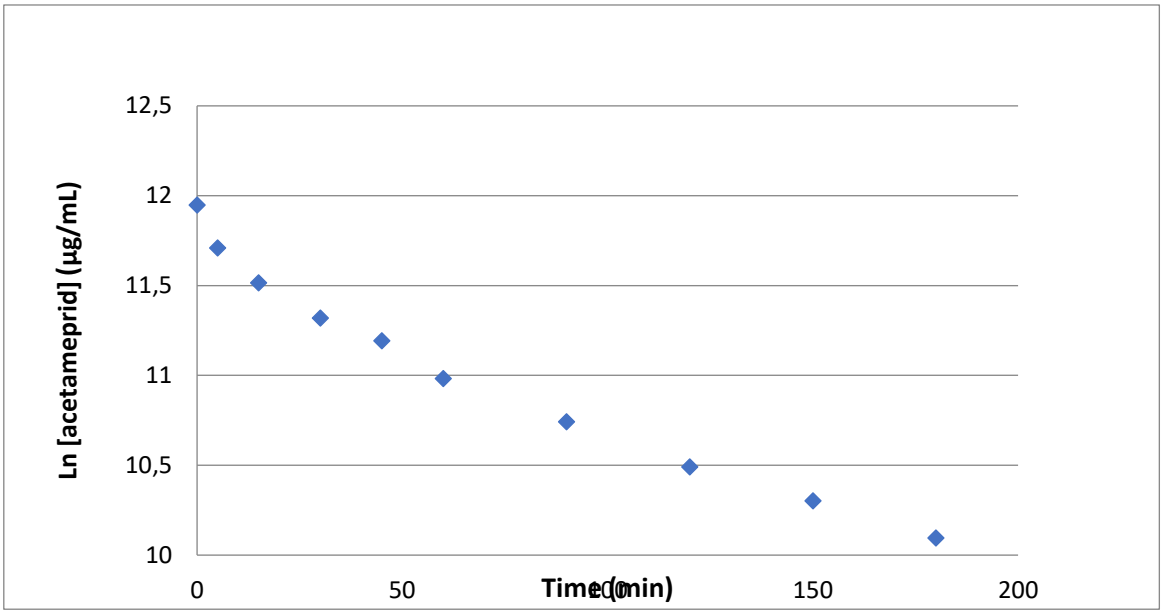

Figure 20. *Ex vivo maternal-to-fetal transfer of acetamiprid in human placenta tissue. Data represents the declining concentrations in the recirculating maternal donor compartment.*

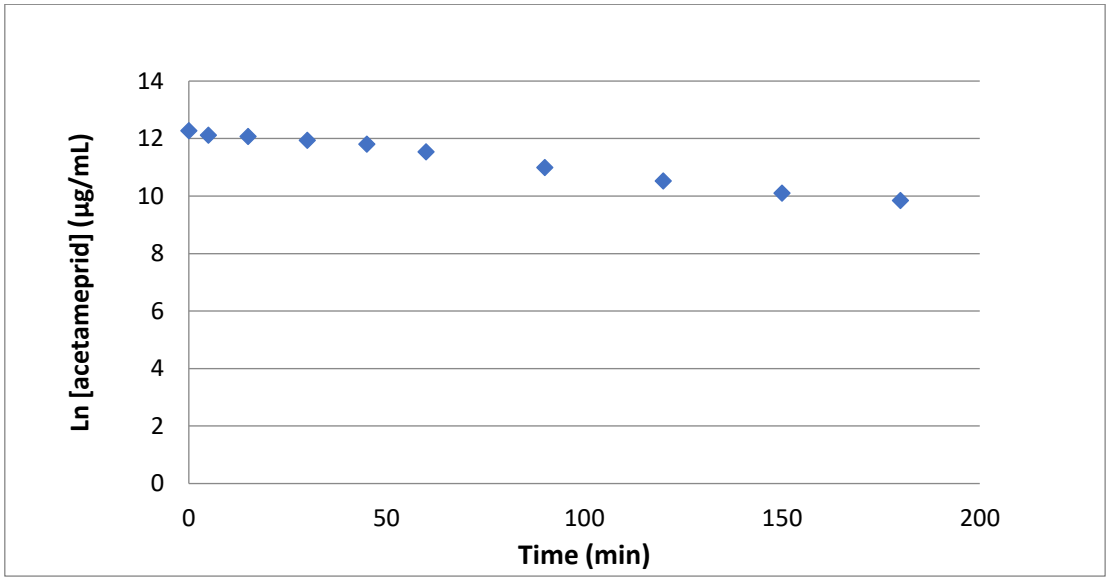

Figure 21. *Ex vivo fetal-to-maternal transfer of acetamiprid in human term placenta tissue. Data represents the declining concentrations in the recirculating fetal donor compartment.*

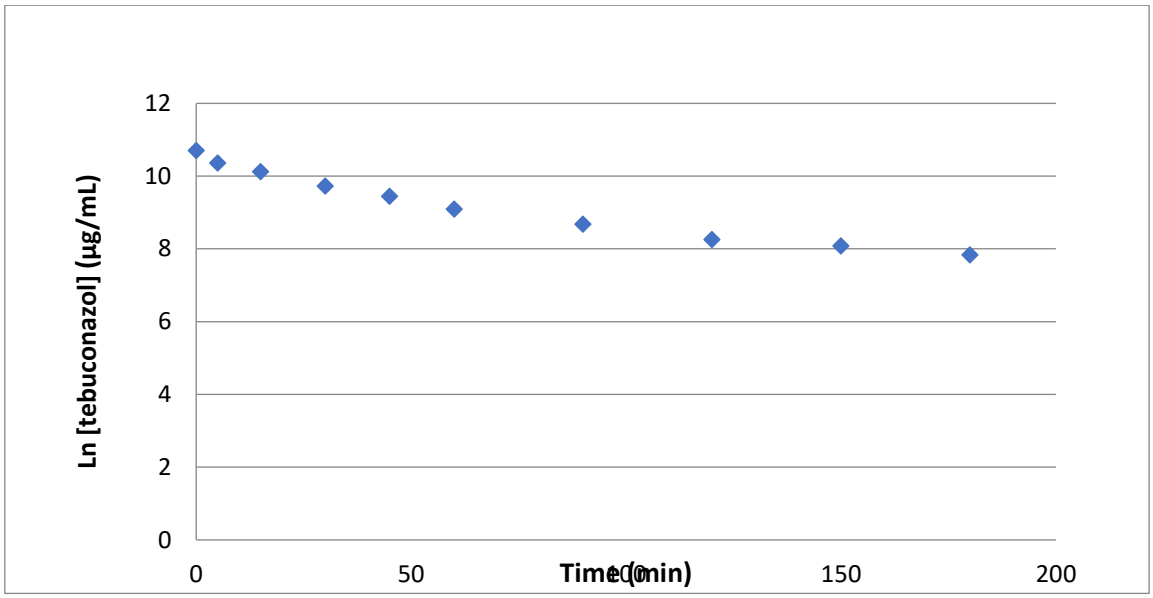

Figure 22. *Ex vivo maternal-to-fetal transfer of tebuconazole in human term placenta tissue. Data represents the declining concentrations in the recirculating maternal donor compartment.*

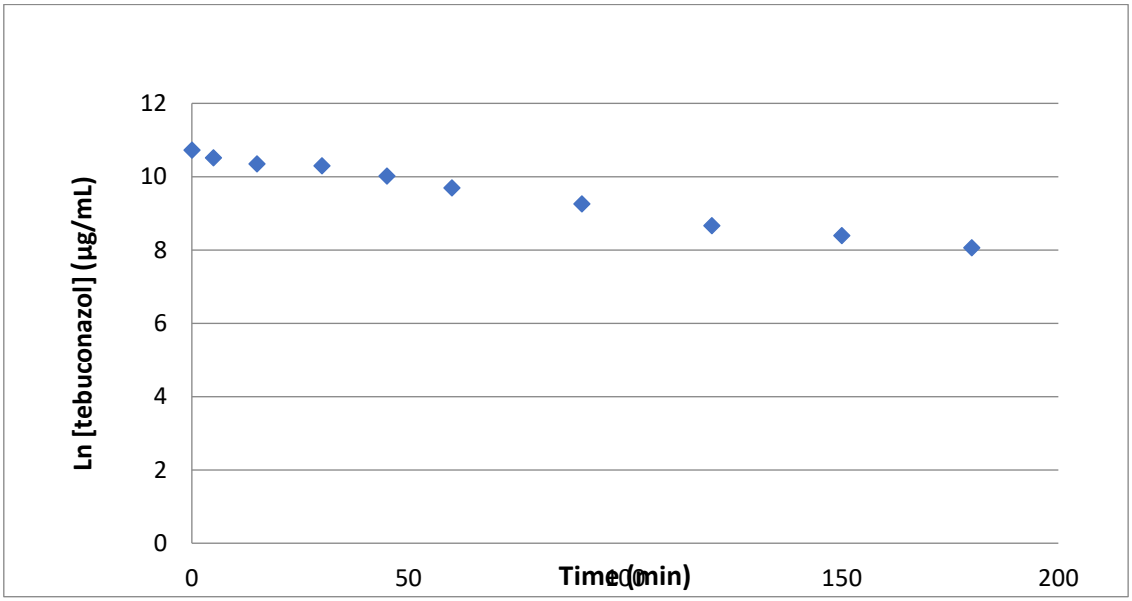

Figure 23. *Ex vivo fetal-to-maternal transfer of tebuconazole in human term placenta tissue. Data represents the declining concentrations in the recirculating fetal donor compartment.*

Next, PBK simulations were conducted to first assess maternal internal exposure. Clearance values and metabolism for tebuconazole were taken from Oerlemans et al. (2019). As shown in **Figure 24**, the maternal venous plasma seems to flatten. This could be related to a relatively slow conversion and saturable metabolism of parent to metabolite in combination with a slow excretion rate, causing the curve to flatten. Compared with acetamiprid, which has an extensive metabolism causing rapid excretion from the maternal venous blood within 400 minutes after oral exposure.

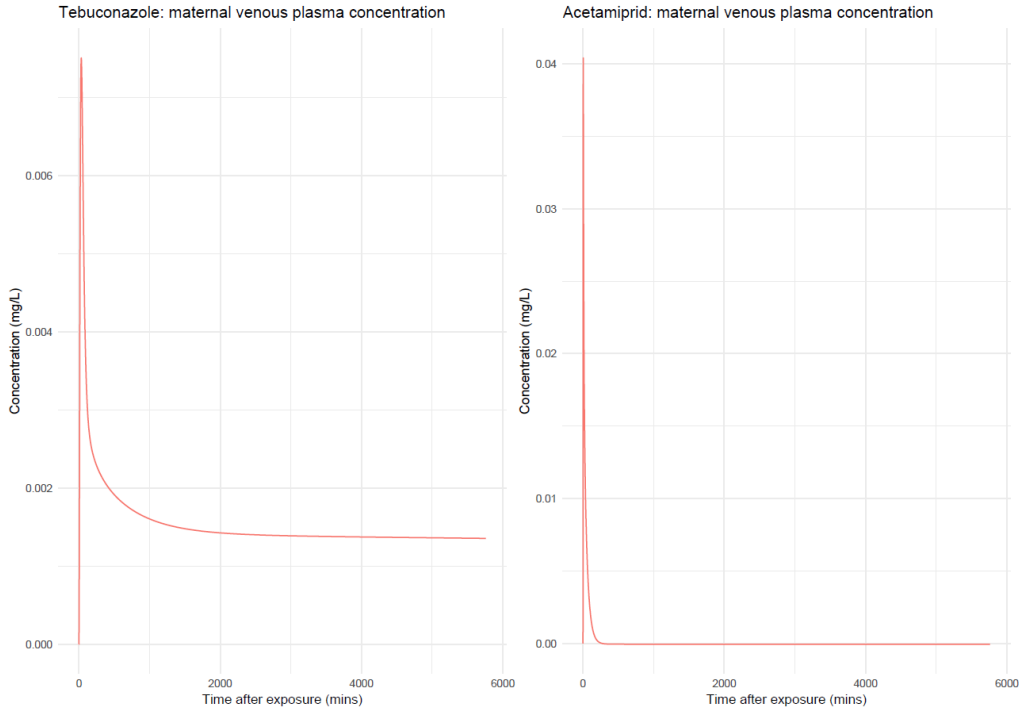

Figure 24. *Maternal concentration time pattern.*

Next, placental transfer clearance values were calculated from the placenta perfusion data and combined with the maternal models. In **Figure 25**, the predicted fetal exposure for acetamiprid is shown, to illustrate the principle of the approach (at the time of writing of the report, modeling for tebuconazole is being finalized). Based on placental transfer data in combination with PBK modeling, it is expected that acetamiprid concentrations in fetal blood follow the same pattern as in maternal blood, with a fast clearance after reaching maximum plasma concentrations. Likely there will be some partitioning into fetal tissues, but little transfer to amniotic fluid is to be expected.

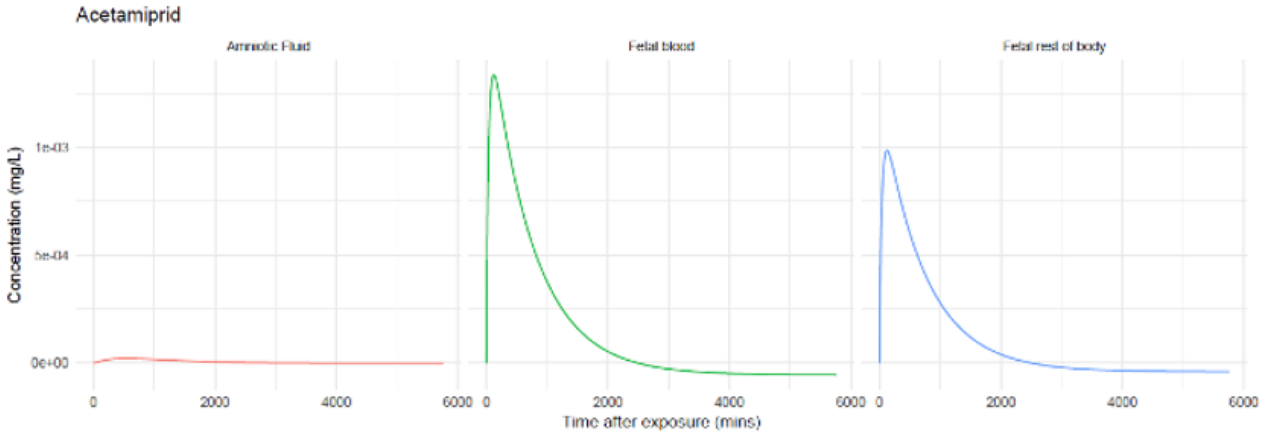

Figure 25. *Fetal concentration-time pattern after exposure of the mother during 3rd trimester pregnancy at 90% of the ADI for 5 days after (oral) exposure for acetamiprid. Concentrations are shown in mg/L for the amniotic fluid, fetal blood plasma, and rest of fetal body.*

4.4. Reverse dosimetry of Human HBM data

4.4.2. Reverse dosimetry using dedicated models

In **Figure 26a** the results of the reverse dosimetry calculations for acetamiprid, glyphosate and tebuconazole are presented. For this calculation it was assumed that all urinary excretion was derived from ingestion for comparison to the ADI of each substance. The uptake is expressed in mg/kg/d, where the bodyweight in kg was assumed to be 70 kg for all participants. The expression of the uptake allows direct comparison with the ADI for each of the substances. Note that the ADI for acetamiprid was reduced from 0.025 to 0.005 mg/kg/d recently. For all substances in all groups the back-calculated median values are below the ADI by a margin of 3-4 orders of magnitude. Expressed as % of the ADI the P5, median and P95 for acetamiprid were 0.004%, 0.03% and 0.36%, resp. For the new ADI of acetamiprid these values were 0.02%, 0.16% and 1.8%. For glyphosate these values were 0.02%, 0.06% and 0.32% and for tebuconazole the values were 0.001%, 0.03% and 0.6%. The acceptable operator exposure level (AOEL) for glyphosate is 0.1 mg/m^3. The back-calculated uptake corresponds to 0.1% of AOEL for the P5, 0.3% for the P50 and 1.6% for the P95 (EFSA, 2021).

Figure 26b shows the same data on a smaller scale (not including the ADI. The estimated uptake is very similar across subgroups consumer, farmer and neighbour. For acetamiprid the farmers have elevated values. For glyphosate and tebuconazole the consumers have somewhat higher values compared to farmers and neighbours. The numbers can be found in **Table 12** and indicate that the number of study participants with estimated uptake above P95 is 2 for acetamiprid, 14 for glyphosate and 0 for tebuconazole. Expressed as percentage of exceedance of P95 of the distribution is 3.9% for acetamiprid, 5 % for glyphosate and 0% for tebuconazole.

In **Figure 27** the estimated uptake shows the same data but disaggregated by the labels 'conventional' and 'organic'. For study participants for which this was not known label 'unknown' was assigned. With this subdivision the differences between groups are more pronounced. For acetamiprid in consumers in the Netherlands and Portugal who reported to consume organic food show a wide variation, suggesting that a substantial number of consumers of organic products have much higher estimated uptake by ingestion compared to conventional consumer and consumers that could not be assigned to either group. For farmers and neighbours there is also a tendency for conventional to be higher than organic (farmers) or organic and unknown (neighbours). For glyphosate the differences within the sub-groups farmers, consumers and neighbours are less pronounced. Within consumer and farmers levels were very similar by conventional/organic/unknown diet assignment. For neighbours the category labelled as 'unknown' has more higher values. For tebuconazole the differences across consumers, farmers and neighbours and according to the dietary label 'conventional, 'organic' and unassigned are the most similar.

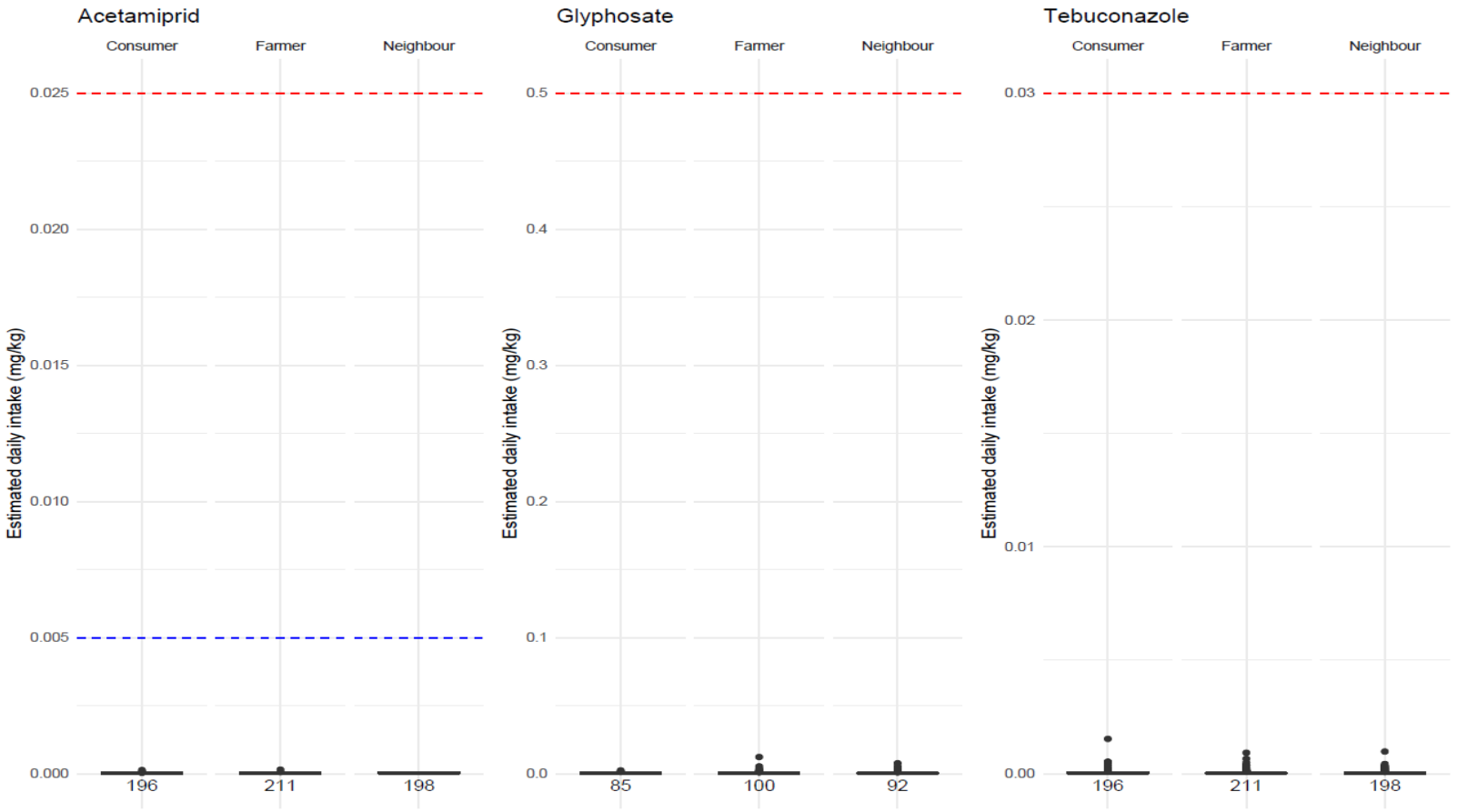

Figure 26a. *Estimated daily intake of acetamiprid, glyphosate and tebuconazole in mg/kg bw disaggregated by subgroup consumer, farmer and neighbour, back-calculated from urinary excretion of glyphosate, acetamiprid-N-desmethyl and 5-hydroxy-tebuconazole. An average body weight of 70 kg was assumed. The red dotted line indicates the current ADI for each pesticide. The blue dotted line represents the proposed ADI for acetamiprid (EFSA, 2024). The number of study participants with 5-hydroxy-tebuconazole excretion > LOQ is provided on X. Disaggregation of the farmers by conventional, organic and unknown status is provided in* ***Figure 27****.*

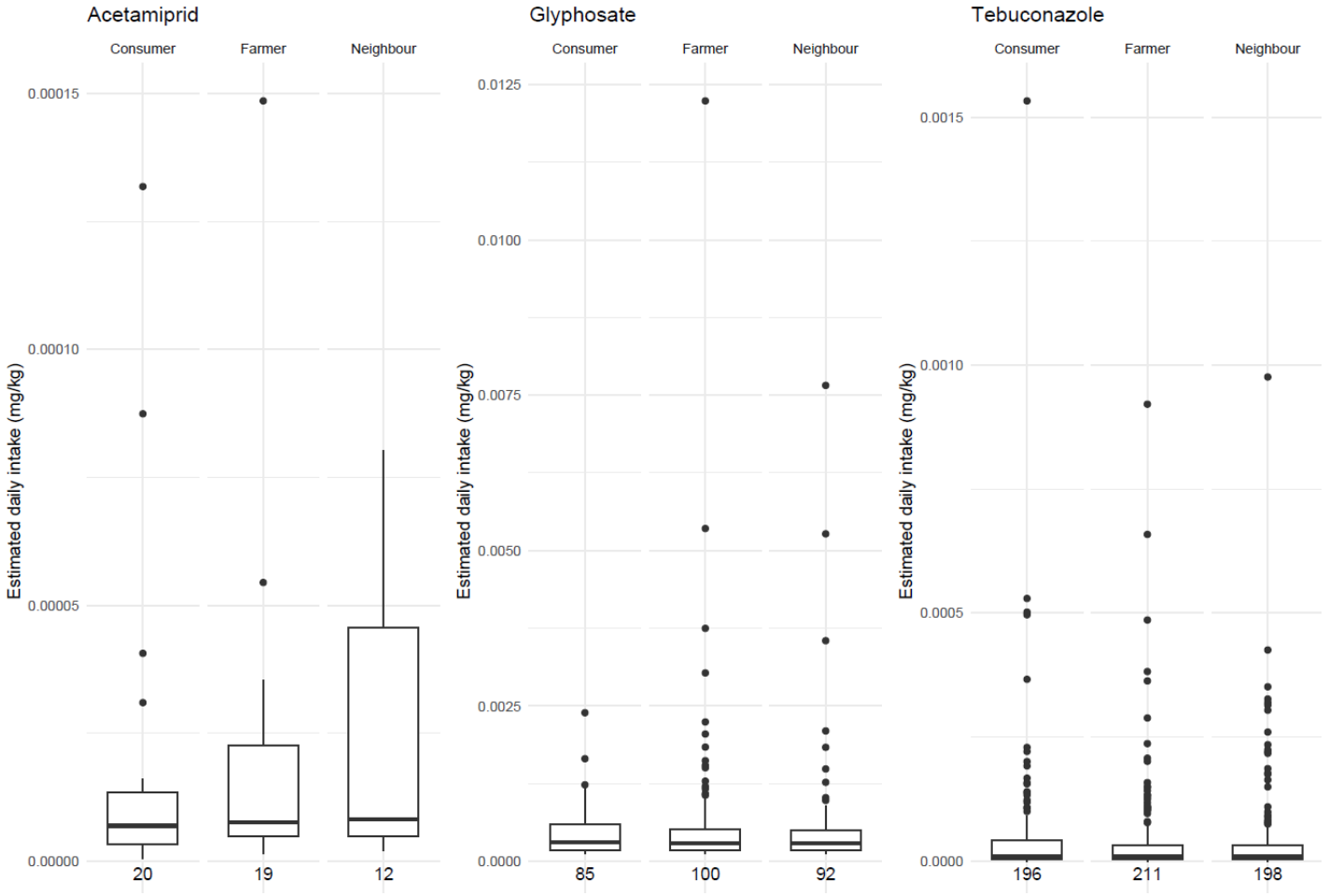

Figure 26b. *Estimated daily intake of acetamiprid, glyphosate and tebuconazole in mg/kg bw disaggregated by subgroup consumer, farmer and neighbour, back-calculated from urinary excretion of glyphosate, acetamiprid-N-desmethyl and 5-hydroxy-tebuconazole. An average body weight of 70 kg was assumed. The red dotted line indicates the current ADI for each pesticide. The number of study participants with desmethyl-N-acetamiprid excretion >LOQ is provided on X. Disaggregation of the farmers by conventional, organic and unknown status is provided in* ***Figure 27****.*

Table 12. ADI and descriptive statistics for uptake estimates back-calculated from urinary excretion parent or metabolite from prioritised pesticides.

Substance	Used HBM-data (urine)	ADI (mg/kg/d)	Back calculated from urine (mg/kg/d)				
			P5 (%ADI)	P50 (%ADI)	P95 (%ADI)	N > P95	% > P95
Acetamiprid[a]	Acetaimiprid-N-desmethyl	0.025[b] 0.005	0.000001 (0,004%) (0.020%)	0.000008 (0.03) (0.16%)	0.00009 (0.36%) (1.8%)	2	3.9
Glyphosate	Glyphosate	0.5[c]	0.0001 (0.020%)	0.0003 (0.06%)	0.0016 (0.32%)	14	5.0
Tebebuconazole	5-hydroxy-Tebuconazole	0.03	0.0000003 (0.001%)	0.0000098 (0.03%)	0.00018 (0.60%)	0	0

P5 is the 5th percentile; P50 is the 50th percentile or median; P95 is the 95th percentile; N > P95 is the number of study participants with urinary excreted metabolite levels higher than the P95 for the entire group. % > P95 is the number of study participants with urinary excreted metabolite levels higher than the P95 for the entire group. [a]Based on available acetamiprid-N-desmethyl data from NL and PT (in other countries this was not reported due to interference in the analysis); [b]The proposed new ADI for acetamiprid is 0.005 (EFSA, 2024). [c]The back-calculated uptake corresponds to 0.1% of the AOEL of glyphosate for the P5, 0.3% for the P50 and 1.6% for the P95.

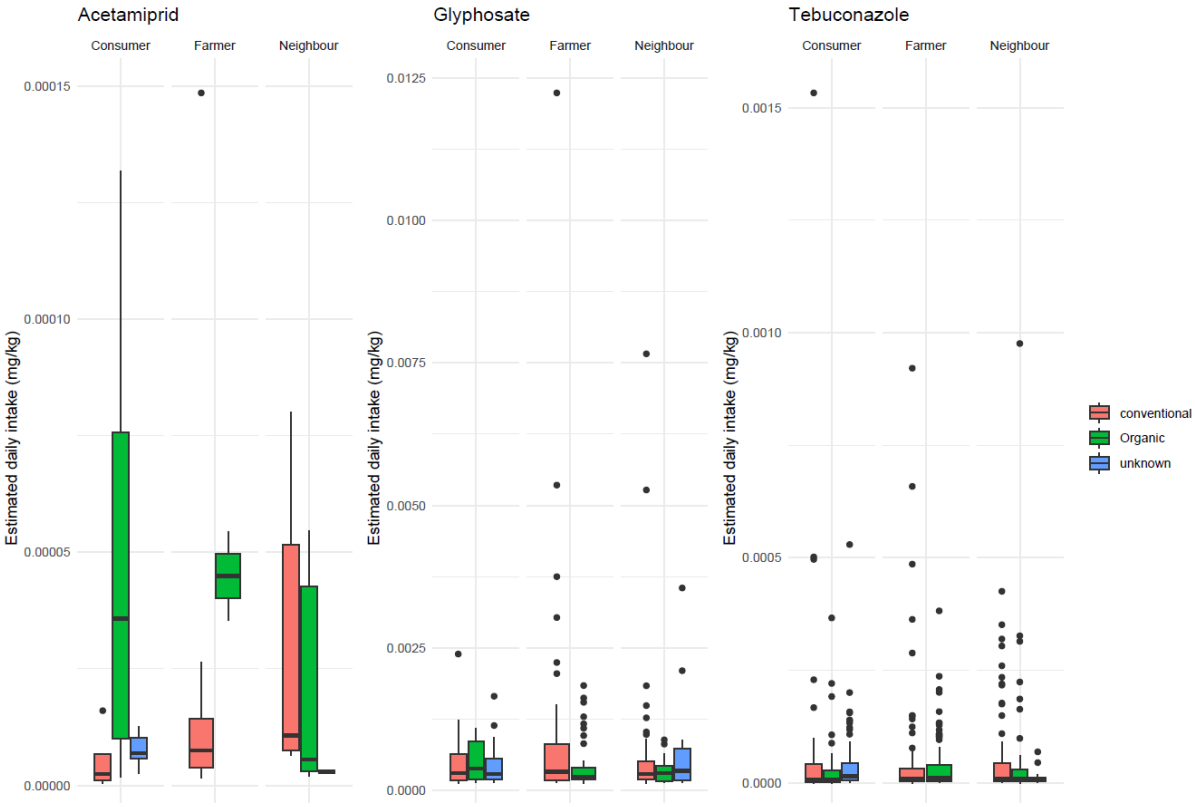

Figure 27. *Estimated daily intake of acetamiprid, glyphosate and tebuconazole in mg/kg bw subdivided between 'conventional', 'organic' and 'unknown' (if this division was not reported), back-calculated from urinary excretion of glyphosate, acetamiprid-N-desmethyl and 5-hydroxy-tebuconazole. An average body weight of 70 kg was assumed. The blue dotted line represents the proposed ADI for acetamiprid (EFSA, 2024).* ***Table 13*** *provides the number of study participants.*

Table 13. Numbers of study participants per subgroup.

Subgroup		Acetamiprid[a]	Glyphosate	Tebuconazole
Consumer	Organic	12	59	59
	Conventional	12	75	75
	Unknown	24	127	127
Farmer	Organic	22	125	125
	Conventional	25	119	119
	Unknown	0	0	0
Neighbour	Organic	11	82	82
	Conventional	26	130	130
	Unknown	8	19	19

[a] From NL and PT

5. PBK modelling for animals

5.1. Generic PBK modelling for each animal species

For cat, chicken, cow, pig, human and rat, the generic PBK models were previously used and reported under similar assumptions as in the current study (Noorlander et al., 2024). Therefore, these models did not need additional model evaluation prior to their use. An oral dose was set for these species at 5 mg/kg BW.

As no experimental data (i.e., plasma concentrations over time) were available for goat and sheep, the plasma concentrations of the model compounds demeclocycline and probenecid, respectively, were used to fit the PBK models. Optimization steps included the adaptation of the physiological and kinetic parameters that had the highest effect on the plasma concentrations, which were found to be CL_{int}, GFR, urine flow and blood:plasma ratio. Importantly, as these parameters were manually changed and are thus deviating from the values obtained from literature, they can be considered as important uncertainty factors. After optimization, the model performance was deemed successful for further use. An oral dose was set at 2 mg/kg BW for goat and sheep.

5.2 Farm animal species

5.2.1. Liver S9 metabolism studies

After the optimization of liver S9 protein concentrations, imidacloprid and glyphosate were excluded from further intrinsic clearance studies due to a lack of conversion in all species. Therefore, Figure 21 contains the intrinsic clearance results of the six remaining pesticides. Species differences in clearance were found to be within two orders of magnitude for each of the pesticides apart from chlorpyrifos, which covered three orders of magnitude difference. Cats were the slowest converter (11.6 µL/min/mg S9 protein) and cow the fastest converter (2,810 µL/min/mg S9 protein). Interestingly, cow, pig and rat showed the highest intrinsic clearance rates for all pesticides, except for chlorpropham and pyrimethanil for which high clearance rates were also observed in human (Figure 28). Overall, the conversion of tebuconazole is the lowest compared to the other pesticides with a clear difference between human, chicken and cat (slow conversion) and rat, cow and pig (fast conversion).

5.2.2. Model outcome with inclusion of the intrinsic clearance

The obtained *in vitro* clearance rates of the selected pesticides (**Figure 28**) were incorporated in the generic PBK models and plasma concentration – time curves were predicted (**Figure 29**). Pyrimethanil showed the highest plasma curves for all species except for human, followed by tebuconazole and chlorpropham. All compounds, except piperonyl butoxide in chicken, were cleared within 12 hours after dosing.

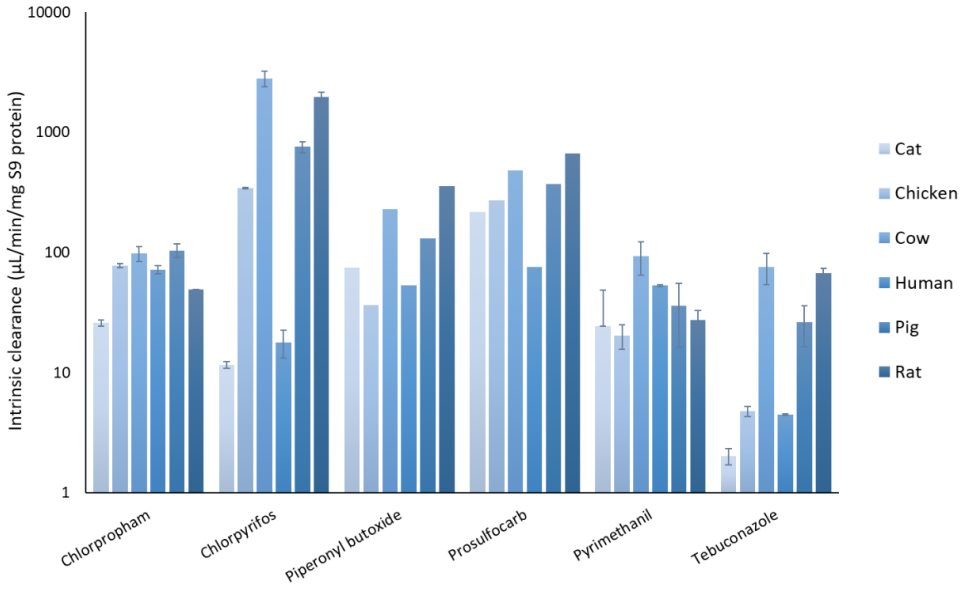

Figure 28. *Determined intrinsic clearance (in µL/min/mg S9 protein) of six pesticides (chlorpyrifos, chlorpropham, piperonyl butoxide, prosulfocarb, pyrimethanil and tebuconazole) found in six species (cat, chicken, cow, human, pig and rat) using liver S9 fractions.*

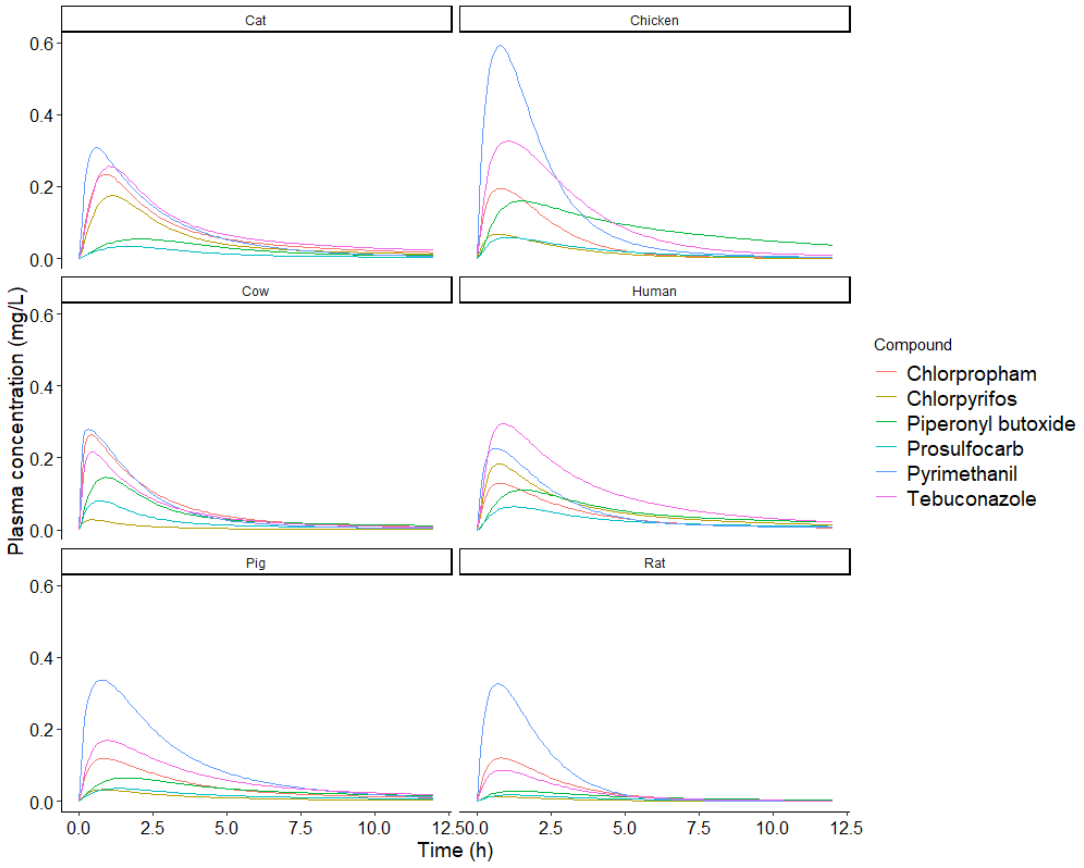

Figure 29. *Predicted plasma concentration - time curves (mg/L) for six species (cat, chicken, cow, human, pig and rat) and six selected pesticides (chlorpropham, chlorpyrifos, piperonyl butoxide, prosulfocarb, pyrimethanil and tebuconazole) at an oral dose of 5 mg/kg BW.*

5.2.3. Predicted transfer from pesticides to milk and eggs

The transfer of the selected pesticides (Figure 28) to milk and eggs was predicted using the PBK models for cow and chicken, respectively. The transfer of pesticides to milk (**Figure 30a**) and eggs (**Figure 30b**) was expressed as percentage of the dose. Chlorpropham and pyrimethanil showed the highest transfer to milk (~0.038%) and eggs (~0.17%), respectively. Overall, transfer to milk and eggs remained below 0.2% of the oral dose.

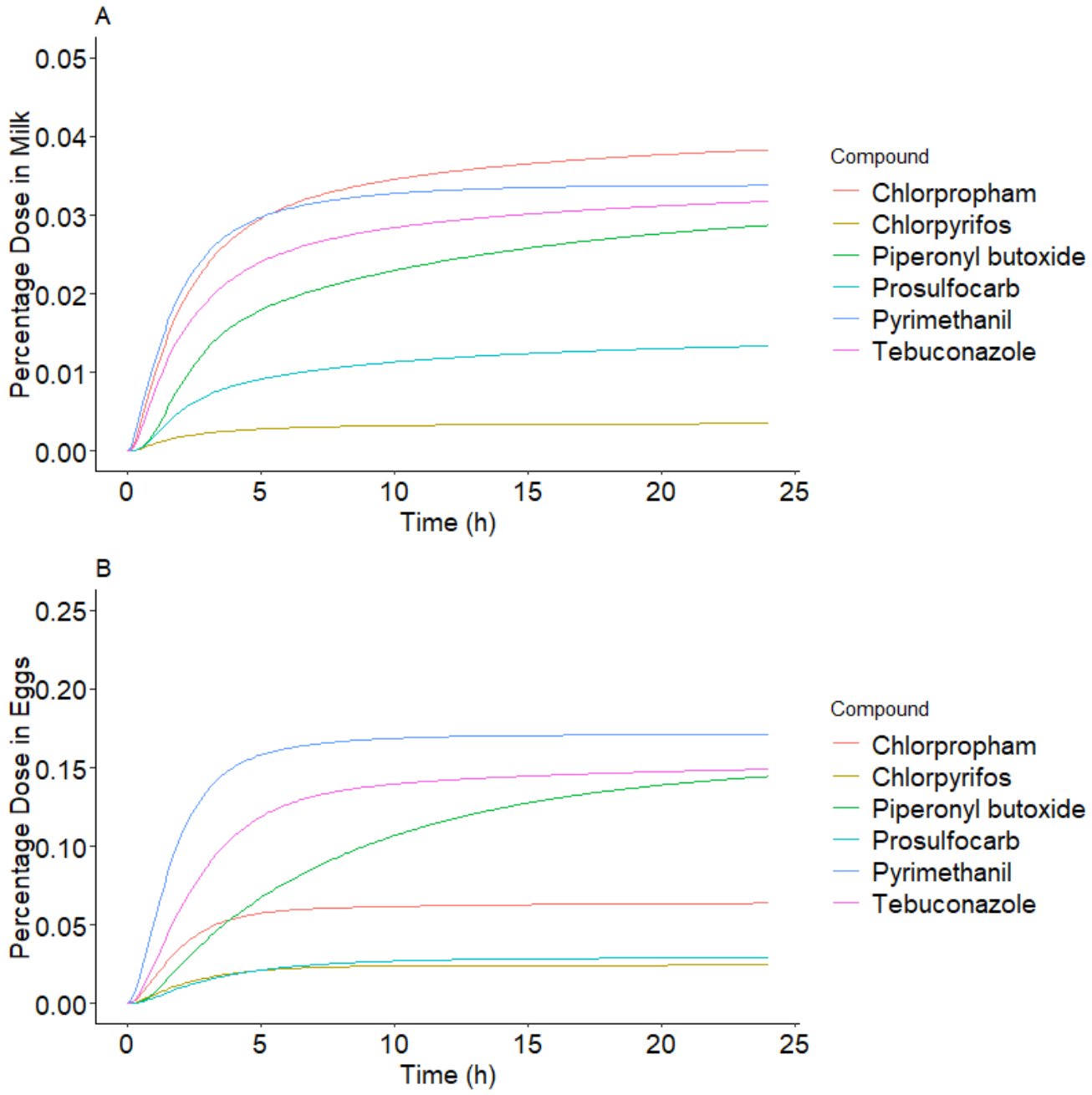

Figure 30. *Predicted transfer of pesticides (as a percentage of the dose) to* ***A****: milk and* ***B****): eggs at an oral dose of 5 mg/kg BW.*

5.2.4. Reverse dosimetry and assessment of pesticide concentrations in feed

In work package 2 of the SPRINT project, blood and urine samples of animals were taken and analysed for the presence of pesticides (in ng/mL). Based on the occurrence of pesticides (defined as detected above LOD), a selection was made per species for reverse dosimetry to estimate the potential exposure to that particular pesticide. No samples of rats were collected and therefore the rat model was excluded from reverse dosimetry calculations. . In general, the predicted exposure for EM was found to be higher than for PM. This finding is explained by the fact that EMs have a higher hepatic clearance, and thus a higher metabolism of the specific substance, which results in the potential to process a higher oral dose than PMs.

5.2.5. Assessment maximum calculated intake of selected pesticides

Using the assumptions stated in the Materials and Methods section 3.1.4, the maximum calculated intake of the selected pesticides in feed were estimated. First, the total intake of concentrate feed per animal was calculated using the nutritional advice indicated on the website of the supplier concentrate feed (Welkoop) (**Table 14**).

Table 14. *Estimation of (concentrate) feed intake per animal per day*

	Cat	Chicken[c]	Cow[d]	Goat	Pig[e]	Sheep
Body weight[a] (kg)	3.8	2.1	526	25.6	108	36
Nutritional advice concentrates feed[b]	50 gram/ 4 kg	100 gram/ 2 kg	800 gram/ 100 kg	500 gram/ adult goat	1.5% of BW	300 gram/ adult sheep
Total intake (kg per day)	0.0475	0.105	4.21	0.5	1.62	0.3

[a] Body weight (BW) as used in the generic PBK models; [b] Nutritional advice from the supplier of concentrate feed www.welkoop.nl; [c] Laying hens producing one egg per day; [d] Dairy cows; [e] Fattening pigs

Next, the MRLs of the selected pesticides for the ingredients found in the (concentrate) feed were collected from the EU Pesticides Database and used to calculate the total concentration of pesticides in feed. Thus, we assumed that the substances were present in feed at MRL, which is a worst-case scenario. To illustrate our approach, the ingredients found in cat feed and the respective MRLs for tri-allate are given in **Table 15**. Then, the intake of the individual ingredients in (concentrate) feed was calculated based on the nutritional advice provided by the supplier (Table 11). These values were multiplied by the MRL values to get the total concentration of the pesticide per kg body weight per day (Table 12). The total concentration of tri-allate in cat feed was 0.00109 mg/kg BW/day (Table 12). This approach was used for all pesticides detected in blood in the different species during the field campaign the case study sites. In **Table 16**, an overview is given for all calculated total concentrations of the corresponding pesticides in (concentrate) feed per species.

Table 15. *Approach to assess the maximum calculated intake of tri-allate in cat dry feed.*

Ingredient	MRL[a] (mg/kg)	Amount of ingredients in feed (%)[b]	Amount of ingredients in feed (kg)	Amount of tri-allate in feed (mg/day)
Wheat	0.1	30.5	0.0144875	0.00145
Barley	0.1	12.3	0.0058425	0.00058
Maize	0.1	13.2	0.00627	0.00063
Maize gluten feed	0.1	31.9	0.0151525	0.00151
Total maximum calculated intake (mg/day)				***0.0042***
Total maximum calculated intake (mg/kg BW/day)				***0.00109***

[a] EU Pesticides Database
[b] Percentages taken from Table 4 of the EFSA Scientific Report on animal dietary exposure (EFSA, 2019b).

Table 16. *Overview of maximum calculated intake (mg/kg BW/day), i.e., the estimated total concentrations of pesticides in (concentrate) feed of different animals, assuming that the substances were present at MRL values.*

	Cat	Chicken	Cow	Goat	Pig	Sheep
Bromoxynil	0.00011		0.00007	0.00016		0.00008
Hexachlorobenzene		0.00056				
Indoxacarb					0.00012	
MCPA	0.00055		0.00095			0.00106
Pendimethalin					0.00061	
Pyrethrin II						0.01875
Tri-allate	0.00109					
2,4-D	0.00798					

5.2.6. Comparison of the predicted pesticide intake with the maximum calculated intake

Applying PBK model-based reverse dosimetry on the detected blood levels of the different pesticides in all species resulted in predicted oral doses/exposures for poor metabolizers (PM) and extensive metabolizers (EM). Next, these values were compared with the estimated maximum calculated intake presented in **Tables 14-16** and these results are depicted in **Figure 17**.

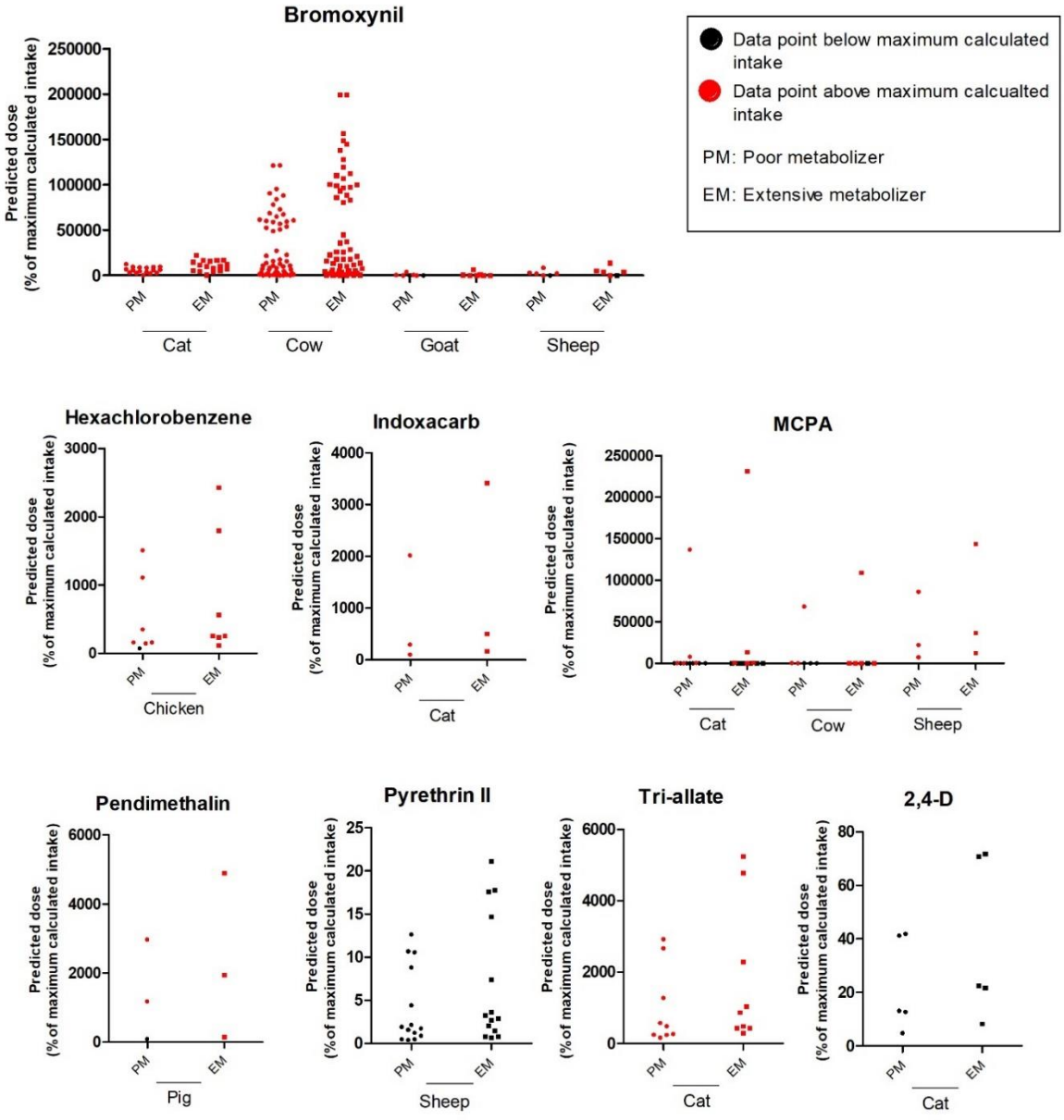

Figure 17. *Predicted dose of a selection of pesticides that were detected in plasma of at least three animals, expressed as % of maximum calculated intake. A black data point indicates that the predicted dose is below the maximum calculated intake for that specific pesticide. Red data points indicate that the predicted dose is above the maximum calculated intake.*

Bromoxynil was found in four species (i.e., cat, cow, goat, sheep) and its predicted oral doses were exceeding the estimated total concentration of bromoxynil in feed when present at MRL values in all species for PM and EM (indicated with the red dots), except for a few data points in goat and sheep (indicated with the black dots). Also, for hexachlorobenzene, indoxacarb, MCPA, pendimethalin and tri-allate, most of the predicted dose levels were exceeding the MRL-based maximum concentration in feed. For MCPA, some of the datapoints calculated for cat and cow were below the MRL-based maximum pesticide concentrations in feed (**Figure 17**). With regard to 2,4-D and pyrethrin II, none of the predicted doses were exceeding the MRL-based maximum concentration in feed, which can be attributable to their higher MRLs compared with the other pesticides.

6. Discussion

Both generic and more refined substance-specific PBK models were used to perform back-calculations as a proof of principle. While the generic model could be applied to the SPRINT-data and no ADI exceedance was found. A lack of data for the majority of the substances in the SPRINT pesticide selection causes limited reliability and applicability of the applied PBK approach. Several assumptions had to be made to make the model workable for a range of compounds due to data gaps. For three pesticides human volunteer study data provided valuable data and showed kinetics vary between individuals and even more so between pesticides. Below the strengths and limitations of PBK modelling to inform the exposure assessment of pesticides will be further discussed for applications in humans and animals, separately.

6.1. Human

Human volunteer data was used to validate the substance specific dedicated PBK models for acetamiprid, glyphosate and tebuconazole. These three pesticides were prioritised in WP3, WP4 and WP5 for targeted research efforts related to inform the links between exposure and effects. The human volunteer studies provided the concentration time pattern of urinary excretion to calculate cumulative excretion until 24 hours after the start of exposure. After this validation and conversion from cumulative excretion to a concentration in urine, a linear relationship between dose and urine sample concentration over a period of 8 hours following the start of exposure. From this dataset an equation was derived to back-calculate intake from the human biomonitoring data, specifically urinary excretion data. After estimating daily uptake in mg of the pesticide by dividing with the average human bodyweight of 70 kg it was found that in none of the study participants of the SPRINT biomonitoring campaign the ADI was exceeded. Additionally, in none of the farmers the acceptable operator exposure level (AOEL) for glyphosate was exceeded.

While the models provide a proof-of-concept for the application of generic and dedicated models to perform back calculation, several assumptions were included to parameterise the models used. For the generic models, these assumptions were less precise than for the dedicated model. For the latter type of more refined model parameters could be fitted to real-life excretion data from the human volunteer study removing away some of the uncertainty in the reverse dosimetry calculations. This comes with one limitation related to back-calculations of inhalation exposure because no validation data was available due to the lack of human volunteer or animal studies for this route of uptake.

When working with parent and metabolite model, robust data on human biotransformation are required. Often, Michaelis-Menten kinetics are assumed which can be parameterised using hepatic in-vitro assays. For acetamiprid only the conversion to acetamiprid-N-desmethyl is taken into account, while it is known that the acetamiprid-N-desmethyl is further converted to secondary metabolites including nicotinic acid derivatives (Wrobel et al., 2023b). In the case of glyphosate, AMPA is a known metabolite although it is unclear which fraction of glyphosate is metabolised in humans. For the pesticides of interest, biotransformation parameters were not always available or of poor quality, especially for the generic model. If metabolism cannot be sufficiently parameterised, back-calculation from urinary samples based on metabolism content is unreliable. One way to circumvent this is by performing back-calculations on plasma

samples, since this is a direct representation of internal kinetics of a compound. Blood collection is an invasive method of sample collection, especially repeated over time such as in a human volunteer study. In the generic model, it was opted to use plasma data for back-calculation while the more data-rich dedicated model could be used to perform a more refined back-calculation for urinary metabolite to parent ingestion. Regarding the availability of feces from the study participants in SPRINT we have also asked the human volunteers to collect stool samples. The feces analysis informs the kinetics qualitatively, regarding enterohepatic recirculation and feces as an excretion pathway for parent and the identification of of human and microbial metabolites. However, for quantitative purposes the feces excretion is more difficult than urinary excretion data due to the lack of knowledge regarding quantitative data on the excretion of parent and the contribution of bacterial biotransformation to inform back-calculation to the parent. Additionally, it is considered more difficult to quantitatively inform the concentration time pattern due to the sampling procedure and interindividual variability in day-to-day defecation patterns in humans subjects.

For a substance to be modelled information on entering a tissue compartment from the circulation is needed. In PBK models this is described in organ-blood partition coefficients. Especially for pesticides, there is a lack of data regarding partitioning between whole blood and organs and tissues. Additionally, there is a lack of data on the concentration of free substance in plasma. The ratio of unbound to bound substance determines the fraction available for diffusion into tissues, clearance by metabolism or urinary excretion. The fraction bound to plasma proteins or distribution of substance available intracellular in erythrocytes (and not available for exchange into organs or tissues) is often not known. For the models presented here QSARs or commonly known methods such as Rodger's and Rowland's formula or Schmitt's method were used. These are all computational techniques which take into account physicochemical characteristics of a compound to predict their behaviour in blood and tissue. Although these are well-established and commonly used methods this use of QSARS can introduce inaccuracies in the modelling.

At the time of writing of this report data on glyphosate in blood plasma from the human volunteer study were not yet available. For this substance it is not clear to what extent our predictions are accurate. For the current model instead of plasma, urinary data was used in the dedicated model for glyphosate. From previous studies it is already known that glyphosate is poorly absorbed in the gut and only a small fraction of administered dose is excreted in urine, indicating that circulating blood concentrations are also expected to be low (Faniband et al. 2021). This needs to be verified as soon as the human glyphosate plasma data are available.

When building a PBK-model, as many organs of interest should be included without making the model too complex. Every organ that is included needs to be parameterised, for example with the aforementioned QSAR methods. In our models some organs were therefore lumped into fast or slowly perfused tissue. Most important organs that affect kinetics and biotransformation, such as liver and kidney, were included. It is not to be expected that this had a large impact on modelled outcomes.

Some of the uncertainties in the models could be reduced by validating the model outcomes with data from human volunteer studies. The results of generic model should be interpreted with more caution because of limited availability of some substance properties and human physiology input parameters. To perform the reverse dosimetry, several assumptions regarding the samples had to be made as well. Urine samples were

as the first void after awakening. An estimated time since exposure was unknown and information on the total urine void volume was not available either. Urine production may vary from person to person in the population studied. For the current proof-of-principle a standardised urine void volume of around 400mL was used. Since it was a morning void, the modelled outcome (cumulative) in urine at 8 hours after exposure was taken. The same applies to body weight which was assumed to be 70kg.

There are opportunities for further development of this modelling approach. Further sensitivity analysis may show which parameters have the greatest influence on model outcomes. Bootstrapping could done to model variability of the population. For example, a normal distribution in body weight and urine production could be included in a probabilistic reverse dosimetry calculation. To assess real-life scenarios, multiple exposure routes could be modelled in such a way that repeated exposure (for example, due to ingestion of pesticides via multiple meals a day) can be included. Dietary intake could be combined with an inhalation and dermal exposure scenario to support occupational exposure assessment.

6.2. Animal

In the current study, PBK models were developed for a number of farm animals as well as humans, cats and rats. For cat, chicken, cow, human, pig and rat, a selection of pesticides was included based on their frequent presence in food/feed (Table 1), to obtain *in vitro* clearance rates for PBK modelling performing liver S9 incubations. With regard to the intrinsic clearance values as determined with *in vitro* liver S9 incubations, substantial species differences were found. Strikingly, less pronounced species differences were found in the predicted plasma concentration – time curves as determined with the PBK models. Most likely, this is due to the fact that the blood flow to the liver is the rate limiting factor for clearance. In contrast, imidacloprid did not show any conversion in the included species, while it was previously reported that this pesticide is metabolized extensively *in vivo* (Schulz Jander et al 2002; Solecki, 2001). Kolanczyk and colleagues (2019) determined the *in vitro* Michaelis-Menten parameters of imidacloprid metabolism in rat microsomes (i.e., the Michaelis-Menten constant (Km) and the maximum velocity (Vmax)). Interestingly, for the formation of 5-hydroxyimidacloprid, these researchers found a Km of 158 µM imidacloprid, while in the current study a concentration of 1 µM of imidacloprid was used. This implies that in the current study, the concentration of imidacloprid might have been too low to be converted into 5-hydroxyimidacloprid and other phase I and phase II metabolites. Also, for glyphosate, no conversion was measured in the current study. This finding was in line with the expectations, as it was previously reported that glyphosate is hardly metabolized in human, rat and chicken (Williams et al, 2020; Brewsteer et al., 1991; Fréville et al., 2023)

For cat, chicken, cow, goat, pig and sheep, a selection of pesticides was included based on their occurrence in blood in at least three animals (as previously measured in the SPRINT project) (Table 1), and reverse dosimetry was performed. The resulting predicted oral doses were compared with the calculated maximum intake via feed, under the assumption that the substance was present at MRL. Strikingly, for six out of eight pesticides, the predicted oral doses highly exceeded the maximum calculated intake (Figure 5). To explain these results there are several possible explanations. First, during the development of the PBK models, a number of parameters were adopted based on assumptions. For example, a hepatic clearance of 0.2 L/hr (for a 'poor metabolizer', PM)

was selected for all animals, which might be an underestimation for some of the animal species. Furthermore, a bioavailability of 100% was assumed, together with a blood:plasma ratio of 1. These can be considered as worst-case scenarios, leading to an overestimation of the predicted exposures. Also, human-based partition coefficients were used, which might have led to inaccuracies. With regard to the reverse dosimetry, several other rather conservative assumptions were made. For example, reverse dosimetry was performed using C_{max} values as the dose metric. However, the concentrations of the substances in blood were measured at only one point in time, which was unknown because the exact time of sample collection was not reported. Thus, the measured concentration can represent any data point on the plasma/time curve, making the reverse dosimetry-based predicted oral dose a highly uncertain outcome.

Altogether, since the PBK models and reverse dosimetry included several uncertainty factors, the outcomes are most probably overestimated, which means that the number of cases where the predicted oral exposure exceeded the maximum calculated intake is most probably lower. A thorough evaluation and optimization of the model parameters should be performed, for example by performing a study in a controlled laboratory environment investigating the kinetics of a selection of pesticides in animal species of interest.

With regard to the predicted oral dose of bromoxynil, a potential cause for the exceedance of the maximum calculated intake could be related to bromoxynil binding to serum albumin (Appah et al., 2017). To investigate this possibility, reverse dosimetry was repeated using a higher fraction unbound in plasma (Fup) (i.e., 0.85 instead of 0.156), which represents the unbound fraction of the substance in the blood circulation. However, the resulting predicted oral doses turned out to be not sensitive to the fraction unbound, implying that even if bromoxynil would bound to albumin, this does not have a major impact on the outcomes of reversed dosimetry calculations.

Another factor that may have contributed to the exceedance of the maximum calculated intake is the actual approach to calculate these values. In these calculations, multiple assumptions were made regarding the feed intake and feed composition. For example, the intake of concentrate feed was based on the nutritional advice (i.e., the maximum recommended intake provided by the supplier), and not on actual feed intake data. This may have resulted in an overestimation of the outcomes. In addition, the exact composition of the feed ingredients was not provided and thus the calculations were based on estimated values, which might have deviated from the actual composition. It might be possible that the animals were additionally exposed to pesticides via other routes than feed. If pesticides were present in the air (via spray drift, evaporation from crops or in in airborne or settled dust), this may lead to additional non-dietary exposure by inhalation and/or dermal absorption. To verify if there was indeed exposure via these alternative routes, it might be worthwhile to analyse wristband data.

Ideally, the pesticides selected for the *in vitro* liver S9 incubations should have matched the pesticides found in blood. In that way, metabolism could have been taken into account more precisely compared to the current less precise approach (apparent PMs and EMs). Priority was given to the analyses of human blood to inform the selection of substances to prioritise for the human volunteer study that needed approximately one year of preparation regarding required ethics approvals. To compensate for this uncertainty, with the use of PM and EM a range of exposures was established, covering

population variability in the analysis. For example, with regard to MCPA in sheep, a blood level of 177 µg/L resulted in the exposure levels ranging from 0.23 – 0.39 mg/kg BW. The model outcome could have been verified by urinary metabolite excretion data as well. However, these data were available for only a very limited number of cows, goats and pigs. Furthermore, most of the detected compounds were metabolites, which were not usable for the current model as it did not contain a metabolite extension.

According to the predicted exposure from the blood levels found in the different farm animals and cat it was revealed that for each animal the observed exposure to pesticides exceeded the calculated maximum intake via feed under the assumption that the substances were present at MRL. Although the back-calculated exposure estimates were based on assumptions and estimations for some of the model parameters, it provides a proof of principle to the assessment of exposure from feed. It was assumed that exposure to the selected pesticides is chronic (originating from feed intake) and that the outcomes could be compared to the Acceptable Daily Intake (ADI) of those substances. The highest predicted exposures were found for MCPA in sheep, cat and cow (1.5, 1.3 and 1 mg/kg BW/day, respectively). Although no studies are available for regulatory purposes performed for these animals, the Joint Meeting on Pesticide Residues in 2012 (Joint Meeting on Pesticide Residues (2012) adopted an ADI for human of 0.1 mg/kg BW/day based on a NOAEL of 12 mg/kg BW/day from four sub-chronic studies in rat, thereby looking at changes in clinical chemistry parameters indicative of kidney toxicity. This indicates that when applying the ADI to sheep, cat and cow, these animals are exposed to levels of MCPA that could potentially lead to adverse effects in kidney and liver. Similar for bromoxynil, an ADI of 0.003 mg/kg BW/day was agreed based upon a short-term NOAEL of 0.3 mg/kg BW/day in a 90-day study in dogs with the liver as the target organ (EFSA, 2006; 2007). Interestingly, many of the predicted doses both for PMs and EMs in cat, cow, goat and sheep exceeded this point of departure to some extent. The highest estimated uptake for cow was 0.13 mg/kg BW/day. In the case of tri-allate in cat, similar results were observed as in both PMs and EMs some predicted doses were exceeding the ADI (0.025 mg/kg BW/day) (EFSA, 2008) by a factor of two (0.057 mg/kg BW/day).

Although the use of hexachlorobenzene has been banned in the European Union since 1981 for agricultural purposes (REF), it has been measured in blood of chicken albeit under the lowest reported NOAEL, which was 0.05 – 0.07 mg/kg BW per day for hepatic effects derived from a subchronic study in pigs and several studies in rat (EFSA, 2006) Potential current sources of exposure to hexachlorobenzene are primarily from chemical industrial where it was formed as a waste product (EPA, 2020). For the remaining pesticides the predicted doses were all below the established ADIs (pyrethrin II: 0.04 mg/kg BW/day II (EFSA, 2013), indoxacarb 0.005: mg/kg BW/day (EFSA, 2017), pendimethalin: 0.125 mg/kg BW/day (EFSA, 2016a) and 2,4-D: 0.02 mg/kg BW/day (EFSA, 2016b.

7. Data gaps and future research

7.1. Human

To expand the application domain of pesticides beyond the current dedicated PBK models, more data on biotransformation and clearance processes in humans have to become available. The *httk* application (https://cfpub.epa.gov/si/si_public_record_report.cfm?dirEntryId=337720&Lab=NCCT) supports high-throughput analyses enabling calculations of input parameters for a range of pesticides. Combining high-throughput assays for pesticides can be a way forward to improving PBK-modelling for application to pesticides. In the current *CompTox* database (https://www.epa.gov/comptox-tools/comptox-chemicals-dashboard) many pesticides are included. Inclusion of next-generation pesticides with fast kinetics and often unknown metabolism can further improve the current domain greatly. With this, generic models could be transformed into dedicated substance-specific models.

1. There are data gaps for most pesticides, specifically related to blood-tissue partitioning, fractions of pesticides bound to unbound in blood plasma and fractions of pesticides available in whole blood compartment, extracellular versus intracellular.
2. There is a lack of data regarding the biotransformation of pesticides regarding the formation of primary and secondary metabolites and related to the Michaelis-Menten characteristics of enzymatic conversions.
3. There are opportunities for sensitivity analysis and when indicated probabilistic modelling can be performed to further take into account variability and uncertainty in some of the substance characteristics and population characteristics.
4. There is a lack of data regarding the kinetics of inhalation. In animal studies this is not required and in the human volunteer study it is considered a risk to the human subjects that cannot be assessed to make an informed decision regarding their safety. This means for setting AOELs the derivation will have to be conservative and based on modelling assumptions combined with appropriate assessment factors to cover uncertainties related to the kinetic aspect next to the lack of inhalation toxicity data.

7.2. Animal

In the current study different PBK models were developed for a selection of pesticides observed in the SPRINT field campaign. For a set of pesticides, the PBK models included intrinsic clearance data that were obtained *in vitro*. PBK models for other pesticides were completely based on literature-derived data, due to a lack of *in vivo* data. Nevertheless, all models showed to perform adequately. Inclusion of specific compartments representing the mammary glands in cows and reproductive organs in chicken offered the opportunity to study transfer to milk and eggs, respectively. This can be considered as highly relevant future extension of the model, as this may provide information on potential pesticide exposure to humans after consumption of milk and eggs. Another goal of this study was to use a reverse dosimetry-based approach to calculate pesticide exposure to (farm) animals. Although the obtained results indicate a high intake, it should be considered that the approach was based on assumptions and calculations and the results should be interpreted with caution. This approach provides a way forward to gain new insights on pesticide exposure of (farm) animals. Several optimization steps could still be considered to further limit the number of assumptions.

1. Further reduce assumptions for modelling, e.g. related to biotransformation
2. Availability of accurate data on feed composition and total feed intake data per day for different farm animal species at EU level.
3. Estimates of non-feed uptake of pesticides from inhalation and or dermal absorption. Such estimates may be supported by the wristband data that have been collected on a limited scale.
4. Extend existing models for chicken to support predictions for pesticide residues in eggs.
5. Extend existing models for dairy cow to support predictions for pesticide residues in milk.

8. Conclusions

The use of PBK modelling for the interpretation of human biomonitoring data is demonstrated as proof of principle. All findings related to estimates generated by PBK modelling should be interpreted with caution, given the assumptions made to cover data gaps.

8.1. Humans

For the use of PBK models in the assessment of pesticide exposures, regarding their human physiology-based toxicokinetics, some of the new insights are the following:

1. Substance specific PBK models were developed using both existing and measured parameter estimates in a human volunteer study for acetamiprid, glyphosate and tebuconazole, including placenta transfer estimates from ex-vivo experiments.
2. Biomonitoring data from study participants recruited in ten countries were used to study pesticide exposure scenarios by reverse dosimetry. A generic model produced less precise back-calculated exposure estimates compared to the substance-specific models.
3. Results are expressed as the median % of the (ADI) with a range of the 5th to 95th percentile (P5-P95). For acetamiprid these values were 0.16% (0.02-1.8%) of the recently reduced ADI. For glyphosate these values were 0.06% (0.02-0.3%) of the ADI and 0.3% (0.1-1.6%) of the AOEL. For tebuconazole these values were 0.03% (0.001-0.6%) of the ADI
4. Placenta transfer was studied in ex vivo human placenta tissue for acetamiprid, glyphosate and tebuconazole. Forward dosimetry studies combining PBK models with ex vivo placental transfer data were completed for acetamiprid, illustrating how this approach can be used to estimate internal fetal exposure following external maternal exposure. For glyphosate and tebuconazole these studies were not completed, pending sample and data analyses.

8.2. Animals

For the use of PBK models in the assessment of pesticide exposure, regarding their animal physiology-based toxicokinetics, some of the new insights are the following:

1. PBK models for farm animals (chicken, cow, pig, goat, sheep and cat) were developed using both existing and newly measured parameter estimates. Added features include specific compartments to study transfer to milk (cows) and eggs (chicken).
2. A limited set of biomonitoring data from the SPRINT field campaign in ten countries were used to study farm animal's pesticide exposures.
3. For hexachlorobenzene, indoxacarb, MPCA, pendimethalin and tri-allate, most of the predicted dose levels were exceeding the MRL-based maximum concentration in feed at MRL-values.
4. For MCPA, some of the datapoints calculated for cat and cow were below the MRL-based maximum concentrations in feed at MRL-values.
5. For bromoxynil in cat, cow, goat, sheep predicted oral doses were exceeding the MRL-based maximum concentrations of bromoxynil in feed at MRL values.
6. For 2,4-D and the pyrethrin II, none of the predicted doses exceeded the MRL-based maximum concentration in feed at MRL values.

9. References

1. Appah E, Elzey B, Fakayode SO. Investigation of the binding and simultaneous quantifications of propanil and bromoxynil herbicide concentrations in human serum albumin. J Environ Sci Health B. 2017 Jul 3;52(7):495-504. doi: 10.1080/03601234.2017.1303323.
2. Ardizzone M, Binaglia M, Cottrill B, Cugier JP, Ferreira L, Gómez Ruiz JÁ, Innocenti M, Ioannidou S, López Puente S, Merten C, Nikolic M, Savoini G. Animal dietary exposure: overview of current approaches used at EFSA. EFSA J. 2019 Nov 15;17(11):e05896. doi: 10.2903/j.efsa.2019.5896. PMID: 32626181; PMCID: PMC7008838.
3. Automeris, WebPlotDigitizer. (Accessed 15-12-2024): https://automeris.io/docs/
4. Berezhkovskiy LM. Volume of distribution at steady state for a linear pharmacokinetic system with peripheral elimination. J Pharm Sci. 2004 Jun;93(6):1628-40. doi: 10.1002/jps.20073.
5. Brewster DW, Warren J, Hopkins WE 2nd. Metabolism of glyphosate in Sprague-Dawley rats: tissue distribution, identification, and quantitation of glyphosate-derived materials following a single oral dose. Fundam Appl Toxicol. 1991 Jul;17(1):43-51. doi: 10.1016/0272-0590(91)90237-x.
6. Brown RP, Delp MD, Lindstedt SL, Rhomberg LR, Beliles RP. Physiological parameter values for physiologically based pharmacokinetic models. Toxicol Ind Health. 1997 Jul-Aug;13(4):407-84. doi: 10.1177/074823379701300401.
7. Charistou A, Coja T, Craig P, Hamey P, Martin S, Sanvido O, Chiusolo A, Colas M and Istace F (2021) Guidance on the assessment of exposure of operators, workers, residents and bystanders in risk assessment of plant protection products European Food Safety Authority (EFSA), 30 November 2021, doi: 10.2903/j.efsa.2022.7032.
8. EFSA (2006) Opinion of the scientific panel on contaminants in the food chain on a request from the commission related to hexachlorobenzene. As undesirable substance in animal feed. Question N° EFSA-Q-2005-185. Adopted on 13 September 2006. Accessed 15-12-2024: https://efsa.onlinelibrary.wiley.com/doi/pdf/10.2903/j.efsa.2006.402
9. EFSA (2007) Peer review of the pesticide risk assessment of the activesubstance bromoxynil (variant evaluated bromoxyniloctanoate) 7 April 2017. doi: 10.2903/j.efsa.2017.4790
10. EFSA Scientific Report (2008) 181, Conclusion on the peer review of tri-allate. (accessed 15-12-2024): https://efsa.onlinelibrary.wiley.com/doi/epdf/10.2903/j.efsa.2009.181r
11. EFSA (2013) EFSA Journal 2013;11(1):3032Suggested citation: European Food Safety Authority; Conclusion on the peer review of the pesticide risk assessment of theactive substance pyrethrins. EFSA Journal 2013;11(1):3032. [76 pp.] doi:10.2903/j.efsa.2013.3032. (accessed 15-12-2024): https://efsa.onlinelibrary.wiley.com/doi/epdf/10.2903/j.efsa.2013.3032
12. EFSA (2016a) doi:10.2903/j.efsa.2016.4420www.efsa.europa.eu/efsajournal EFSA Journal 2016;14(3):4420Peer review of the pesticide risk assessment of theactive substance pendimethali. (accessed 15-12-2024): https://efsa.onlinelibrary.wiley.com/doi/epdf/10.2903/j.efsa.2016.4420
13. EFSA, 2016b) Peer review of the pesticide risk assessment of theactive substance 2,4-DB doi: 10.2903/j.efsa.2016.4500 (accessed 15-12-2024): https://efsa.onlinelibrary.wiley.com/doi/epdf/10.2903/j.efsa.2016.4500

14. EFSA (2017) Peer review of the pesticide risk assessment of the activesubstance indoxacarb doi: 10.2903/j.efsa.2018.5140. (accessed 15-12-2024): https://efsa.onlinelibrary.wiley.com/doi/epdf/10.2903/j.efsa.2018.5140
15. EFSA (2019) doi: 10.2903/j.efsa.2019.5896Animal dietary exposure: overview of current approaches used at EFSA. (accessed 15-12-2024): https://efsa.onlinelibrary.wiley.com/doi/epdf/10.2903/j.efsa.2019.5896
16. EPA (accessed 15-12-2024): https://www.epa.gov/sites/default/files/2016-09/documents/hexachlorobenzene.pdf
17. EPA High-Throughput Toxicokinetics (httk) R Package. (accessed 15-12-2024): https://www.epa.gov/comptox-tools/high-throughput-toxicokinetics-httk-r-package
18. EU Pesticides Database (accessed 15-12-2024): https://food.ec.europa.eu/plants/pesticides/eu-pesticides-database_en)
19. Faniband MH, Norén E, Littorin M, Lindh CH. Human experimental exposure to glyphosate and biomonitoring of young Swedish adults. Int J Hyg Environ Health. 2021 Jan;231:113657. doi: 10.1016/j.ijheh.2020.113657. Epub 2020 Oct 30. PMID: 33130428.
20. FAO/WHO 2007 Pesticide residues in food 2007. Joint FAO/WHO Meeting on Pesticide Residues. Report of the Joint Meeting of the FAO Panel of Experts on Pesticide Residues in Food and the Environment and the WHO Core Assessment Group on Pesticide Residues. Geneva, Switzerland.
21. Freriksen JJM, Schalkwijk S, Colbers AP, Abduljalil K, Russel FGM, Burger DM, Greupink R. Assessment of Maternal and Fetal Dolutegravir Exposure by Integrating Ex Vivo Placental Perfusion Data and Physiologically-Based Pharmacokinetic Modeling. Clin Pharmacol Ther. 2020 Jun;107(6):1352-1361. doi: 10.1002/cpt.1748.
22. Fréville M, Henri J, Estienne A, Serra L, Ramé C, Ganier P, Chahnamian M, Froment P, Dupont J. Determination of the elimination half-life of Glyphosate and its main metabolite, AMPA, in chicken plasma. Toxicol Lett. 2023 Nov 1;389:19-25. doi: 10.1016/j.toxlet.2023.10.009.
23. Goh MY, Millard MS, Wong ECK, Berlowitz DJ, Graco M, Schembri RM, Brown DJ, Frauman AG, O'Callaghan CJ. Comparison of diurnal blood pressure and urine production between people with and without chronic spinal cord injury. Spinal Cord. 2018 Sep;56(9):847-855. doi: 10.1038/s41393-018-0081-3.
24. Guerrini VH, Filippich LJ, English PB, Schneider J, Cao GR, Bourne DW. Pharmacokinetics of probenecid in sheep. J Vet Pharmacol Ther. 1985 Jun;8(2):128-35. doi: 10.1111/j.1365-2885.1985.tb00936.x. PMID: 4020944.
25. Jha VK, Jayachandran C, Singh MK. Disposition kinetics and distribution of demeclocycline in various biological fluids in female goats. Vet Res Commun. 1989;13(3):225-30. doi: 10.1007/BF00142048. PMID: 2506691.
26. Jha VK, Jayachandran C, Singh MK (2013). Pharmacokinetics of demeclocycline and doxycycline after intramuscular administration in goat. The Indian Journal of Animal Sciences, 67(9). https://epubs.icar.org.in/index.php/IJAnS/article/view/34964
27. Joint Meeting on Pesticide Residues (2012) MCPA. MCPA 653–724 JMPR 2012
28. Jónsdóttir SO, Reffstrup TK, Petersen A, Nielsen E (2016) Physicologically based toxicokinetic models of tebuconazole and application in human risk assessment. Chem Res Toxicol 29(5):715–734. https://doi.org/10.1021/acs.chemrestox.5b00341
29. Kirchheiner J, Heesch C, Bauer S, Meisel C, Seringer A, Goldammer M, Tzvetkov M, Meineke I, Roots I, Brockmöller J. Impact of the ultrarapid metabolizer genotype of cytochrome P450 2D6 on metoprolol pharmacokinetics and pharmacodynamics. Clin Pharmacol Ther. 2004 Oct;76(4):302-12. doi: 10.1016/j.clpt.2004.07.002. PMID: 15470329.

30. Kolanczyk RC, Tapper MA, Sheedy BR, Serrano JA. In vitro metabolism of imidacloprid and acetamiprid in rainbow trout and rat. Xenobiotica. 2020 Jul;50(7):805-814. doi: 10.1080/00498254.2019.1694197.
31. Lautz LS, Melchers TC, Noorlander A, Stoopen G, Arrizabalaga-Larrañaga A. Application of a generic PBK model for beef cattle: Tissue/fluid correlations of paracetamol and NSAIDs. Food Chem Toxicol. 2024 Aug;190:114812. doi: 10.1016/j.fct.2024.114812. Epub 2024 Jun 13. PMID: 38879144.
32. Lautz LS, Stoopen G, Ginting AJ, Hoogenboom RLAP, Punt A. Fipronil and fipronil sulfone in chicken: From in vitro experiments to in vivo PBK model predictions. Food Chem Toxicol. 2022 Jul;165:113086. doi: 10.1016/j.fct.2022.113086. Epub 2022 Apr 29. PMID: 35500697.
33. Mazuryk J, Klepacka K, Kutner W, Sharma PS. Glyphosate: Hepatotoxicity, Nephrotoxicity, Hemotoxicity, Carcinogenicity, and Clinical Cases of Endocrine, Reproductive, Cardiovascular, and Pulmonary System Intoxication. ACS Pharmacol Transl Sci. 2024 Apr 8;7(5):1205-1236. doi: 10.1021/acsptsci.4c00046. PMID: 38751624; PMCID: PMC11092036.
34. Moser VC, Barone S Jr, Smialowicz RJ, Harris MW, Davis BJ, Overstreet D, Mauney M, Chapin RE. The effects of perinatal tebuconazole exposure on adult neurological, immunological, and reproductive function in rats. Toxicol Sci. 2001 Aug;62(2):339-52. doi: 10.1093/toxsci/62.2.339. PMID: 11452147.
35. Musther H, Harwood MD, Yang J, Turner DB, Rostami-Hodjegan A, Jamei M. The Constraints, Construction, and Verification of a Strain-Specific Physiologically Based Pharmacokinetic Rat Model. J Pharm Sci. 2017 Sep;106(9):2826-2838. doi: 10.1016/j.xphs.2017.05.003. Epub 2017 May 8. PMID: 28495566.
36. Netherlands trial register. Modelling human pesticide kinetics based on oral and dermal exposure data derived in a controlled setting NL84110.091.23. Accessed 29-11-2024 at https://onderzoekmetmensen.nl/en/trial/53236.
37. Noorlander A, Lautz L, Jansen Holleboom W, Mulder PPJ, Stoopen G, Punt A EFSA Project on the use of NAMs to explore interspecies metabolic differences on essential oils as feed additives. EFSA Journal 25 July 2024 https://doi.org/10.2903/sp.efsa.2024.EN-8820
38. Pearce RG, Setzer RW, Strope CL, Wambaugh JF, Sipes NS. httk: R Package for High-Throughput Toxicokinetics. J Stat Softw. 2017 Jul 17;79(4):1-26. doi: 10.18637/jss.v079.i04.
39. QIVIVE Tools web applications accessible at https://www.qivivetools.wur.nl/
40. Punt A, Lautz L, Stoopen G, Pinckaers N, Rijkers D, Essers M, Hoogenboom R. In vitro metabolism of lidocaine in subcellular post-mitochondrial fractions and precision cut slices from cattle liver. Toxicol In Vitro. 2021 Oct;76:105228. doi: 10.1016/j.tiv.2021.105228. Epub 2021 Jul 24. PMID: 34311064.
41. Schmitt W. General approach for the calculation of tissue to plasma partition coefficients. Toxicol In Vitro. 2008 Mar;22(2):457-67. doi: 10.1016/j.tiv.2007.09.010. Epub 2007 Nov 5. Erratum in: Toxicol In Vitro. 2008 Sep;22(6):1666.
42. Schulz-Jander DA, Casida JE. Imidacloprid insecticide metabolism: human cytochrome P450 isozymes differ in selectivity for imidazolidine oxidation versus nitroimine reduction. Toxicol Lett. 2002 Jun 7;132(1):65-70. doi: 10.1016/s0378-4274(02)00068-1.
43. Seneff S, Orlando LF (2018) Is Glyphosate a Key Factor in Mesoamerican Nephropathy? J Environ Anal Toxicol 2018, 8:1
44. Solecki R (2001) Imidacloprid. Toxicological evaluations. Pesticide residues in food 2001.

45. Welkoop feed supplier information. Accessible at https://www.welkoop.nl/
46. Williams GM, Kroes R, Munro IC. Safety evaluation and risk assessment of the herbicide Roundup and its active ingredient, glyphosate, for humans. Regul Toxicol Pharmacol. 2000 Apr;31(2 Pt 1):117-65. doi: 10.1006/rtph.1999.1371.
47. Wrobel SA, Bury D, Belov VN, Klenk JM, Hauer B, Hayen H, Martino-Andrade AJ, Koch HM, Brüning T, Käfferlein HU. (2023a) Rapid quantification of seven major neonicotinoids and neonicotinoid-like compounds and their key metabolites in human urine. Anal Chim Acta. 2023 Jan 25;1239:340680. doi: 10.1016/j.aca.2022.340680. Epub 2022 Nov 30. PMID: 36628758.
48. Wrobel SA, Bury D, Koslitz S, Hayen H, Koch HM, Brüning T, Käfferlein HU. (2023b) Quantitative Metabolism and Urinary Elimination Kinetics of Seven Neonicotinoids and Neonicotinoid-Like Compounds in Humans. Environ Sci Technol. 2023 Dec 5;57(48):19285-19294. doi: 10.1021/acs.est.3c05040. Epub 2023 Nov 8. PMID: 37939249.
49. Ying Y, Pan P, Zou C, Wang Y, Tang Y, Hou X, Li Y, Xu Q, Lin L, Lu J, Ge RS. Tebuconazole exposure disrupts placental function and causes fetal low birth weight in rats. Chemosphere. 2021 Feb;264(Pt 2):128432. doi: 10.1016/j.chemosphere.2020.128432.
50. Youness M, Sancelme M, Combourieu B, Besse-Hoggan P. Identification of new metabolic pathways in the enantioselective fungicide tebuconazole biodegradation by Bacillus sp. 3B6. J Hazard Mater. 2018 Jun 5;351:160-168. doi: 10.1016/j.jhazmat.2018.02.048.

Annexes

Annex 1. Model code for the generic model.

Annex 2. Human tissue parameters.

Annex 3. Physiological parameters for humans and all animal species of interest

Annex 4. MRM details on the LC-MS/MS analysis for seven pesticides.

Annex 5. Substance-specific modelling parameters.

Annex 1. Model code for the generic model

```
METHOD RK4
STARTTIME = 0
STOPTIME = 24
DT = 0.02
;-----------------------------------------------------------------------------------------
; INPUTS
;-----------------------------------------------------------------------------------------
; Volumes in Litres
; The model outputs are provided in the following units:
; #>  umol: Agutlumen, Atubules, Ametabolized
; #>  uM: Cgut, Cliver, Cven, Clung, Cart, Crest, Ckidney, Cplasma
; #>  uM*days: AUC

bw = 70                                          ; bodyweight
Clmetabolismc = 0.203
hematocrit = 0.44
kgutabs = 1
Kkidney2pu = 0
Kliver2pu = 0
Krest2pu = 0
Kgut2pu = 0
Klung2pu = 0

; BLOOD FLOWS
Qcardiacc = 4.8
Qgfrc = 0.108
Qgutf = 0.205
Qkidneyf = 0.221
Qliverf = 0.0536

; VOLUMES
Vartc = 0.0487
Vgutc = 0.0158
Vkidneyc = 0.00119
Vliverc = 0.02448
Vlungc = 0.00723
Vrestc = 0.77654
Vvenc = 0.0487

; BLOOD PARTITIONING
Fraction_unbound_plasma = 0.0682
Rblood2plasma = 0.0

Clmetabolism = 0.0
```

```
Qcardiac = 0.0
Qgfr = 0.0
Qgut = 0.0
Qkidney = 0.0
Qliver = 0.0
Qrest = 0.0

Vart = 0.0
Vgut = 0.0
Vkidney = 0.0
Vliver = 0.0
Vlung = 0.0
Vrest = 0.0
Vven = 0.0

;----------------------------------------------------------------------------------------------
; INITIALIZERS
;----------------------------------------------------------------------------------------------
kgutabs_sc = kgutabs * 24                                    ; scaled
Clmetabolism = Clmetabolismc * 24 * BW
Qcardiac = Qcardiacc * 24 * BW^0.75
Qgfr = Qgfrc * BW^0.75 * 24
Qgut = Qcardiac * Qgutf
Qkidney = Qcardiac * Qkidneyf
Qliver = Qcardiac * Qliverf
Qrest = Qcardiac - ( Qgut + Qkidney + Qliver )

Vart = Vartc * BW
Vgut = Vgutc * BW
Vkidney = Vkidneyc * BW
Vliver = Vliverc * BW
Vlung = Vlungc * BW
Vrest = Vrestc * BW
Vven = Vvenc * BW

;----------------------------------------------------------------------------------------------
; CONCENTRATIONS FORMULAS
;----------------------------------------------------------------------------------------------
Cgut = Agut / Vgut
Cliver = Aliver / Vliver
Cven = Aven / Vven
Clung = Alung / Vlung
Cart = Aart / Vart
Crest = Arest / Vrest
Ckidney = Akidney / Vkidney
Cplasma =Aven / Vven / Rblood2plasma
```

```
;-----------------------------------------------------------------------------------------
; DIFFENTRIAL EQUATIONS
;-----------------------------------------------------------------------------------------
; INITIAL CONCENTRATIONS

INIT Aplasma = 0
INIT Agutlumen = 1
INIT Agut = 0
INIT Aliver = 0
INIT Aven = 0
INIT Alung = 0
INIT Aart = 0
INIT Arest = 0
INIT Akidney = 0
INIT Atubules = 0
INIT AUC = 0
INIT Ametabolized = 0

Aplasma' = Aven / Rblood2plasma * ( 1 - hematocrit )

Agutlumen' = - kgutabs_sc * Agutlumen
Agut' = (kgutabs_sc * Agutlumen + Qgut * Aart / Vart) - (Agut / Vgut * (Rblood2plasma / Kgut2pu /
Fraction_unbound_plasma))

Aliver' = (Qliver *Aart / Vart) + (Qgut * Agut / Vgut * (Rblood2plasma / Kgut2pu /
Fraction_unbound_plasma)) - ( Qliver + Qgut ) * (Aliver / Vliver / Kliver2pu /
(Fraction_unbound_plasma * Rblood2plasma)) - (Clmetabolism * Aliver / Vliver / (Kliver2pu /
Fraction_unbound_plasma))

Aven' = (( Qliver + Qgut ) * Aliver / Vliver / Kliver2pu + Qkidney * Akidney / (Vkidney / Kkidney2pu) +
Qrest * (Arest / Vrest / Krest2pu)) * (Rblood2plasma / Fraction_unbound_plasma) - Qcardiac * Aven
/ Vven

Alung' = Qcardiac * ( Aven / Vven - Alung / Vlung * (Rblood2plasma / Klung2pu /
Fraction_unbound_plasma))
Aart' = Qcardiac * ( Alung / Vlung * (Rblood2plasma / Klung2pu / Fraction_unbound_plasma - Aart /
Vart))
Arest' = Qrest * ( Aart / Vart - Arest / Vrest * (Rblood2plasma / Krest2pu /
Fraction_unbound_plasma))
Akidney' = Qkidney * (Aart / Vart) - Qkidney * Akidney / ((Vkidney / Kkidney2pu) * (Rblood2plasma /
Fraction_unbound_plasma)) - (Qgfr * (Aart / Vart / Rblood2plasma) * Fraction_unbound_plasma)
Atubules' = (Qgfr * Aart) / ((Vart / Rblood2plasma) * Fraction_unbound_plasma)

Ametabolized' = Clmetabolism * (Aliver / Vliver / Kliver2pu)
AUC' = Aven / Vven / Rblood2plasma
```

Annex 2. Human tissue parameters

Tissue	Source	Unit	Value
adipose	Davies and Morris 1993	Flow (mL/min/kg^(3/4))	10.740000
bone	Davies and Morris 1993	Flow (mL/min/kg^(3/4))	9.719000
brain	Davies and Morris 1993	Flow (mL/min/kg^(3/4))	28.930000
gut	Davies and Morris 1993	Flow (mL/min/kg^(3/4))	47.520000
heart	Davies and Morris 1993	Flow (mL/min/kg^(3/4))	9.917000
kidney	Davies and Morris 1993	Flow (mL/min/kg^(3/4))	51.240000
liver	Davies and Morris 1993	Flow (mL/min/kg^(3/4))	59.920000
lung	Davies and Morris 1993	Flow (mL/min/kg^(3/4))	5.785000
muscle	Davies and Morris 1993	Flow (mL/min/kg^(3/4))	30.990000
skin	Davies and Morris 1993	Flow (mL/min/kg^(3/4))	12.400000
spleen	Davies and Morris 1993	Flow (mL/min/kg^(3/4))	3.182000
thyroid	ILSI-RSI 1994	Flow (mL/min/kg^(3/4))	3.700000
rest	Davies and Morris 1993	Flow (mL/min/kg^(3/4))	4.190000
adipose	ILSI-RSI 1994	Vol (L/kg)	0.208600
bone	ILSI-RSI 1994	Vol (L/kg)	0.072310
brain	ILSI-RSI 1994	Vol (L/kg)	0.019310
gut	ILSI-RSI 1994	Vol (L/kg)	0.015800
heart	ILSI-RSI 1994	Vol (L/kg)	0.004563
kidney	ILSI-RSI 1994	Vol (L/kg)	0.004190
liver	ILSI-RSI 1994	Vol (L/kg)	0.024480
lung	ILSI-RSI 1994	Vol (L/kg)	0.007235
muscle	ILSI-RSI 1994	Vol (L/kg)	0.384200
skin	ILSI-RSI 1994	Vol (L/kg)	0.033200
spleen	ILSI-RSI 1994	Vol (L/kg)	0.002467
thyroid	ILSI-RSI 1994	Vol (L/kg)	0.000300
rest	ILSI-RSI 1994	Vol (L/kg)	0.051820
adipose	EPA, Physiological Parameters Database for PBPK Modeling	Density (g/cm^3)	0.916000
bone	EPA, Physiological Parameters Database for PBPK Modeling	Density (g/cm^3)	1.976000
brain	EPA, Physiological Parameters Database for PBPK Modeling	Density (g/cm^3)	1.035000
gut	EPA, Physiological Parameters Database for PBPK Modeling	Density (g/cm^3)	1.044000
heart	EPA, Physiological Parameters Database for PBPK Modeling	Density (g/cm^3)	1.030000
kidney	EPA, Physiological Parameters Database for PBPK Modeling	Density (g/cm^3)	1.050000
liver	EPA, Physiological Parameters Database for PBPK Modeling	Density (g/cm^3)	1.050000
lung	EPA, Physiological Parameters Database for PBPK Modeling	Density (g/cm^3)	1.050000

muscle	EPA, Physiological Parameters Database for PBPK Modeling	Density (g/cm^3)	1.041000
placenta	Del Nero (2002)	Density (g/cm^3)	1.020000
red blood cells	Sun and Sethu (2017)	Density (g/cm^3)	1.080000
skin	EPA, Physiological Parameters Database for PBPK Modeling	Density (g/cm^3)	1.117000
spleen	EPA, Physiological Parameters Database for PBPK Modeling	Density (g/cm^3)	1.054000
thyroid	EPA, Physiological Parameters Database for PBPK Modeling	Density (g/cm^3)	1.051000
adipose	Schmitt 2008	pH	7.100000
bone	Schmitt 2008	pH	7.000000
brain	Schmitt 2008	pH	7.100000
gut	Schmitt 2008	pH	7.000000
heart	Schmitt 2008	pH	7.100000
kidney	Schmitt 2008	pH	7.220000
liver	Schmitt 2008	pH	7.230000
lung	Schmitt 2008	pH	6.600000
muscle	Schmitt 2008	pH	6.810000
placenta	Httk estimate, various references needed; Lee 1972	pH	7.320000
red blood cells	Schmitt 2008	pH	7.200000
skin	Schmitt 2008	pH	7.000000
spleen	Schmitt 2008	pH	7.000000
thyroid	Pilari et al. 2017; Chow et al. 1982	pH	7.300000
adipose	Schmitt 2008	Fa_PLc	0.007859
bone	Schmitt 2008	Fa_PLc	0.040000
brain	Schmitt 2008	Fa_PLc	0.167800
gut	Schmitt 2008	Fa_PLc	0.050000
heart	Schmitt 2008	Fa_PLc	0.030900
kidney	Schmitt 2008	Fa_PLc	0.068530
liver	Schmitt 2008	Fa_PLc	0.050510
lung	Schmitt 2008	Fa_PLc	0.140000
muscle	Schmitt 2008	Fa_PLc	0.078840
placenta	Httk estimate, various references needed; Lee 1972	Fa_PLc	0.073800
red blood cells	Schmitt 2008	Fa_PLc	0.100000
skin	Schmitt 2008	Fa_PLc	0.138200
spleen	Schmitt 2008	Fa_PLc	0.072870
thyroid	Pilari et al. 2017; Chow et al. 1982	Fa_PLc	0.014000
adipose	Schmitt 2008	Fn_PLc	0.056070
bone	Schmitt 2008	Fn_PLc	0.110000

brain	Schmitt 2008	Fn_PLc	0.458800
gut	Schmitt 2008	Fn_PLc	0.260000
heart	Schmitt 2008	Fn_PLc	0.079010
kidney	Schmitt 2008	Fn_PLc	0.294000
liver	Schmitt 2008	Fn_PLc	0.225100
lung	Schmitt 2008	Fn_PLc	0.560000
muscle	Schmitt 2008	Fn_PLc	0.381700
placenta	Httk estimate, various references needed; Lee 1972	Fn_PLc	0.298700
red blood cells	Schmitt 2008	Fn_PLc	0.500000
skin	Schmitt 2008	Fn_PLc	0.501900
spleen	Schmitt 2008	Fn_PLc	0.393000
thyroid	Pilari et al. 2017; Chow et al. 1982	Fn_PLc	0.064000
adipose	Schmitt 2008	Fn_Lc	0.936100
bone	Schmitt 2008	Fn_Lc	0.850000
brain	Schmitt 2008	Fn_Lc	0.373400
gut	Schmitt 2008	Fn_Lc	0.690000
heart	Schmitt 2008	Fn_Lc	0.890100
kidney	Schmitt 2008	Fn_Lc	0.637500
liver	Schmitt 2008	Fn_Lc	0.724400
lung	Schmitt 2008	Fn_Lc	0.300000
muscle	Schmitt 2008	Fn_Lc	0.539400
placenta	Httk estimate, various references needed; Lee 1972	Fn_Lc	0.627300
red blood cells	Schmitt 2008	Fn_Lc	0.400000
skin	Schmitt 2008	Fn_Lc	0.359900
spleen	Schmitt 2008	Fn_Lc	0.534100
thyroid	Pilari et al. 2017; Chow et al. 1982	Fn_Lc	0.920000
adipose	Schmitt 2008	FPc	0.046010
bone	Schmitt 2008	FPc	0.210000
brain	Schmitt 2008	FPc	0.083410
gut	Schmitt 2008	FPc	0.150000
heart	Schmitt 2008	FPc	0.166800
kidney	Schmitt 2008	FPc	0.169800
liver	Schmitt 2008	FPc	0.183300
lung	Schmitt 2008	FPc	0.183000
muscle	Schmitt 2008	FPc	0.177000
placenta	Httk estimate, various references needed; Lee 1972	FPc	0.153500

red blood cells	Schmitt 2008	FPc	0.330700
skin	Schmitt 2008	FPc	0.289800
spleen	Schmitt 2008	FPc	0.190700
thyroid	Pilari et al. 2017; Chow et al. 1982	FPc	0.160000
adipose	Schmitt 2008	FLc	0.934000
bone	Schmitt 2008	FLc	0.020000
brain	Schmitt 2008	FLc	0.112300
gut	Schmitt 2008	FLc	0.070000
heart	Schmitt 2008	FLc	0.137500
kidney	Schmitt 2008	FLc	0.064070
liver	Schmitt 2008	FLc	0.092310
lung	Schmitt 2008	FLc	0.013160
muscle	Schmitt 2008	FLc	0.023870
placenta	Httk estimate, various references needed; Lee 1972	FLc	0.008300
red blood cells	Schmitt 2008	FLc	0.005010
skin	Schmitt 2008	FLc	0.283100
spleen	Schmitt 2008	FLc	0.039460
thyroid	Pilari et al. 2017; Chow et al. 1982	FLc	0.050000
adipose	Schmitt 2008	FWc	0.020020
bone	Schmitt 2008	FWc	0.260000
brain	Schmitt 2008	FWc	0.804300
gut	Schmitt 2008	FWc	0.780000
heart	Schmitt 2008	FWc	0.695700
kidney	Schmitt 2008	FWc	0.766100
liver	Schmitt 2008	FWc	0.724400
lung	Schmitt 2008	FWc	0.803800
muscle	Schmitt 2008	FWc	0.799100
placenta	Httk estimate, various references needed; Lee 1972	FWc	0.793000
red blood cells	Schmitt 2008	FWc	0.664300
skin	Schmitt 2008	FWc	0.427000
spleen	Schmitt 2008	FWc	0.769900
thyroid	Pilari et al. 2017; Chow et al. 1982	FWc	0.690000
adipose	Schmitt 2008	Fint	0.140000
bone	Schmitt 2008	Fint	0.100000
brain	Schmitt 2008	Fint	0.005000
gut	Schmitt 2008	Fint	0.096000

heart	Schmitt 2008	Fint	0.250000
kidney	Schmitt 2008	Fint	0.165000
liver	Schmitt 2008	Fint	0.230000
lung	Schmitt 2008	Fint	0.200000
muscle	Schmitt 2008	Fint	0.150000
placenta	Httk estimate, various references needed; Lee 1972	Fint	0.276000
red blood cells	Schmitt 2008	Fint	0.000000
skin	Schmitt 2008	Fint	0.600000
spleen	Schmitt 2008	Fint	0.255000
thyroid	Pilari et al. 2017; Chow et al. 1982	Fint	0.140000
adipose	Schmitt 2008	Fcell	0.860000
bone	Schmitt 2008	Fcell	0.900000
brain	Schmitt 2008	Fcell	0.995000
gut	Schmitt 2008	Fcell	0.900000
heart	Schmitt 2008	Fcell	0.750000
kidney	Schmitt 2008	Fcell	0.835000
liver	Schmitt 2008	Fcell	0.770000
lung	Schmitt 2008	Fcell	0.800000
muscle	Schmitt 2008	Fcell	0.850000
placenta	Httk estimate, various references needed; Lee 1972	Fcell	0.724000
red blood cells	Schmitt 2008	Fcell	1.000000
skin	Schmitt 2008	Fcell	0.400000
spleen	Schmitt 2008	Fcell	0.745000
thyroid	Pilari et al. 2017; Chow et al. 1982	Fcell	0.860000

Annex 3: Physiological parameters for humans and all animal species of interest.

Para-meter	Parameter (only for goat & sheep)	Description	Cat	Chicken	Cow	Human	Pig	Rat	Sheep	Goat
BW	BW	Body Weight	3,8	2,11	526,1	70	108	0,25	36,8	25,56
GFR	GFR	Glomerular Filtration Rate	0,418	0,32494	57,871	6,7	25,92	0,0786	6,38	2.8938
FVad	VAdc	Fraction of adipose tissue	0,117	0,107	0,184	0,213	0,176	0,07	0,2098	0,0914
FVbo		Fraction of bone	0,136	0,203	0,091	0,085629	0,09	0,0659		
FVbr		Fraction of brain	0,008	0,0027	0,0008	0,02	0,0018	0,0052		
Fvgu	VGIc	Fraction of gut	0,033	0,039	0,017	0,0171	0,03	0,026	0,0445	0,0991
FVhe		Fraction of heart	0,005	0,006	0,0038	0,0047	0,0035	0,0044		
FVki	VKc	Fraction of kidney	0,007	0,0084	0,003	0,0044	0,0034	0,0092	0,0023	0,0038
FVli	VLc	Fraction of liver	0,033	0,024	0,013	0,021	0,017	0,036	0,0127	0,0189
FVlu		Fraction of lungs	0,008	0,0082	0,0072	0,0076	0,0077	0,0052		
FVmu	VMuc	Fraction of muscle	0,499	0,408	0,34	0,4	0,45	0,488	0,2478	0,1009
FVoo		Fraction of reproductive organ (chicken) and mammary gland (cow)	0,000001	0,028	0,032	0,000001	0,000001	0,000001		
FVve		Fraction of venous blood	0,033333	0,047333	0,026667	0,0514	0,023333	0,0429		
	VBc	Fraction of blood							0,0486	0,0549
FVar		Fraction of arterial blood	0,016667	0,023667	0,013333	0,0257	0,011667	0,0215		
FVre	VRc	Fraction of rest compartment	0,104	0,0947	0,2682	0,149471	0,1856	0,2257	0,4343	0,3461
QC	QC	Cardiac output	27,47	43,044	3577,48	389,9	712,8	4,8	419,9195	208,8252
FQad	QAdc	Fraction of blood flow to adipose tissue	0,06	0,015	0,068	0,05	0,11	0,059	0,0618	0,0618

Para-meter	Parameter (only for goat & sheep)	Description	Cat	Chicken	Cow	Human	Pig	Rat	Sheep	Goat
FQbo		Fraction of blood flow to bone	0,025	0,124	0,03	0,05	0,108	0,101		
FQbr		Fraction of blood flow to brain	0,054	0,004	0,009	0,12	0,02	0,014		
FQgu	QGIc	Fraction of blood flow to gut	0,158	0,177	0,3	0,146462	0,173	0,101	0,2699	0,2699
FQhe		Fraction of blood flow to heart	0,067	0,055	0,02	0,04	0,04	0,04		
FQki	QKc	Fraction of blood flow to kidney	0,084	0,114	0,07	0,19	0,098	0,145	0,119	0,1298
FQh	QLc	Fraction of blood flow to liver	0,198	0,243	0,35	0,215385	0,22	0,242	0,012	0,012
FQlu		Fraction of blood flow to lungs	1	1	1	1	1	1		
FQmu	QMuc	Fraction of blood flow to muscle	0,13	0,198	0,2	0,17	0,3	0,237	0,1009	0,1009
FQoo		Fraction of blood flow to reproductive organs		0,143	0,165					
FQre	QRc	Fraction of blood flow to rest compartment	0,382	0,104	0,088	0,164615	0,104	0,162	0,4256	0,4256
Qtransfer		Fraction of transfer to eggs (chicken) or milk (cow)		0,012	1,27					

Annex 4. Substance-specific modelling parameters.

Para-meter	Parameter (only for goat & sheep)	Descrip-tion	Bromoxynil	Chlorpropham	Chlorpyrifos	Hexachlorobenzene	Indoxacarb	MCPA	Pendimethalin	Piperonyl butoxide	Prosulfocarb	Pyrethrin II	Pyrimethanil	Tri-allate	2,4-D	Tebuconazole
MW		Molecular weight (g/mol)	276,91	213,66	350,6	284.8	527,8	200,62	281,31	338,4	251,39	372,5	199,25	304,7	221,03	307,82
logP			2,7	3,51	4,96	5,73	4,65	3,25	5,2	4,75	4,48	4,3	2,84	4,6	2,81	3,7
type		Protonation	Mono-protic base	neutral	neutral	neutral	neutral	Mono-protic acid	Mono-protic acid	neutral	neutral	neutral	neutral	neutral	Mono-protic acid	neutral
pKa			3,86					2,64	2,8						2,64	
Ka		Absorption rate from gut	1	1	1	1	1	1	1	1	1		1	1	1	1
Fa		Fraction absorbed	1	1	1	1	1	1	1	1	1		1	1	1	1
Kpad	PAdc	Partition coefficient adipose tissue	5,9	23,26	102,51	150,59	79,83	0,1	0,1	164,36	107,87	56,17	7,8	76,25	0,1	31,52
Kpbo		Partition coefficient bone	4,77	4,34	15,63	16,93	14,75	3,06	13,8	21,81	15,39	13,43	1,8	14,59	1,83	5,57
Kpbr		Partition coefficient brain	4,54	9,57	14,32	15,48	13,52	2,97	12,66	48,39	34,13	12,33	3,91	13,37	1,86	12,3
Kpgu	PGIc	Partition coefficient gut	3,62	10	11,3	12,21	10,67	2,39	10	50,22	35,44	9,74	4,13	10,56	1,52	12,83

*For goat and sheep, the partition coefficient of the rest compartment was the average of bone, brain, heart, lung, skin and spleen.

Para-meter	Parameter (only for goat & sheep)	Descrip-tion	Bromoxynil	Chlorpro-pham	Chlorpyrifos	Hexachloro-benzene	Indoxacarb	MCPA	Pendi-methalin	Piperonyl butoxide	Prosulfo-carb	Pyrethrin II	Pyri-methanil	Tri-allate	2,4-D	Tebu-conazole
Kphe		Partition coefficient heart	1,36	4,1	3,51	3,77	3,33	0,98	3,14	20,1	14,22	3,07	1,77	3,3	0,74	5,23
Kpki	PKc	Partition coefficient kidney	1,93	4,73	5,42	5,84	5,13	1,34	4,82	23,37	16,52	4,71	2,02	5,08	0,94	6,04
Kpli	PLc	Partition coefficient liver	2,95	5,06	8,94	9,66	8,45	1,97	7,92	24,96	17,64	7,72	2,16	8,36	1,29	6,46
Kplu		Partition coefficient lung	0,72	6,14	1,25	1,32	1,2	0,59	1,15	30,51	21,56	1,14	2,59	1,2	0,53	7,86
Kpmu	PMuc	Partition coefficient muscle	1,94	2,99	5,5	5,93	5,21	1,35	4,89	14,79	10,45	4,77	1,3	5,15	0,94	3,82
Kpsk		Partition coefficient skin	2,28					1,55				5,81				
Kpspl		Partition coefficient spleen	1,96					1,36				4,79				
Kpoo		Partition coefficient reproductive organs		2,99	5,5	5,93	5,21		4,89	14,79	10,45		1,3	5,15	0,94	3,82
Kpre*	PRc	Partition coefficient rest compartment	2,605	2,99	5,5	5,93	5,21	1,752	4,89	14,79	10,45	6,762	1,3	5,15	0,94	3,82
fup		Fraction unbound plasma	0,156	0,074	0,018	0,008	0,024	0,024	0,005	0,022	0,005	0,034	0,138	0,025	0,035	0,2

*For goat and sheep, the partition coefficient of the rest compartment was the average of bone, brain, heart, lung, skin and spleen.

Annex 5. MRM details on the LC-MS/MS analysis.

MRM details of the LC-MS/MS analysis of the included pesticides for the quantification of their metabolism in vitro are presented in the table below.

Compound	Precursor (m/z)	Product (m/z)	Dwell time (s)	Cone energy (V)	Collision energy (V)
Chlorpropham	172	154	0.163	20	10
	172	126	0.163	20	20
Tebuconazole	308	151	0.08	30	20
	308	124.7	0.08	30	30
Imidacloprid	256	175	0.163	29	27
	256	209	0.163	25	29
Piperonyl butoxide	356	119	0.163	26	35
	356	177	0.163	26	20
Prosulfocarb	252	91	0.163	20	15
	252	128	0.163	20	10
Pyrimethanil	200	82	0.163	20	20
	200	107	0.163	20	20
Chlorpyrifos	349.9	96.9	0.163	20	35
	349.9	198	0.163	20	20